10-6-2016 12:00 AM

Adipose-Derived Stem Cell Differentiation in Cell Aggregates Supplemented with Micronized, Decellularized Extracellular Matrix

Danielle Heinbuch
The University of Western Ontario

Supervisor
Dr. Lauren Flynn
The University of Western Ontario

Graduate Program in Biomedical Engineering
A thesis submitted in partial fulfillment of the requirements for the degree in Master of Engineering Science

Abstract

In the human body there are tissues with limited regenerative potential, raising the need for cell-based regenerative therapies. The main objective of this thesis was to examine how tissue-specific extracellular matrix (ECM) affects the differentiation of human adipose-derived stem/stromal cells (ASCs). The effects of incorporating milled, decellularized adipose (DAT) or cartilage (DCT) ECM particles on ASC lineage-specific differentiation in 3-D cell aggregate cultures were explored. The results demonstrated that the addition of ECM improved differentiation for both adipogenesis and chondrogenesis. Analysis of adipogenic gene and protein expression indicated enhanced differentiation in the DAT+ASC aggregates relative to the DCT+ASC and ASC-alone groups at 14 days. Additionally, chondrogenic studies showed that incorporating DCT had a positive effect on collagen II deposition and late chondrogenic marker expression at 28 days when compared to DAT+ASC or ASC-alone groups. Overall, these findings support the further investigation of ECM as a cell-instructive platform for ASC differentiation.

Keywords

Adipose-derived stem/stromal cells, extracellular matrix, decellularization, decellularized adipose tissue, adipose tissue, adipogenesis, decellularized cartilage tissue, cartilage, chondrogenesis, differentiation, cell-ECM aggregates, cell-based therapy, tissue engineering, regenerative medicine.

Acknowledgments

First and foremost, I would like to thank my supervisor, Dr. Lauren Flynn for her support and guidance throughout this project. Her undeniable devotion to her students, research, and the future of science is inspiring and did not go unnoticed. Her writing and editing skills are superior to many and she was an irreplaceable mentor throughout the writing process. She was also extremely patient and understanding and gave me an incomparable experience here at Western.

Secondly, I would like to thank my advisory committee members, Dr. Alan Getgood and Dr. Harvey Goldberg, for their commitment to seeing this project through with their helpful guidance and suggestions over the last two years.

Thank you to my fellow Flynn lab members, who I have come to know as friends. Your quirks and charms made coming to the lab every day an adventure. I would like to thank Claire Yu for enduring the trials of PCR and attempts at chondrogenesis, and for her guidance in many other lab procedures. Special thanks goes to Cody Brown for familiarizing me with basic lab techniques, setting up and keeping the lab tidy, functional, fully stocked, and in proper working order. Additionally, I would like to thank Anna Kornmuller for assisting me with a final pilot study that included fluorescent staining of my ECM particles for IHC analysis.

I would like to thank my parents, Tom and Rose Heinbuch, for always encouraging me academically and setting me up with the inquisitive attitude that led me to science. Your support both financially and emotionally have kept me on track. You are dedicated to your children and our successes are thanks to you.

Finally, I would like to thank my Husband, Wesley Greig. You have been one of my biggest supporters throughout my university career. Your continual encouragement and emotional support has helped me in so many ways.

Table of Contents

List of Tables

List of Figures

List of Abbreviations

2-D	2-dimensional
3-D	3-dimensional
ABAM	antibiotic-antimycotic
ADIPOQ	adiponectin
AGG	aggrecan
ASCs	adipose-derived stem/stromal cells
BMI	body mass index
BMSCs	bone marrow-derived mesenchymal stem/stromal cells
BSA	bovine serum albumin
C/EBPα	CCAAT/enhancer-binding protein-alpha
C/EBPβ	CCAAT/enhancer-binding protein-beta
C/EBPδ	CCAAT/enhancer-binding protein-delta
COMP	cartilage oligomeric matrix protein
DAT	decellularized adipose tissue
DCT	decellularized cartilage tissue
DEX	dexamethasone
dH2O	distilled water

ECM	extracellular matrix
EDTA	ethylenediaminetetraacetic acid
EtOH	ethanol
FACIT	fibril associated collagen with interrupted helices
FBS	fetal bovine serum
FFAs	free fatty acids
GAGs	glycosaminoglycans
GAPDH	glyceraldehyde-3-phosphate dehydrogenase
Gly	glycine
GLUT4	glucose transporter-4
GPDH	glycerol-3-phosphate dehydrogenase
I	induced
IBMX	3-isobutyl-1-methylxanthine
IFATS	International Federation for Adipose Therapeutics and Science
IGF-IRs	insulin-like growth factor-I receptors
IHC	immunohistochemistry
IL1	interleukin-1
IL6	interleukin-6
IL10	interleukin-10

IL11	interleukin-11
IPO8	importin 8
LPL	lipoprotein lipase
ISCT	International Society for Cellular Therapy
MMPs	matrix metalloproteinases
MSCs	mesenchymal stem/stromal cells
NI	not induced
PBS	phosphate buffered saline
PDGF	platelet-derived growth factor
Pen-strep	penicillin/streptomycin
PFA	paraformaldehyde
PGA	poly-glycolic acid
PGE2	prostaglandin E2
PLA	poly-L-lactic acid
PMSF	phenylmethylsulfonyl fluoride
PPARϒ	peroxisome proliferator activated receptor-gamma
RPL13A	ribosomal protein L13A
RPM	revolutions per minute
RT-qPCR	quantitative reverse transcriptase-polymerase chain reaction

RUNX2	runt-related transcription factor 2
SDS	sodium dodecyl sulphate
SEM	scanning electron microscopy
SOX5	sex-determining region Y-related high motility group box 5
SOX6	sex-determining region Y-related high motility group box 6
SOX9	sex-determining region Y-related high motility group box 9
SPB	Sorenson's phosphate buffer
SVF	stromal vascular fraction
TBP	tributyl phosphate
TBS	tris buffered saline
TCPS	tissue culture polystyrene
TG	triglycerides
TGF-β	transforming growth factor-beta
TIMPs	tissue inhibitor of metalloproteinases
UBC	ubiquitin C
VEGF	vascular endothelial growth factor
Wnt	wingless-related integration site

List of Appendices

Chapter 1

1 Introduction

In the emerging field of tissue engineering, many strategies have been developed to overcome obstacles related to tissue loss associated with injury or disease. Tissues with limited regeneration potential require stimulation to assist with the repair process in order to prevent scar tissue formation and promote recovery of function. Many studies exploit the use of bioactive materials and various cell types to stimulate *in situ* tissue formation. The concept that stem cell fate is regulated by the extracellular environment *in vivo* is well founded in research [1][2]. Recent studies suggest that cellular behavior of stem/stromal cells is mediated in part though biochemical and biomechanical interactions with the extracellular matrix (ECM), as well as through other environmental cues (e.g. oxygen tension) and signaling with surrounding cells [3][4].

The ECM is a complex 3-dimensional network of proteins, proteoglycans, and glycoproteins that are tissue-specific in structure and composition [3]. The ECM is known to influence cellular responses such as cell survival, development, shape, and migration through interactions with adhesion molecules, binding proteins and various enzymes [4][5]. Physical and biomechanical cues such as matrix architecture and surface chemistry also play an important role in mediating cellular functions [6]. A large area of tissue engineering and cell-based therapy research is focused on designing novel scaffolds and biomaterials to mimic the 'tissue-specific niche' and simulate the biomechanical and biochemical cues present *in vivo* in order to stimulate regeneration [5][7][8].

For the development of cellular therapies, adipose tissue represents an attractive source of adult mesenchymal stem/stromal cells (MSCs) [9]. Adipose-derived stem/stromal cells (ASCs) can be isolated from the stromal vascular fraction (SVF) of digested adipose tissue using established procedures. The stem/stromal population is selected through serial passaging of the tissue culture polystyrene (TCPS)-adherent cell population [10]. ASCs are a promising cell source for regenerative therapies due to their relative abundance and ease of access when compared with other MSC sources, such as bone marrow-derived MSCs [9]. Further, ASCs are a heterogeneous

cell population that includes multipotent adult stem cells, capable of differentiating along the adipogenic, chondrogenic, and osteogenic lineages, as well as displaying cell surface markers of the neuronal, endothelial, and hematopoietic lineages [11][12]. ASCs may be incorporated into scaffolds, where they assist in modulating the cell niche by stimulating the recruitment and differentiation of host cells through paracrine signaling [10].

1.1 Project Motivation

The ECM is a key component of the tissue-specific natural microenvironment for cells. Therefore ECM-derived biomaterials are of interest as stem cell delivery vehicles, to improve cell attachment and survival *in vivo* [13][14]. The heterogeneity of the ECM composition within various tissues provides a rationale for applying a tissue-specific approach to bio-scaffold design. The selection of naturally derived, tissue-specific scaffolds comprised of ECM as a platform for tissue regeneration is well supported, as it is recognized that cells exchange signals with both neighboring cells and the surrounding matrix [15][2][16]. An ideal scaffold should mimic the properties of the native tissue, supporting the rationale for the use of tissue-specific scaffolds. Many approaches target tissue decellularization as a method of obtaining tissue-specific ECM from sources such as heart, adipose tissue, cartilage, bone, kidney and lung [9], [17]–[21]. However, limited research has been done to date to compare the effects of tissue-specific ECM on the lineage-specific differentiation of MSCs [22][18][9].

1.2 Project Rationale

To study the effects of tissue-specific ECM on the adipogenic and chondrogenic differentiation of human ASCs *in vitro*, culture conditions must allow for adipogenesis and chondrogenesis to occur in their preferred environment, which is a 3-dimensional (3-D) culture with high cell density [23][24][25]. A high cell density is often achieved by culturing ASCs clustered in an aggregate, often referred to as a pellet culture. Incorporating decellularized ECM sourced from adipose tissue or cartilage into the cell aggregate cultures will give insight into the potential importance of using tissue-specific ECM to guide differentiation and/or to act as a natural scaffold for the regeneration of adipose or cartilage tissue. For this reason, decellularized adipose tissue (DAT) and decellularized cartilage tissue (DCT) were lyophilized, milled, and incorporated into 3-D aggregates fabricated by centrifuging a suspension of ASCs and ECM

particles. *In vitro* cell culture studies were conducted to explore adipogenesis and chondrogenesis of ASCs in the cell-ECM aggregates. The level of adipogenic and chondrogenic differentiation within the various aggregates was assessed in both proliferation medium and differentiation medium to examine the potential inductive effects of the ECM on ASC differentiation. ASCs were also cultured in cell aggregate cultures without ECM as a control.

1.3 Hypothesis

With support from the literature that tissue-specific ECM has the ability to influence cellular behaviors, it was hypothesized that the ECM will stimulate ASCs to differentiate towards the lineage specific to that of the native tissue. Therefore, cells cultured with DAT particles will demonstrate an increased tendency for differentiation towards the adipogenic lineage and the ECM will have an inductive effective on adipogenic differentiation under proliferation conditions. Similarly, ASCs cultured with DCT particles will be induced towards the chondrogenic pathway. It was expected that differentiation levels will be higher in all aggregates containing ECM, and that differentiation towards the adipogenic lineage will be highest in the samples combining DAT with adipogenic medium. Likewise, chondrogenic differentiation was expected to be highest when ASCs were cultured with DCT in chondrogenic medium.

1.4 Specific Objectives

The objectives of this Master's project were:

1) To establish methods for decellularizing porcine auricular cartilage based on existing decellularization protocols in the literature.
2) To refine protocols for cryo-milling the DAT and DCT, and to characterize the particles using SEM and dynamic light scattering.
3) To conduct *in vitro* cell culture studies to investigate adipogenesis and chondrogenesis in cell aggregates comprised of (i) ASCs and DAT (ii) ASCs and DCT, and (iii) ASCs alone, cultured in both differentiation and proliferation media.

Chapter 2

2 Literature Review

2.1 Adipose-derived Stem/Stromal Cells (ASCs)

Research conducted by *Friedenstein et al.* identified some of the first reported evidence of tissue culture polystyrene (TCPS)-adherent bone marrow-derived mesenchymal stem/stromal cells (BMSCs) that were capable of expansion and differentiation towards osteogenic lineages [26]. Further examination led to the identification of stem/stromal cells within other adult tissues, and since this time mesenchymal stem/stromal cells (MSCs) have been discovered within many human tissues [27]–[29]. This work revolutionized modern cell therapy strategies as MSCs became more readily available, and could be expanded in culture and differentiated towards multiple lineages [30]. Adipose-derived stem/stromal cells (ASCs) are attractive as a cell source due to their relative abundance, the ease of access to adipose tissue (fat) with minimal discomfort to patients, and the larger cell yield when compared to BMSC populations [29]. While BMSCs have been studied extensively, limitations to using this cell type include low yields (1 BMSC in every 3.4×10^4 bone marrow nucleated cell population) and painful collection procedures [31]. It is for these reasons that ASCs are being extensively researched in the field of regenerative cell therapies.

Another benefit of ASCs is the potential to be an autologous stem/stromal cell source for patients, as the cells are easily obtained from subcutaneous fat stores within the body. Cellular procurement may be accomplished through minimally invasive procedures such as lipoaspiration [29] or from excess tissues collected during elective breast or abdominal reduction surgeries [32]. There are varying methods of ASC isolation, but common protocols involve enzymatic digestion and centrifugation steps to yield the stromal vascular fraction (SVF). Current views of ASCs suggest that they co-exist with resident endothelial cells and pericytes within the perivascular niche *in vivo.* After isolation, the SVF contains a heterogeneous mixture of endothelial progenitor cells, pericytes, fibroblasts, blood cells, smooth muscle cells, macrophages, pre-adipocytes, and MSCs [33]–[35]. Expansion of the heterogeneous SVF aids in the selection of adherent cell populations to yield a purer ASC culture. Donor variability,

isolation procedures, growth conditions, and sites of tissue harvesting have been noted as potential reasons for differences seen within varying ASC populations [36]–[38].

Recent studies found that an increased donor age, increased body mass index (BMI), and reduced donor health have been linked to decreased proliferation and differentiation capacities and an increase in cell senescence markers [39]–[41]. Interestingly, donor depot has also been linked to differences in ASC characteristics [42]. Studies by Schipper *et al.* found that the upper arm and medial thigh depots consistently yielded ASCs with a greater proliferation and differentiation capacity when compared to the depots of the abdomen or trochanter [42]. Russo *et al.* reported that adipogenesis was enhanced in ASCs isolated from subcutaneous, pericardial, and thymic remnant adipose tissue, while osteogenic differentiation levels were upregulated in ASCs sourced from the omentum [43]. Other potential differences have also been noted between male and female donors, however more research is needed to confirm these findings [43], [44]. These findings highlight the need for larger studies to assess significant differences between donor gender, depot site, age, and BMI and the effect these factors may have on ASC proliferation and differentiation capacity and ASC immunophenotypes.

2.1.1 ASCs in Regenerative Tissue Engineering

According to Gimble *et al.*, ASCs retain the ability to give rise to genetically identical daughter cells through the process of mitotic division [38]. ASCs are also capable of differentiation towards cells of the mesodermal lineage, including adipocyte, chondrocyte, osteoblast, myocyte, and peripheral nerve lineages [29], [45]. Based on yields obtained from isolations, expected cellular demands for therapeutic applications can require approximately 10^9 stem cells [46]. ASCs have the potential to meet that need, making them promising sources for musculoskeletal research applications. Comparatively, reports on ASC isolations suggest that cell yields can reach 40 times more than BMSCs [29], [47], [48].

ASCs have the ability to be cultured in various conditions such as 2-D and 3-D cultures, under normoxic and hypoxic conditions, static and dynamic cultures, and under different media formulations [45]. This is beneficial from a culturing perspective as methods can be altered to examine cellular behavior from a multitude of perspectives in culture. Due to the ability of ASCs

to be cultured under various conditions, cultures may be tailored to conditions seen in a specific tissue of interest *in vivo*, including in diseased states.

ASCs are also capable of secreting paracrine factors that can modulate wound healing [49]. A variety of growth factors such as platelet-derived growth factor (PDGF), vascular endothelial growth factor (VEGF), as well as cytokines such as interleukin-10 (IL10) and prostaglandin E2 (PGE2) have been shown to be secreted by ASCs within wound healing sites [50]–[52]. Evidence also suggests that ASCs are capable of modulating macrophage behavior and recruiting cells to promote tissue remodeling [53]. Transplantation of ASCs *in vivo* demonstrates minimal evidence of immune rejection and as a result, allogeneic ASCs may hold potential for use in cell therapy applications [46].

2.1.2 Immunophenotype of ASCs

The International Society for Cellular Therapy (ISCT) and the International Federation for Adipose Therapeutics and Science (IFATS) have defined a set of parameters with the intention of characterizing ASCs. The following criteria were proposed for the characterization of ASCs: (1) plastic-adherent, (2) express the standard immunophenotypic profile (Table 2.1), and (3) maintain multipotency towards the adipogenic, osteogenic, and chondrogenic lineages [54].

ISCT and IFATS suggest that immunophenotype analysis should include at least two primary positive markers, one secondary positive marker, two primary negative markers, and one secondary negative marker when characterizing ASCs [54]. Positive expression of primary markers should be greater than 80% but less than 2% for primary negative markers. Additionally, cell viability should be greater than 90% [54]. It is worth noting that some discrepancies have been published in terms of expression levels of some markers between culture conditions and passage number, highlighting the need for guidelines for characterizing ASC populations, as well as standardization of isolation and culture methods. In addition, studies have noted that immunophenotypes of ASCs may be altered in 2-D cultures when compared to cells found *in vivo* or when cultured in 3-D cultures [46].

Table 2.1 ASC Immunophenotype

Marker type	Antigen
Primary positive (>80%)	CD90 (Thy-1) CD105 (endoglin) CD73 (ecto-5'-nucleotidase) CD44 (hyaluronic acid receptor) CD29 (β1-integrin) CD13 (aminopeptidase-N) CD34 (progenitor associated marker)* CD146 (melanoma cell adhesion molecule (MCAM))*
Secondary positive	CD10 (nephrilysin) CD26 (dipeptidyl peptidase-4) CD48d (α4-integrin)* CD49e (α5-integrin) CD36 (fatty acid translocase)
Primary negative (<2%)	CD31 (platelet endothelial cell adhesion molecule (PECAM)) CD45 (leukocyte-common antigen-antigen D related)
Secondary negative	CD3 (T-cell co-receptor) CD11b (α6-integrin) CD49F (αM-integrin) CD106 (vascular cell adhesion protein 1 (VCAM-1))

**Variable levels of expression*

2.1.3 Adipogenesis

It is known that ASCs are capable of differentiating along multiple pathways, including the adipogenic pathway [29]. In general, ASCs undergoing adipogenesis prefer close cell-cell contact, suggesting that a high cell density is preferred prior to differentiation towards this lineage. ASCs have been shown to differentiate both on 2-D TCPS and on 3-D scaffolding materials [32]. Glucocorticoid agonists such as hydrocortisone and dexamethasone (DEX) initiate the induction of ASCs toward the adipogenic pathway (Figure 2.1) [55]. Presence of hydrocortisone and DEX, along with supra-physiological insulin concentrations, initiate a signaling cascade [56], [57]. This in turn activates receptors in pre-adipocytes to stimulate the activation of early transcription factors CCAAT/enhancer-binding protein-β (C/EBPβ) and CCAAT/enhancer-binding protein-δ (C/EBPδ) [58]. This causes the upregulation of the primary transcription factors peroxisome proliferator activated receptor-ϒ (PPARϒ) and CCAAT/enhancer-binding protein-α (C/EBPα) [55], [57]. Cell proliferation is inhibited by the activation of C/EBPα while sensitivity to insulin is maintained. A positive feedback loop ensues

between PPARϒ and C/EBPα to maintain increased expression as the cells accumulate lipid during maturation and move closer to terminal differentiation [59], [60]. Adipocyte-specific genes such as lipoprotein lipase (LPL), glucose transporter-4 (GLUT4), glycerol-3-phosphate dehydrogenase (GPDH) and insulin receptors are all upregulated, driving the cells to further maturation and lipid accumulation [55].

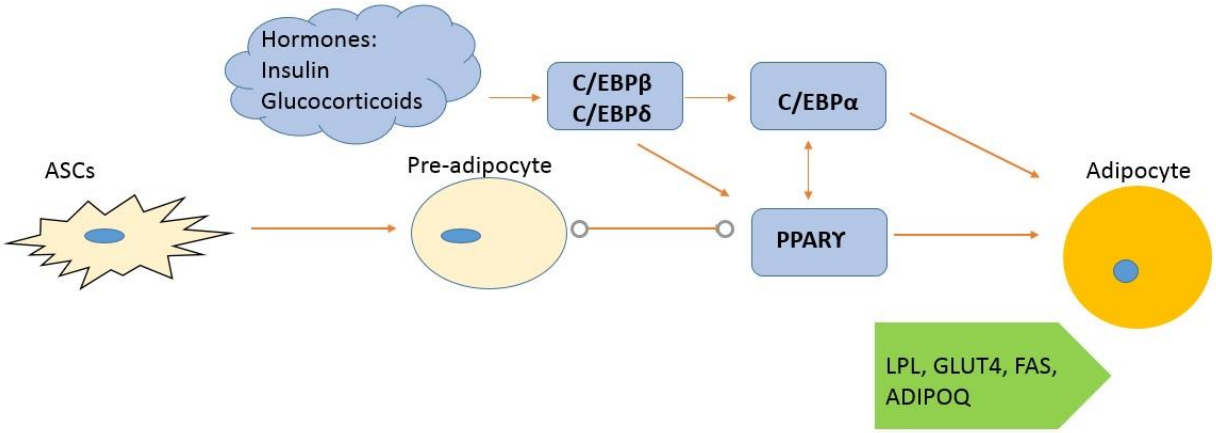

Figure 2.1 Transcriptional control of adipogenesis.

There is a delicate balance of factors that mediate adipogenesis along the transcriptional signaling cascade. Fatty acids and prostaglandins act as ligands or precursor ligands for PPARϒ or may help to induce the adipogenic factors C/EBPβ and C/EBPδ [61]–[63]. Glucocorticoids also promote adipogenesis through activating C/EBPδ and PPARϒ expression [64], [65]. Nuclear co-activated receptors, like PPAR binding protein, work through PPARϒ to promote adipogenesis [60]. Insulin-like growth factor-I receptors (IGF-IRs) also function to increase insulin sensitivity of the cells, driving maturation. Conversely, factors such as wingless-related integration site (Wnt) signaling, transforming growth factor-β (TGF-β), tumor necrosis factor-α (TNF-α), and interleukins (IL-1, IL-6, IL-11) inhibit adipogenesis through inhibition of PPARϒ and CEBPα [55], [57], [66]. Upregulation of adipogenesis *in vitro* often includes the addition of supplements such as insulin, DEX, hydrocortisone, troglitazone, and 3-isobutyl-1-methylxanthine (IBMX) to serum free media [67], [68].

2.1.4 Chondrogenesis

ASCs have the ability to differentiate towards the chondrogenic lineage, however, this cannot be accomplished in 2-D on TCPS. The cells require the high cell density and close cell-cell contact that can only be accomplished in 3-D cultures [69], [70]. It is for this reason that pellet cultures are often used during chondrogenesis [71]. This culture format mimics the mesenchymal condensation process that occurs during chondrogenesis *in vivo* and allows the cells to initiate differentiation towards the chondrogenic pathways [72].

Sex-determining region Y-related high motility group box 9 (SOX9) is an important transcription factor in chondrogenesis [73]. Transcription of SOX5 and SOX6 is induced by SOX9, which act in turn to enhance SOX9 activity and maintain chondrogenic phenotypes, preventing hypertrophy [74]. SOX9 induces chondrogenesis by upregulating cartilage-matrix specific genes to help maintain pre-chondrocyte phenotypes [75]. Chondrogenic factors such as TGF-β and bone morphogenic proteins (BMPs) are key to initializing the chondrogenic signaling cascade that leads to the condensation process [76]–[79]. ASCs begin to differentiate into chondroblasts following condensation. In this stage, the cells are highly proliferative and begin matrix deposition of collagens II, IX, XI, and aggrecan (Figure 2.2) [78], [80]. Subsequently, cartilage oligomeric matrix protein (COMP) is upregulated while collagen I is downregulated [71], [72], [59]. It is for this reason that ratios of collagen II:collagen I are often compared using immunohistochemistry (IHC) to assess chondrogenesis.

Late stages of chondrogenesis may see chondroblasts become hypertrophic chondrocytes, where collagen X is upregulated and calcification begins [80]. This signals terminal differentiation of chondrogenesis and marks the beginning of osteo-chondrogenesis. Runt-related transcription factor 2 (RUNX2) is upregulated during this time [81]. Since none of this can occur without the initial condensation process that triggers upregulation of SOX9 and cartilage-specific ECM synthesis, it can be stated that chondrogenesis is highly dependent not only on transcriptional control but may be partially controlled by cells responding to signals within their immediate surroundings, including the ECM [72], [73], [75], [82].

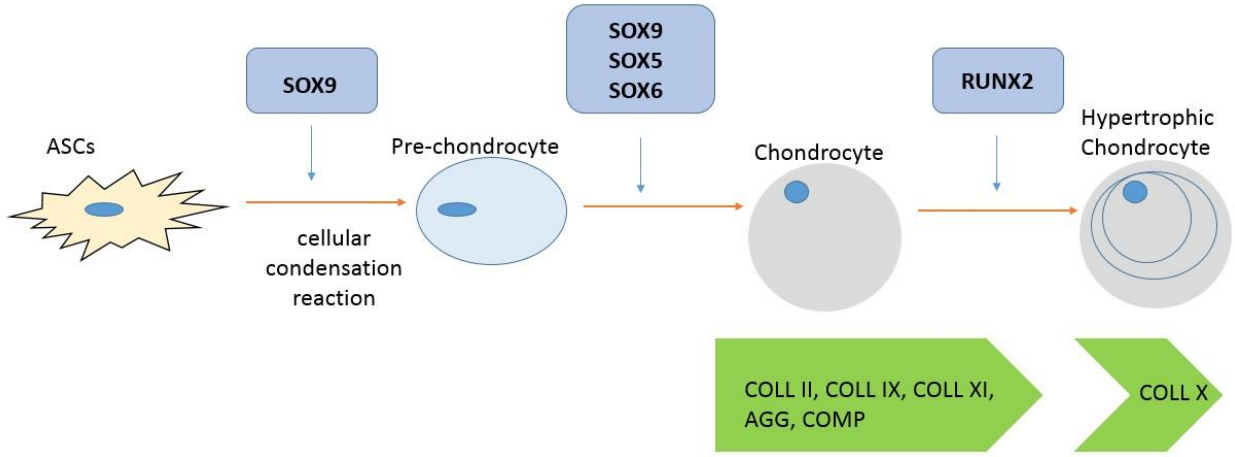

Figure 2.2 Transcriptional control of chondrogenesis.

2.2 The Extracellular Matrix (ECM)

Tissue loss acquired through disease or trauma poses problems where tissue regeneration is limited due to scar tissue formation and/or the loss of function in the afflicted area. This loss of function can impact the health and well-being of the patient. This raises the need for the development of cell-based therapies for connective tissue loss and is a major area of research in tissue engineering. In the field of tissue engineering, there is growing evidence to support the application of cell-based therapies to promote the regeneration of soft connective tissues in order to restore structure and function following tissue damage [29], [82]. Recent studies have suggested that the proliferation and differentiation of stem/stromal cells can be mediated through interactions with the ECM [6], [83]–[85]. Therefore, cell-based approaches that combine stem/stromal cell-based therapies with biomaterials have become a highly researched field of study.

Tissues within the body are comprised of cells and an extracellular matrix that is comprised of an intricate network of proteins and polysaccharides [86]. The macromolecules within the ECM are locally secreted by the cells and assembled and organized into tissue-specific structures [3], [5], [87]. There is a dynamic relationship that exists between the cells and the ECM. The ECM is active in regulating cellular behaviors and processes such as attachment, proliferation, and survival [88]. Likewise, as the cells within the niche respond to their environment, they secrete factors that induce alterations or remodeling of their surroundings [88], [89]. For example, cells

can secrete matrix metalloproteinases (MMPs) that enzymatically degrade the ECM to allow for cellular migration and release of ECM-bound molecules [90], [91]. This dynamic state highlights the interdependent relationship of cells and the ECM, supporting the rationale for incorporating ECM-based biomaterials into therapeutic strategies.

There are two main types of ECM, the basement membrane/basal lamina and connective tissue ECM [92], [93]. The basal lamina is a thin, highly bioactive structure that is often associated with various pathologies such as epidermolysis bullosa [94]. Connective tissue ECM is very important in cell regulation as it provides both structural and chemical cues to the cells [95]. The cells within a tissue help to create and maintain the integrity of the ECM by constant remodeling in response to stimuli [96].

The main macromolecules secreted by the cells within the matrix are: (1) fibrous proteins that include collagen and elastin, (2) glycosaminoglycans (GAGs), (3) proteoglycans, and (4) glycoproteins [97]. The specificity of the matrix is determined by the relative amounts of the different macromolecules within the matrix and the organization of those components to give tissue-specific structures and functions. Regulation of cellular behavior is achieved by interactions with cells and the surrounding matrix. Cell surface receptors called integrins bind cells to the ECM and can trigger a signaling cascade via the cytoskeleton in response to mechanical stimuli [86]. Functions such as cell shape, survival, proliferation, migration, and tissue cohesion may be determined, in part, by the ECM [89]. For this reason, it is important to have an understanding of the components of the cell-secreted ECM. This section will focus on the main types of macromolecules present in the ECM. The specific structure and composition of adipose tissue and cartilage ECM will be discussed in detail in Sections 2.4.1 and 2.5.1 respectively.

2.2.1.1 Fibrous Proteins

Fibroblasts synthesize collagens, GAGs, and glycoproteins and are responsible for a large majority of matrix production and remodeling in many tissues in the body [90]. In adipose tissue, adipocytes and pre-adipocytes are responsible for the majority of ECM production, however other cells types such as fibroblasts, vascular cells, and macrophages can be involved in matrix synthesis and modification [98]–[101]. In comparison, cartilage ECM is deposited mainly by

chondrocytes [102], [103]. Proteins embedded within the matrix act as sites for cell adhesion and signaling. Collagen plays a major role within the ECM and is one of the main components that make up these complex structures [104].

Collagen fibers impart structural integrity, organization, strength and resilience to the ECM and therefore play an important role in cell attachment, growth and differentiation through receptor mediated signaling [105]. Collagens are the most abundant fibrous proteins within the interstitial ECM, comprising 20-40% of total protein within the body. This family of structural and bioactive proteins functions to regulate cell adhesion, support cellular migration, and direct tissue development [106]. The right-handed triple helix comprised of three α-chain subunits is a defining characteristic of collagen (Figure 2.3a) [104]. These α-chain subunits are stabilized by hydrogen bonds and are each encoded by a unique gene. Within these long polymers, there are repeated amino acid sequences of (Gly-X-Y) where approximately 30% of the time X is proline and Y is hydroxyproline [104]. To date, 28 different types of collagen have been identified and can be classified as either (1) fibrillar, (2) fibril associated collagen with interrupted helices (FACIT), (3) short chain, (4) basement membrane, or (5) microfibrillar [105]. Each of these collagen types is associated with unique amino acid sequences and conformational structures that give individual functions, such as basement membrane collagens like collagen IV [97]. The α-chains within collagen IV lack a glycine residue in every third amino acid, allowing the chains to be covalently crosslinked and assembled into flexible sheet-like structures [105], [104].

The ability of tissues to deform from mechanical stimuli and recoil back to their original state can be attributed to the properties of the insoluble fibrous protein, elastin (Figure 2.3) [107]. Elastin is comprised of multiple tropoelastin monomers that are crosslinked by lysyl oxidase to form desmosine residues (Figure 2.3b) [108], [109]. Non polar amino acid residues comprise much of these monomers, which are rich in proline and lysine [110]. Elastin and collagen are often in close association, as the stretch of elastin is limited by the tight associations with collagen fibrils [106].

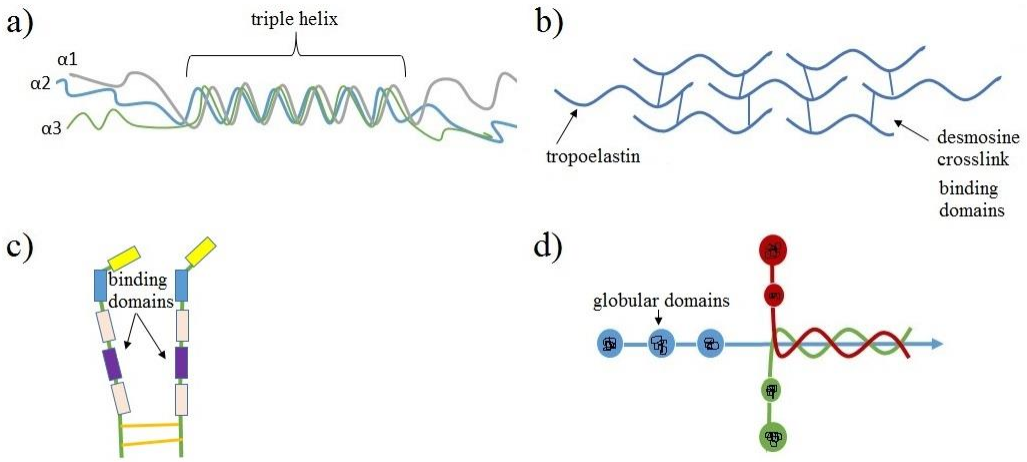

Figure 2.3 Representative images of (a) collagen, (b) elastin, (c) fibronectin, and (d) laminin. Images adapted from *Lange Histology and Cell Biology, 2010* [111].

2.2.1.2 Glycosaminoglycans

GAGs are comprised of repeating disaccharide units, where one of the two sugars is always an amino sugar (N-acetylglucosamine or N-acetylgalactosamine), and the other sugar is usually an uronic acid (glucuronic or iduronic). These sugars typically contain carboxyl or sulphate groups, and create an anionic charge [97]. GAGs may be further subcategorized into four main types, distinguished by the sugars, the linkage of those sugars, and the number and location of the sulphate groups. The main types of GAGs are: hyaluronan, chondroitin sulphate, heparan sulphate, keratin sulphate, dermatan sulphate and heparin, which may be found in varying amounts within different tissues [97], [106]. Hyaluronan is found in skin and load bearing joints, and chondroitin sulphate is most commonly found in ligaments, tendons, and cartilage [112]. GAGs aid in resisting compressive forces through their negative charges. The highly negative nature of GAGs attracts ions such as Na^+, allowing the matrix to become hydrated [106], [112]. The osmotic pressure created, such as that within the knee joint, allows the tissue to withstand large compressive forces [97], [113]. For example, hyaluronan is a type of GAG that is found in load-bearing joints that not only aids in resisting compressive forces, but also contributes to joint lubrication [97]. With the exception of hyaluronan, GAGs are covalently attached to proteins to create proteoglycans [97].

2.2.1.3 Proteoglycans

Proteoglycans consist of polysaccharide chains bound to a protein where at least one of the sugar side chains is a GAG, thus distinguishing them from glycoproteins [114]. Proteoglycans may contain more sugars by weight (up to 95%) when compared to glycoproteins, and may have many long unbranched GAG chains [115], [116]. Proteoglycans are remarkably diverse, possessing a variety of structures and functions. Aggrecan, for example, is one of the most important ECM proteins in cartilage that aids in the load distributing properties that are present in weight-bearing joints [114], [117]. Proteoglycans also promote the rapid diffusion of nutrients, metabolites and cytokines by aiding in the hydration of the ECM [118].

Proteoglycans also play a role in chemical signaling between cells. They attach to cell surfaces and bind to fibrous collagens or fibronectin on the ECM to act in a similar manner to cell-adhesion molecules [117]. As most proteoglycans are extracellular in nature, they have the ability to affect signaling cascades and influence intracellular events [119]. Not only do the molecules function as structural components of the ECM, but they have the ability to sequester and present many growth factors [117].

2.2.1.4 Glycoproteins

Glycoproteins contain many short, branched oligosaccharide chains and are 1-60% carbohydrate by weight [97]. For example, fibronectin is an important matrix glycoprotein that it is involved with cellular adhesion through integrins. In addition, fibronectin is thought to be involved in directing organization of the ECM [106]. The multi-domain structure of fibronectin plays an active role in ECM assembly by forming a bridge between cell surface receptors such as integrins, and collagens, proteoglycans, and other focal adhesion molecules (Figure 2.3c) [115]. Various binding domains present on the fibronectin backbone bind cells as well as molecules such as fibrin, heparin, and collagens [115]. As another example, laminin is the most abundant glycoprotein in the basement membrane and is able to bind various receptors on the cell surface to elicit cellular responses [93]. Laminins are proteins that form sheet-like networks within the basal lamina of the ECM (Figure 2.3d) [97]. They are known to contribute to the structure of the ECM and modulate cellular functions such as adhesion, migration, resistance to apoptosis, stability of phenotype, and differentiation [115].

2.2.2 Extracellular Matrix-Derived Scaffolding Materials

Cell types may vary widely from one type of tissue to another, but the ECM of various tissues contains the same base components. Knowing this, research has centralized around the idea of tissue-engineered biomaterials and scaffolds as a method for synthesizing tissue constructs [6], [82], [120], [121]. Scaffold design is a major area of research as the scaffold plays an important role in tissue repair. An ideal 3-D scaffold should mimic the properties of the native tissue but as this is extremely challenging to achieve, general guidelines for scaffolds include [122]:

(1) The scaffold must promote cell-biomaterial interactions, adhesion, and ECM deposition;

(2) The scaffold must permit transport of gases, nutrients, and regulatory factors as necessary for cell survival, proliferation, and differentiation;

(3) The scaffold must biodegrade at a controllable rate that approximates the rate of tissue regeneration under culture conditions of interest;

(4) The scaffold must not elicit a chronic inflammatory response or toxicity *in vivo.*

Through the use of rationally-designed scaffolds, tissue engineering strategies have demonstrated the ability to improve tissue repair *in vivo* [32]. It has been established that the ECM plays a vital role in the support and regulation of cellular behavior, providing the rationale for using ECM as a scaffold for tissue repair. In theory, ECM-based biomaterials can meet the above requirements, and may potentially provide cell-instructive guidance for tissue repair.

2.2.2.1 Tissue-Specific Scaffolds for Tissue Engineering

As it has been previously stated, all tissues have their own tissue-specific composition and structure that distinguishes them from other tissues within the body. It is this rationale that leads to the belief that tissue therapies should use materials to mimic the native ECM of that tissue as a tissue-specific approach is hypothesized to be superior to a non-specific approach [3]. Replicating the ECM of the native tissue for regenerative purposes would require an in-depth knowledge of the native ECM composition of a particular tissue. Even if replicating the components was trivial, structural arrangement would still pose a problem that hinders “bottom-up” strategies to recapitulate the native microenvironment. As an alternative approach, tissue

decellularization provides a straightforward method in which tissue samples are treated to remove cellular components and extract the tissue-specific ECM [82].

Decellularized tissues have been used in their intact form but the lack of a tunable geometry can pose a potential limitation for some applications [123]. For this reason, the ability to manipulate the various properties of the scaffolds is an area of significant research interest. The use of lyophilization and milling to create fine powders and/or enzymatic digestion creates the potential to manipulate the ECM into desired architectures and formats [1], [124], [125]. Hydrogels, foams, microcarriers, sheets, powders, and injectable pastes have been developed, with varying properties including stiffness, porosity, and architecture [1], [126]–[130].

The use of decellularized materials is a promising strategy in tissue engineering. Depending on processing, the decellularized tissue may provide a complex array of chemical and mechanical properties through the retention of ultrastructure and signaling proteins that is challenging to mimic through the use of synthesized biomaterials [18]. This natural, tissue-specific scaffold can then be used in its intact format or fabricated and manipulated into various forms depending on the target application [126], [131], [95], [132], [133].

2.3 Tissue Decellularization

Decellularization involves the mechanical, chemical, and/or enzymatic processing of tissues of the body to remove cellular components while ideally maintaining the structural and functional integrity of the proteins comprising the ECM. In turn, this will minimize the potential for immune rejection [82]. Advantages of these methods include that the scaffolds may retain the native ECM architecture, leading to similar biomechanical properties as seen *in vivo*. It is also possible that cell adhesion ligands may still be intact, thereby improving biochemical interactions [134]. This framework provides a structural lattice for cellular migration and tissue organization in a way that is difficult to replicate artificially. In the past, decellularization of both whole organs and tissues has been accomplished [82].

Tissue decellularization has been accomplished by perfusing solutions through existing vasculature of the tissue, as seen in lung or heart decellularization, or by agitation of tissue blocks or sections immersed in solutions [18], [19]. While perfusion decellularization may

provide the advantage of better retaining the original shape/structure of the tissues, this requires the vascular network of the tissue to be intact. Cannulation is also technically challenging and may lead to rupture of blood vessels. Not all tissues are extensively vascularized however, and so immersion and agitation in fluids may be required for proper decellularization. The most common practices involve the use of acids and bases, hypo- and hypertonic solutions, detergents, alcohols, enzymes, and mechanical stimulation for decellularization [135].

2.3.1 Chemical Decellularization Methods

Acids and bases are commonly used to either cause or catalyze degradation of biomolecules. Varying concentrations of acetic acid are commonly used to remove collagens, thereby reducing ECM strength without disrupting sulphated GAGs [135]. Dermal samples are often subjected to harsh bases to remove hair in early decellularization. However, treatment with bases is typically quite harsh and may eliminate growth factors and decrease ECM structural properties by cleaving collagen fibrils, which is a downside to using bases in decellularization practices [135].

Hypertonic and hypotonic solutions can be most effective when alternated through several cycles to rinse cell residue from within the tissues following cells lysis [82], [135]. The combination of the two creates osmotic stress, resulting in cell lysis. Hypotonic saline solutions are used to lyse cell membranes without causing major changes to the ECM, and can also help to dissociate DNA from proteins within the cells [82], [136].

Detergents are effective in removing cellular material by solubilizing cell membranes and dissociating DNA from proteins [135]. While detergents are effective at removing cellular DNA, they are also known for disrupting and dissociating proteins in the ECM, as evidenced by their use in proteomics [137], [138]. Detergents can be broadly separated into three categories: (1) ionic, (2) non-ionic, and (3) zwitterionic [135]. The most commonly used detergents in decellularization practices are Triton X-100, sodium dodecyl sulphate (SDS) and 3-[(3-cholaminopropyl)dimethylammonio]-1-propanesulfonate (CHAPS). Triton X-100 (non-ionic) can be effective at removing cellular residues from some dense tissues, like cartilage. Like Triton, SDS (anionic) is also widely used for decellularizing thick or dense tissues and has demonstrated superior removal of cellular DNA when compared to Triton X-100. However, SDS is also much more disruptive to the ECM and is known to remove important growth factors,

although the effects may be highly tissue dependent [135]. For this reason, sodium deoxycholates have been explored as an alternative where retention of ECM growth factors is important [139], [140]. CHAPS is a zwitterionic detergent that is most effective at removing cellular material from thin tissues such as lung, while better maintaining the ultrastructure of the ECM [82], [135]. Care must be taken to remove remaining detergents from tissues, as cytotoxicity is possible even in small concentrations [20], [135]. Removing anionic detergents such as SDS can prove to be more difficult than non-ionic detergents [135], [136].

Alcohols such as isopropanol, glycerol, and ethanol dehydrate tissues and lyse cells, making them useful reagents in decellularization protocols. Alcohols have been shown to remove intracellular lipids, making them very effective in adipose decellularization protocols [131]. Alcohols are also used as a fixative in histology practices and to precipitate out proteins so evaluating the effects of alcohols on the ECM is important in order to avoid excess damage to the ECM [141].

Other solvents such as acetone and tributyl phosphate (TBP) are also used as chemical agents for decellularization. Acetone can be used to remove lipids, but is also known to produce stiffer scaffolds by crosslinking the ECM [142]. TBP is an organic solvent that appears to be particularly good at removing cellular contents from dense tissues, such as tendon [136], [143]. While there have been various reports on the effects it has on the biochemical and mechanical properties of the ECM, TBP has shown potential as a decellularizing agent over either Triton X-100 or SDS in dense tissues for retention of mechanical properties while removing cellular contents [135], [139], [140].

Enzymes such as trypsin, lipase, collagenase, and various nucleases (RNases and DNases) have been used in various protocols to disrupt proteins, remove cell residues, and digest nucleic acids [131], [135]. Enzymes may be used to extract specific components, but use of enzymes alone is not sufficient for decellularization. Additionally, non-enzymatic agents such as chelators and serine protease inhibitors are used to aid in cell dissociation from the ECM and minimize ECM damage. Antibiotics and antimycotics are also used to minimize microbial contamination during decellularization and are often added to many decellularization solutions [135], [144].

2.3.2 Mechanical Decellularization Methods

In many cases, mechanical methods must be used in conjunction with chemical decellularization to achieve effective decellularization. Freeze/thaw cycles are often used to lyse cells within tissues [135]. Multiple freeze/thaw cycles may be used, with subsequent washes to remove cellular contents [135]. Some studies have shown that temperature disruption may also reduce adverse immune responses in vascular ECM scaffolds [145]. Cellular contents can also be removed through the forces associated with agitation in fluids, gravity separation of lipids through centrifugation, mechanical abrasion, and tissue compression [131], [95], [135]. These methods have proven particularly effective, and may cause less disruption to the ECM than chemical agents. In relatively acellular tissues, such as articular cartilage, freeze/thaw cycles and pulverizing the tissue through the use of cryogenic milling have been used as the main forms of decellularization [22], [144]. Limitations of these methods include that freeze/thaw cycles have limited efficacy on load bearing and mechanically robust tissues, and that pulverizing the tissue disrupts ECM architecture and has the potential to damage or eliminate important matrix proteins [133], [146].

2.3.3 Optimizing Methods for Tissue Decellularization

Tissues are comprised of both cellular material and ECM but the physical and chemical bonds vary in degrees of compactness [82]. The ECM must be adequately disrupted for the cellular materials to be removed, while minimizing the disruption to the tissue so as to maintain biomechanical and biochemical components of the ECM. The decellularization process must also leave the tissue free of added chemicals, such as detergents, if the ECM is to retain the native composition and limit toxicity *in vitro* or *in vivo* [6], [82]. Protease inhibitors may be used to preserve the ECM during the decellularization process [82], [147].

The specificity of the ECM for each tissue raises the need for unique decellularization practices with investigation into optimal methods for each tissue. Often, both chemical and mechanical methods are combined in decellularization protocols to deal with the varying requirements for tissue-specific decellularization [9], [82]. To test the effectiveness of decellularization, Masson's trichrome, DAPI nuclear staining, and DNA quantification, such as using the PicoGreen® dsDNA assay, are often used to measure cellular remnants. The use of ECM as a cell-instructive

therapy has been a large area of research in recent years. As such, recent studies have investigated the results of ASCs seeded on tissue-specific decellularized ECM scaffolds in the form of intact scaffolds, powders, hydrogels, foams, electrospun fibres and sheets for the purposes of tissue engineering [32], [38], [125], [148].

2.4 Adipose Tissue

Adipose tissue, derived from pre-adipocytes, is a loose connective tissue found throughout the body. Its primary role is to act as a regulator of energy metabolism by storing excess energy taken in through diet [149]. Energy is taken up by the adipose tissue in the form of free fatty acids (FFAs) with the aid of lipoprotein lipase (LPL). The FFAs are then converted to triglycerides (TG) within the adipocytes. When the body is in a state of caloric deficit, the stores of TG are liberated from the adipocytes by lipase in the form of FFAs and glycerol, to be oxidized and used as energy throughout the body [150], [151]. Due to its role in energy metabolism, adipose tissue is one of the few organs within the body that is capable of large changes in mass during adulthood. The typical adult female is approximately 30% fat by body weight, whereas males are typically around 20% body fat [151].

Adipose tissue is also an important regulator of body temperature and acts to insulate the body and protect internal organs against mechanical damage [100]. Adipose tissue immediately surrounding the internal organs is termed ‘visceral fat’, while the anatomical depot underlying the dermis is considered ‘subcutaneous fat’ [152]. Due to the fact that adipose tissue is highly vascularized and innervated, it is no surprise that it is also a highly active endocrine organ [153]. Adipose tissue is capable of not only responding to afferent signals, but secreting factors of its own. Adipokines such as leptin and adiponectin are secreted by this endocrine organ [149], [153]. Leptin, more commonly known as the ‘satiety signal’, is known for regulating energy metabolism by regulating appetite [153], [154]. Leptin is released by visceral adipose tissue to signal the body to stop eating. When energy stores are low, leptin levels are decreased and this allows the body to feel hunger, acting as a negative feedback loop to regulate food intake [154]. Adiponectin aids in the breakdown of FFAs and assists in controlling blood glucose levels [149], [100], [155]. Metabolism of sex steroids and glucocorticoids also takes place within adipose tissue, suggesting that hormones play an important role in the different distributions of body fat that are present between males and females [149], [153].

The type of adipose tissue found within adults is termed white adipose tissue. There is another form of adipose tissue found in infants and young children termed brown adipose tissue [156]. The primary role of brown adipose tissue is to regulate body temperature though heat production [156]. Brown fat uses a large amount of energy to produce heat in a method called non-shivering thermogenesis [154]. As people age, brown adipose tissue is replaced by white adipose tissue as other processes are able to take over temperature regulation [157]. Adipose tissue acquired for the purposes of cell isolations or decellularization procedures is white adipose tissue.

2.4.1 Adipose ECM Composition

As previously mentioned, the ECM is a complex mixture of proteins, proteoglycans, and glycoproteins secreted by cells. Adipose tissue ECM also contains a variety of adhesion proteins, growth factors and cytokines [100]. Integrins connect the ECM to the intracellular cytoskeleton, which can lead to signaling cascades in response to mechanical stimulation that can spread to neighboring cells [86]. Cellular cohesion is important in adipose tissue as it is a very dynamic environment. MMPs enzymatically digest structural components of the ECM to allow for cellular migration and release of ECM-bound molecules [91].

Collagen makes up a large component of adipose tissue ECM. Adipocytes are surrounded by a collagen IV-rich matrix that protects the lipid-filled cells from rupturing [101]. The ECM of adipose tissue is primarily comprised of collagens I, II, III, IV, XII XIV, XV, and XVII, as well as laminin, fibronectin, elastin, GAGs, and various proteoglycans. Among these, collagen I and IV are the most abundant [86]. Type I collagen is a fibril-forming collagen with a right-handed triple helix structure, with two of the α-chains being identical [105]. This is the most prevalent type of collagen in adipose tissue. As previously discussed, collagen IV is the most abundant structural component of basal lamina ECM. Collagen IV is a network-type collagen that does not form fibres, but rather it is arranged into a highly crosslinked mesh [105], [104], which surrounds the adipocytes, and contains laminins, nidogens, heparin sulphates, and other basement membrane components [101], [99].

Adipose tissue ECM also includes bioactive components such as GAGs and proteoglycans, as well as growth factors. GAGs help to keep the tissue hydrated and are often bound to proteins to form proteoglycans. The most common proteoglycans in adipose tissue are small leucine-rich

proteoglycans called decorin and biglycan [158], [159]. These proteoglycans can have major effects on lipid transport/absorption, along with other cellular behaviors [160], [161]. VEGFs are pro-angiogenic proteins that are present within the ECM, which are secreted by ASCs and associated with regulating the bioactivity of adipose tissue through signaling for the formation of new blood vessels [162].

2.4.2 Decellularized Adipose Tissue Scaffolds

Decellularized adipose tissue (DAT) has many applications as a scaffolding material. Building on the framework of Flynn *et al.*, recent studies have demonstrated the widespread applications of DAT scaffolds for cell-based therapies [131]. Microcarriers, porous bead foams, foams, and powders have demonstrated that DAT is adipo-inductive, suggesting that adipogenesis can be induced by the matrix alone [125], [163]. DAT scaffolds have also shown promise with regards to promoting angiogenesis *in vivo* [53].

Generally, adipose decellularization approaches require multiple freeze/thaw cycles in hypotonic buffers to aid in initial cell lysis, and open up membranes for additional exposure to elements of decellularization [82], [136], [164]. Enzymatic digestion is also common with the use of trypsin/EDTA, to disrupt cell-cell adhesion [82]. Subsequent enzymatic treatments with endo- and exo-nucleases such as DNase and RNase to remove any remaining nuclear material that may cause an immunogenic response are common [18]. The use of detergents to ensure sufficient removal of cellular material from the ECM and disrupt interactions between lipids and proteins is also a common procedure [82], [131]. Several methods for decellularizing adipose tissue involve the use of collagenase to break down the tissue, mechanical massaging, and rinses in various concentrations of SDS, sodium deoxycholate, or Triton X-100, and isopropanol, followed by lyophilization [165]. However, there is growing evidence to support the notion that detergents degrade the ECM and if residual detergent remains in the ECM, it can by cytotoxic to cells [166], [167]. Flynn *et al.* recognized the importance of developing a uniquely detergent free decellularization protocol and pioneered new methods to better preserve the native ECM [9].

The Flynn method of decellularization is a 5-day protocol that involves a combination of freeze/thaw cycles in hypotonic solutions followed by high salt rinses, enzymatic digestion in trypsin/EDTA and endonucleases, mechanical digestion, and washes in isopropanol [131]. An

optimized 3-day protocol was also developed that removes the requirement of enzymatic digestion with DNase and RNase, but continues the use of trypsin/EDTA. Studies to characterize the resulting ECM have been accomplished, demonstrating that collagen I and IV, laminin, fibronectin, VEGF-A and adiponectin are retained in the DAT [168].

In the intact form, DAT is an amorphous white substance that when lyophilized, has many applications. DAT can be used in the intact form, however, the ability to use it as a tunable ECM source to fabricate varied scaffold designs shows promise for widespread applications in tissue engineering [46], [131], [165]. Additionally, not many studies have investigated the use of tissue-specific ECM on adipogenic differentiation, highlighting the need for further research in this area.

2.5 Cartilage Tissue

Cartilage tissue can be classified into three categories: hyaline (articular) cartilage, elastic cartilage, and fibrocartilage [169]. Hyaline or articular cartilage is typically found on joint surfaces, in the bridge of the nose, and trachea. It contains a white, shiny elastic matrix of various proteoglycans such as aggrecan, chondroitin sulphate, keratin sulphate, biglycan, fibromodulin, and decorin [170], [171]. Elastic cartilage is found in parts of the larynx but is most commonly associated with the outer ear. It is more yellow in color and is contained within a perichondrium. The perichondrium surrounds the surface of most cartilage within the body and is comprised of a dense, irregular connective tissue [112], [154], [172]. Fibrocartilage is found in the intervertebral discs, pubic symphasis, and the menisci of the knee [173]. The exception to this is in the case of injury; the body may remodel damaged articular cartilage into fibrocartilage during scar formation [174]. Fibrocartilage is the toughest of the three cartilage types as it consists of dense bundles of collagen fibres and chondrocytes. This tissue does not contain a perichondrium [175].

It is generally accepted that cartilage has a limited capacity for self-repair due to minimal vascularity of cartilage tissues and low cell numbers [164]. In general, cartilage is considered to be both avascular and aneural, except for the small blood vessels and nerves found within the perichondrium [173], [175], [176]. This greatly increases the need for tissue regeneration

strategies, particularly for articular cartilages found within joints, and the fibrous cartilage of the meniscus. These are the two areas that see the most common tissue damage [177].

Articular cartilage functions to protect the surface of the joints and prevent high friction on the ends of endochondral bone and is the most abundant of the three types of cartilage found within the body [123]. Type IV collagen can be found within the pericellular region of cartilage, a distinct region just outside the cell membrane [92]. Cartilage is a dense matrix of collagen II, aggrecan, and GAGs that are produced by the resident chondrocytes, as outlined in detail in the next section. These chondrocytes are typically found within spaces called lacunae [172].

Chondrocytes have a rounded or ovoid morphology and are known for secreting large amounts of matrix, primarily collagen II and various GAGs [178], [179]. The large water and collagen contents combined with minimal vascularization give the 'white' appearance that is often associated with cartilage [112]. Fibronectin has also been found in the ECM of meniscal cartilage [175]. Healthy articular cartilage is approximately 70-85% water, allowing for appropriate joint lubrication at articular surfaces [173], [175]. Cartilage remodeling is a slow process that involves careful balance of MMPs and tissue inhibitors of metalloproteinases (TIMPs) [176]. Cartilage is a very dense tissue, with chondrocytes comprising only 5-10% of the tissue [170], [180]. For this reason, harvesting cells from cartilage yields low cell numbers and raises the need for cell-based therapies to aid in tissue regeneration [176].

2.5.1 Cartilage ECM Composition

Within cartilage, resident chondrocytes secrete the structural and bioactive molecules that comprise the ECM. As discussed above, 70-85% of whole cartilage tissue is comprised of water [123], the majority of which resides within the ECM [173]. Collagens, proteoglycans, glycoproteins, and small traces of elastin comprise 20-30% of the wet weight of articular cartilage. Of that 20-30% wet weight, approximately 16% is comprised of collagens [112]. Elastic cartilage is very similar in composition to articular cartilage, except that it contains an extensive network of elastic fibres [111], [115]. Various assays such as the dimethylmethylene blue (DMMB) assay or hydroxyproline assay are typically used to estimate GAG or collagen content respectively [181]–[184].

Collagen types I – VI, IX, X, and XI have been reported within the ECM of various cartilage tissues, with collagen type II being the most abundant [173], [185]. Cross-links form between collagen type II molecules to create collagen fibres. The intramolecular bonds formed create a strong collagen lattice that gives rise to the tensile properties of cartilage tissue [186]. Within the cartilage ECM, the high molecular weight proteoglycan aggrecan, which contains chondroitin 4-sulphate, chondroitin 6-sulphate, and keratin sulphate, interacts with hyaluronic acid to form large aggregates that impart resistance to compressive loads [111], [173]. In addition, chondronectin is an important glycoprotein, as it binds collagens, GAGs, and integrins in order to mediate chondrocyte adherence in the ECM [111]. Cartilage oligomatrix protein (COMP) is commonly used as a marker of cartilage turnover and encodes a non-collagenous protein that aids in cell binding and attachment [187].

Collagens within the ECM have unique fibre orientations that directly contribute to biomechanical functions and strength. When imaged microscopically, sheets of longitudinally arranged fibres can be seen in fibrocartilage [188]. The meniscus of the knee has three distinct layers, each arranged in different directions, which resist tensile stresses placed on the tissue [113], [175]. Fibrous and hyaline cartilage both have superficial and deep zones. Hyaline cartilage has an additional intermediate zone and a calcified zone [170], [189], [190]. The superficial zone protects deeper layers from biomechanical stress and the collagen fibres are tightly packed in parallel to the articular surface [170]. The intermediate zone is a transitional zone that contains slightly thicker collagen fibres and more spherical cells. The deep zone, representing 30% by volume, provides the greatest resistance to compressive forces and contains collagen fibres that are arranged perpendicular to the articular surface [113], [191]. Within the deep zone, chondrocytes are typically arranged in columns and show markers of ossification and hypertrophy as the cartilage is anchored to the bone by collagen fibrils [170].

2.5.2 Decellularized Cartilage Tissue (DCT) Scaffolds

Decellularized cartilage has shown promise in tissue engineering of articular cartilage, menisci, tracheal cartilage, and temporomandibular joint disc [130], [192]–[195]. Like adipose tissue, common cartilage decellularization protocols involve the use of multiple freeze/thaw cycles, rinses in hypotonic buffers, enzymatic digestion, and washes in detergents [21], [22], [143],

[147]. Commonly used detergents include Triton X-100, SDS, sodium deoxycholate, and TBP. Although cartilage tissue contains fewer cells than adipose tissue, the dense nature of the tissue poses a challenge when attempting to extract cellular material. Rinses must occur at higher agitation to perform proper extraction. Mechanical disruption of the tissue by increasing surface area is speculated to assist in the decellularization process [1], [127]. There is no standard decellularization method for cartilage tissue, highlighting the need for studies in this area. After decellularization, the resulting ECM can be used to create 3-D scaffolds or cell constructs.

To date, approaches have used the intact scaffold such as an ECM plug to promote chondrogenesis [143], [164]. DCT has also been examined in its powder form as a potentially injectable ECM source [1]. However, as discussed previously, cartilage is a very dense tissue and the nature of the ECM makes cell infiltration into decellularized cartilage ECM quite difficult. Various studies have suggested that the thickness of DCT plays an important role in cell infiltration, and is therefore a key consideration in cartilage tissue engineering [196]. Gong *et al.* attempted to combat this by developing a 'sandwich model' where twenty 10 μm- or 30 μm-thick articular cartilage sheets were stacked with a 5 μL suspension containing 100×10^6 cells/mL between each sheet and cultured for 16 weeks [130]. The sheets containing 10 μm slices demonstrated greater collagen staining when compared to the 30 μm sheets. In general, poor cellular infiltration in cartilage tissue engineering may be combated by using thin sections of DCT or DCT particles [197], [183], [56]. Some studies have also tried to incorporate *in vitro* cell-derived DCT with a polymer such as collagen or alginate as a template [198], [199]. In a study by Sutherland *et al.* both cell-derived DCT and devitalized DCT particles demonstrated upregulation of collagen II and down-regulation of collagen I, X, and RUNX2 [22]. Cell-derived DCT was composed of cell-secreted matrix from *in vitro* cultures, whereas devitalized particles were derived from native tissue. While several different methods of incorporating various types of DCT into 3-D scaffolds have been explored, the best method for fabricating cell-ECM constructs for chondrogenesis has yet to be determined [8], [20], [143], [147], [183], [200].

Challenges of using intact DCT scaffolds remain that rigorous decellularization protocols may lead to greater destruction of the ECM. Additionally, thinner DCT scaffolds may decrease the biomechanical resilience of the native tissue and may have some unknown effects on chondrogenesis [200]. There is a great need for studies in the area of cartilage tissue engineering,

as regeneration remains challenging due to the avascular and aneural nature of the tissue. If standard methods of cartilage decellularization could be established that minimize damage to the ECM, DCT scaffolds could represent a promising new cell instructive bioscaffolding platform for tissue regeneration and/or cell delivery.

Chapter 3

3 Methods

All chemical reagents for this project were purchased from Sigma-Aldrich Canada Ltd. (Oakville, Ontario) unless otherwise indicated.

3.1 Objective 1: Tissue Procurement and Decellularization

3.1.1 Adipose Tissue Procurement and Decellularization

Subcutaneous human adipose tissue was obtained with informed consent from patients undergoing routine breast reduction surgeries at the University Hospital in London, Ontario, with Research Ethics Board approval from Western University (HREB# 105426). The tissues were transported to the lab on ice in 10 mM Tris buffer (pH 8.0) within 2 hours of excision. Cauterized tissue was removed and the remaining adipose tissue was stored in 10 mM Tris buffer at -80°C. Adipose tissue decellularization was performed using established detergent-free methods [9]. A working volume of 100 mL was used for all processing steps and all decellularization solutions were supplemented with 1% (v/v) antibiotic-antimycotic (ABAM) (Gibco®, Invitrogen, Burlington, Ontario) and 0.27 mM phenylmethylsulfonyl fluoride (PMSF).

In brief, the adipose tissue was subjected to three freeze-thaw cycles in "solution A" comprised of 10 mM Tris buffer containing 5 mM ethylenediaminetetraacetic acid (EDTA) at pH 8.0. After the final thawing step, the samples were incubated for 2 hours in fresh solution A under agitation at 120 RPM and 37°C, and then centrifuged at 1500 x g for 30 minutes. The adipose tissue was incubated again in solution A for 2 hours, and then transferred into 0.25% trypsin/EDTA (Gibco®, Invitrogen, Burlington, Ontario) and incubated overnight under agitation at 120 RPM and 37°C (minimum 8 hours). The following morning, the tissue was incubated in 100% isopropanol for 3 hours under agitation at 120 RPM and 37°C to extract lipids. Subsequently, the tissue was compressed with stainless steel filters to enhance lipid separation, placed in 50 mL conical tubes containing fresh 100% isopropanol, and centrifuged at 1500 x g for 30 minutes. The isopropanol extraction, mechanical compression, and centrifugation steps were repeated once before the tissue was incubated in isopropanol under agitation at 120 RPM and 37°C overnight. The following morning, the sample was manually compressed to remove residual

lipid, and incubated in isopropanol for an additional 4 hours under agitation at 37°C. The decellularized adipose tissue (DAT) was then mechanically compressed once more and rehydrated in Sorenson's phosphate buffer (SPB) rinse solution, containing 8 g/L NaCl, 200 mg/L KCl, 1 g/L Na_2HPO_4, and 200 mg/L KH_2PO_4 (pH 8.0), through three 30 minute rinses at 37°C under agitation at 120 RPM. The DAT was then rinsed several times in deionized water (dH_2O) prepared with the Barnstead GenPure xCAD Plus system (Thermo Fisher Scientific, Ottawa, ON, Canada) prior to being lyophilized, as described in section 3.2.1.

3.1.2 Cartilage Tissue Procurement and Decellularization

Porcine ears were obtained from Mount Brydges Abattoir in Mount Brydges, Ontario for use as an auricular cartilage source. The tissues were transported to the lab on ice within one hour of sacrifice. To enhance the cartilage surface area in contact with the decellularization reagents, the dermis was removed with a scalpel and the cartilage was sectioned into small discs using a 5 mm biopsy punch. The tissue samples were placed in phosphate buffered saline (PBS) and rinsed three times under agitation at 200 RPM for 10 minutes at room temperature.

Adapting protocols from Xu *et al.* [136], two decellularization protocols were initially tested. A solution volume of 50 mL was used and all solutions were supplemented with 1% (v/v) ABAM and 0.27 mM PMSF. The two protocols were very similar, differing only in the buffer used during the incubation with deoxyribonuclease (DNase) and ribonuclease (RNase).

First, the tissue samples were subjected to three freeze-thaw cycles in 10 mM tris buffer (pH 8.0). Next, the samples were incubated in a high salt tris buffer containing 1.5 M KCl and 2% Triton X-100 at 37°C and 200 RPM for 48 hours, with solution changes twice per day. Subsequently, the tissue was rinsed three times in PBS for 30 minutes each at 37°C under agitation at 200 RPM. The cartilage was then rinsed in SPB rinse three times for 30 minutes under agitation at 200 RPM and 37°C. To test two different enzymatic digestion conditions, cartilage samples were then transferred into one of the following buffers supplemented with 12.5 mg RNase Type III A (from bovine pancreas) and 15,000 U DNase Type II (from bovine pancreas) for 72 hours under agitation at 200 RPM and 37°C:

Protocol 1A: a 10:1 ratio of PBS to 0.5% trypsin/EDTA

Protocol 1B: a 10:1 ratio of 50 mM tris buffer to 0.5% trypsin/EDTA

All solutions were replaced twice daily. The enzymatic digestion stage was followed by incubation in PBS at 37°C and 200 RPM for 24 hours, with the solutions replaced once. The samples were then incubated at 37°C and 200 RPM in 50 mM Tris buffer (pH 9.0) for 48 hours and finally, the decellularized cartilage was rinsed several times in PBS and dH_2O. The samples were then prepared for histological analysis, as described in section 3.1.3.

Based on the initial histological results, three different decellularization protocols were subsequently tested, based on the work of Woods and Grazter [201]. For all three protocols, the cartilage discs were first subjected to three freeze-thaw cycles in 10 mM tris buffer containing 5 mM EDTA (pH 8.0). The samples were then incubated in a high salt Tris buffer containing 1.5 M KCl and 1% Triton X-100 for 48 hours at 37°C and 200 RPM, with solution changes twice per day. The samples were then rinsed three times in SPB rinse for 30 minutes under agitation at 200 RPM and 37˚C. Next, the samples were enzymatically digested in Sorenson's phosphate buffer digest (SPB Digest) (55 mM Na_2HPO_4, 17 mM KH_2PO_4, 4.9 mM $MgSO_4 \cdot 7H_2O$) supplemented with 12.5 mg RNase Type III A (from bovine pancreas) and 15,000 U DNase Type II (from bovine pancreas) for 5 hours under agitation at 200 RPM and 37 ˚C. Following digestion, the tissues were then processed using one of three conditions to extract residual cellular debris under agitation at 200 RPM and 37 ˚C for 48 hours:

Protocol 2A: 1% tributyl phosphate (TBP) in 50 mM tris buffer

Protocol 2B: 2% Triton X-100 in 50 mM tris buffer

Protocol 2C: 1% sodium deoxycholate (SDC) in 50 mM tris buffer

The decellularized cartilage samples were then rinsed three times in PBS and three times in dH_2O for 30 minutes each, and incubated in 50 mM Tris buffer (pH 9.0) under agitation at 200 RPM and 37 ˚C for 48 hours. Finally, the decellularized cartilage was rinsed several times in PBS and dH_2O and prepared for histological analysis as described in Section 3.1.3.

Based on the results of the second decellularization trial, a slightly modified decellularization method was tested in which the concentration of Triton X-100 in the initial detergent extraction

phase was increased from 1% to 2%. This final cartilage decellularization protocol (Protocol 2D) is summarized in Table 3.1, and was used as the approach for all subsequent experiments.

Table 3.1: Final Cartilage Decellularization Protocol

Day 1	• 3 x 15 minute rinse in PBS • Three freeze/thaw cycles in 10 mM Tris buffer containing 5 mM EDTA (pH 8.0). Replace solutions after each thaw. • Incubate cartilage in 10 mM Tris buffer containing 5 mM EDTA for 24 hours, changing solutions twice
Days 2-3	• Incubate in high salt Tris buffer containing 1.5 M KCl + 2% Triton X-100 for 48 hours • Change solutions twice per day
Days 4 - 5	• 3 x 30 minutes in SPB rinse • Incubate in SPB digest + RNase + DNase for 5 hours • Incubate in 50 mM Tris buffer + 1% TBP for 48 hours • Replace solutions twice per day
Days 6 - 7	• 3 x 30 minutes in dH_20 • 3 x 30 minutes in PBS • 48 hour rinse in 50 mM Tris buffer (pH 9.0) • Replace solutions twice per day
Day 8	• 3 x 30 minutes in PBS • 3 x 30 minute rinse in 70% ethanol at room temperature under agitation • 3 x 15 minute rinse in sterile PBS at room temperature under agitation • Store in sterile PBS supplemented with ABAM and PMSF

*Note: All processing steps carried out under agitation at 200 RPM and 37˚C, and all solutions supplemented with 1% ABAM and 0.27 mM PMSF.

3.1.3 Histological Analysis

Processed cartilage samples from the different decellularization trials, along with native porcine auricular cartilage control samples, were fixed overnight in 4% paraformaldehyde (PFA). The samples were then rinsed in dH_2O, placed in 70% ethanol, and brought to Robarts Molecular Pathology Laboratory in London, Ontario, for processing. The samples were then embedded in paraffin and sectioned (7 μm sections) using a Leica RM2235 microtome (Leica Biosystems, Concord, ON, Canada). The sections were deparaffinzed by incubating the slides in xylene for

10 minutes (2X) and then rehydrated in an ethanol series (100% (2X), 95%, 90%, 80% 70% EtOH in dH_2O for 5 minutes each), followed by dH_2O. Masson's trichrome staining, 0.1 % safranin O/fast green staining, and DAPI staining using fluoroshield mounting medium (ab104139, Abcam) were performed to characterize the tissues.

3.2 Objective 2: Milling and Characterization of ECM Particles

Breast adipose tissue from three human donors (N=3) was decellularized and pooled to generate a DAT stock that was used for all subsequent studies. Similarly, porcine auricular cartilage from three pigs (N=3) was decellularized and combined to yield a DCT stock. This approach was undertaken to eliminate batch-to-batch variability in the ECM sources when assessing the effects of the decellularized ECM on ASC differentiation.

3.2.1 Lyophilization and Cryogenic Milling

The DAT and DCT samples were rinsed in dH_2O and frozen at -80°C for 8 hours in 50 mL conical tubes covered in perforated aluminum foil. The tubes were then transferred on dry ice to the Labconco Freezone 4.5 lyophilizer (Labconco, Kansas City, MO, United States) and dried for 48 hours. After lyophilization, the pooled DAT or DCT was finely minced with scissors, and transferred into a Retsch 25 mL cryo-milling grinding jar. Two thirds of the milling jar was filled with minced ECM, and two 10 mm stainless steel milling balls were placed in the milling jar. The cap was tightened, and the jar was immersed in liquid nitrogen for 3 minutes. The tissues were then milled for 3 minutes at a frequency of 30 Hz using the Retsch Mixer Mill MM 400 milling system. The cycle of immersion in liquid nitrogen and milling were repeated at least once to obtain a fine powder; during humid weather, additional cycles were required. The particles were then separated based on size using stainless steel sieves (W.S. Tyler, St. Catharines, ON, Canada) of decreasing mesh sizes in the following order: 300 µm, 250 µm, 125 µm, and 45 µm.

3.2.2 Particle Size Analysis

Particle size analysis was completed for both the DAT and DCT particles collected between the 45 µm and 125 µm sieves using a Malvern Mastersizer 2000 (Malvern Instruments Ltd., Worcestershire, United Kingdom). Approximately 1 g of dehydrated ECM particles was placed in 500 mL of dH_2O with 5 drops of Triton X-100 detergent to disrupt surface tension and reduce

aggregation of the ECM particles. The samples were then analyzed following the manufacturer's instructions. For each pooled ECM source, 3 technical replicates (n=3) were analyzed. The data was plotted as the mean ± standard deviation (SD). A Kolmogorov–Smirnov test with $p < 0.05$ was performed using GraphPad Prism 6 (GraphPad Software, San Diego, CA) to assess whether the particle size distributions for the DAT and DCT particles were statistically equivalent.

3.2.3 Scanning Electron Microscopy

Scanning election microscopy (SEM) was performed on both the DAT and DCT particles collected between the 45 µm and 125 µm sieves to visualize the ECM ultrastructure after milling and sieving. Lyophilized, cryo-milled DAT and DCT particles were mounted onto stubs with conductive carbon tape and coated with 10 nm of osmium before visualization with a LEO 1530 scanning electron microscope. The samples were imaged at 700 and 1000 times magnification with an accelerating voltage of 1.00 kV and a working distance of 6 mm.

3.3 Objective 3: In vitro cell culture studies

3.3.1 ASC Isolation

Subcutaneous human adipose tissue was obtained with informed consent from patients undergoing routine breast reduction surgeries at the University Hospital in London, Ontario (HREB# 105426). Adipose tissue samples were transferred to the lab on ice in PBS supplemented with 20 mg/mL bovine serum albumin (BSA), and processed within 2 hours of tissue extraction. Adipose-derived stem/stromal cell (ASC) isolation was performed using established protocols [202]. Cauterized tissue was removed and the adipose tissue was finely minced using scissors. The minced adipose was then digested for 45 minutes with 2 mg/mL collagenase type I (Worthington Biochemical Corporation, Lakewood, NJ, United States) in sterile Kreb's Ringer bicarbonate buffer supplemented with 3 mM glucose, 25 mM HEPES and 20 mg/mL BSA at 37°C under agitation at 100 RPM. The digested sample was filtered through a 250 µm stainless steel filter into a 50 mL conical tube, and the mature adipocyte layer was removed by aspiration following gravity separation. An equal volume of complete medium comprised of DMEM/Ham's F12 supplemented with 10% fetal bovine serum (FBS) (Gibco®, Invitrogen, Burlington, Ontario) and 100 U/mL of penicillin with 0.1 mg/mL streptomycin (pen-strep) (Gibco®, Invitrogen, Burlington, Ontario) was added to the sample, which was then

centrifuged at 1200 x g for 5 minutes. The supernatant was discarded and the pellet was resuspended in an erythrocyte lysing buffer (0.154 M ammonium chloride, 10 mM potassium bicarbonate, and 0.1 M EDTA in sterile dH_2O) for 10 minutes at room temperature under gentle agitation. The sample was then centrifuged for 5 minutes at 1200 x g, resuspended in complete media, filtered through a 100 μm filter, and re-centrifuged. The cell pellet was then resuspended in complete medium and plated on T-75 culture flasks at a density of 30,000 cells/cm^2. The media was exchanged every 2-3 days. When the cells were at approximately 80% confluence, they were passaged 1:4 using 0.25% tryspin-EDTA and re-plated in new T-75 culture flasks.

3.3.2 ASC Immunophenotype

The immunophenotype of passage 2 ASCs was analyzed using a Guava® 8HT flow cytometer (EMD Millipore Corporation, Darmstadt, Germany) following published protocols [152]. Single marker staining was performed (n=3 technical replicates, N=3 cell donors) with monoclonal, fluorochrome-conjugated antibodies (eBioscience, San Diego, CA). The positive markers assessed were CD90, CD44, CD29, CD73, and CD105. CD34 was also analyzed, which is reported to be expressed in early passage ASCs, but declines with passaging [54]. CD146 was also analyzed as a marker of pericyte-like cells [54]. The negative markers assessed were CD31 (endothelial) and CD45 (hematopoietic). All trials included controls with unlabeled cells.

3.3.3 Validation of Cell Aggregate Culture Methods

The initial method used to fabricate 3-D cell aggregates involved transferring 1 mL of ASC suspension at a concentration of $1x10^6$ cells/mL into an uncapped 1.5 mL microcentrifuge tube positioned inside of a 15 mL vented-cap conical tube, which was then centrifuged at 300 x g for 10 minutes and then maintained in culture for 48 hours [38]. Based on histological analysis using Masson's trichrome staining (Figure 3.1), this approach generated non-spherical cell aggregates that were easily disrupted. As such, an alternate approach was adopted based on the methods of Gimble *et al.* [10]. In this strategy, 1 mL of ASC suspension at a lower concentration of $2.5x10^5$ cells/mL was transferred directly into a 15 mL vented-cap conical tube, centrifuged at 300 x g for 5 minutes and cultured for 48 hours to yield robust spherical cell aggregates (Figure 3.1).

a) Culture in 1.5 mL Microcentrifuge Tube **b) Culture in 15 mL Conical Tube**

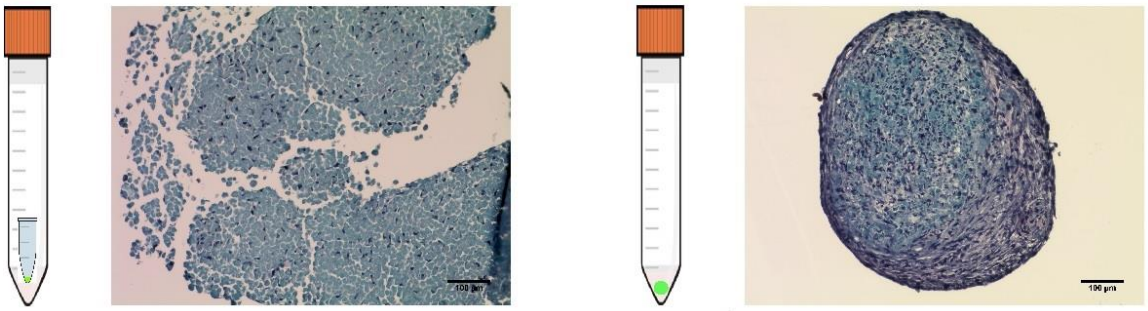

Figure 3.1 Methods used for generating cell aggregates. (a) 1 million cells cultured in 1.5 mL microcentrifuge tubes (b) $2.5x10^5$ cells cultured in 15 mL conicals. (scale bars=100 μm).

3.3.4 Validation of Chondrogenic Medium Formulation

A pilot study was performed on ASC aggregates generated using the refined approach described in the previous section to verify that the cells cultured in this configuration could be successfully induced to express chondrogenic markers when maintained in chondrogenic differentiation medium for 28 days. The chondrogenic medium formulation was selected based on the work of Neupane *et al.* [203], [12] and was comprised of DMEM:Ham's F12 supplemented with 10% FBS, 1% pen-strep, 50 μM ascorbate-2-phosphate, 6.25 μg/mL insulin, 100 nM dexamethasone, and 10 ng/mL TGF-β1 (R&D Systems, CAT#: 100-B-001). For comparison, a second medium formulation reported by Guilak *et al.* [71] was also tested, which was comprised of DMEM:Ham's F12 supplemented with 10% FBS, 1% pen-strep, 50 μM ascorbate-2-phosphate, 1% ITS+premix supplement (Collaborative Research, CAT#: 40352), 100 nM dexamethasone, and 10 ng/mL TGF-β3 (R&D Systems, CAT#: 243-B3-010). Non-induced control aggregates were maintained in complete medium for the duration of the 28-day culture period. To assess chondrogenic differentiation, cell aggregate samples (n=3) were embedded in OCT and cryo-sectioned for immunohistochemical (IHC) analysis of collagen II and collagen I expression, described in detail below. Additional samples (n=3) were fixed in 4% PFA, paraffin-embedded and sectioned for histological analysis of GAG accumulation by safranin O staining. Native porcine cartilage was included as a positive control for the IHC and histological analyses.

For IHC analysis, samples were cryo-sectioned (7 μm) with a Leica RM2235 microtome (Leica Biosystems, Concord, ON, Canada) and collected onto Superfrost® Plus microscope slides

(Thermo Fisher Scientific, Ottawa, ON, Canada). The sections were warmed at 60˚C for 40 minutes before being transferred to the -20˚C freezer for storage. Immediately prior to staining, the slides were warmed to room temperature and subjected to antigen retrieval using DAKO citrate buffer (DAKO, Mississauga, ON, Canada) at 95˚C for 30 minutes, then allowed to cool to room temperature. The slides were subsequently rinsed in Tris buffered saline (TBS) containing 0.025% Triton X-100, and blocked with 10% goat serum for 1 hour to control for non-specific binding of the primary antibody. The samples were then incubated in rabbit anti-collagen II antibody (ab34712, Abcam) diluted to 1:500 in TBS supplemented with 1% BSA solution overnight at 4˚C, or mouse anti-collagen I antibody (ab90395, Abcam) diluted to 1:500 in TBS supplemented with 1% BSA for 1 hour at room temperature. Following this, the sections were rinsed with TBS and incubated in Dylight® 650 goat anti-mouse IgG H&L (ab96882, Abcam) for collagen I and Dylight® 650 goat anti-rabbit IgG H&L (ab96902, Abcam) for collagen II, each diluted to 1:500 in TBS supplemented with 1% BSA for one hour at room temperature. The sections were rinsed, and mounted with mounting medium containing DAPI before imaging with an Evos FL cell imaging system (Thermo Fisher Scientific, Ottawa, ON, Canada).

To assess GAG accumulation within the pellets by safranin O staining, the paraffin-embedded and sectioned samples were collected onto Superfrost® Plus microscope slides and deparaffinized with xylene, followed by rehydration in an ethanol series, and finally to dH_20. The sections were then stained with 0.1% safranin O for 5 minutes before being dehydrated with 95% ethanol for 2 minutes, 100% ethanol for 2 minutes, and cleared in xylene. The slides were mounted using Permount™ mounting medium (Fisher Scientific, Ottawa, ON, Canada) for imaging with an Evos XL Core imaging system (Fisher Scientific, Ottawa, ON, Canada).

3.3.5 ASC + ECM Aggregate Formation

Using the milled DAT or DCT particles collected between the 45 µm and 125 µm sieves, ASC+ECM aggregates comprised of $2.5x10^5$ ASCs and 0.075 mg ECM per aggregate were fabricated. To fabricate the aggregates, milled DAT or DCT was placed under UV light for 30 minutes before being weighed using a Sartorius CPA225D scale (Sartorius, Bradford, MA, United States). The milled ECM particles were rehydrated in complete medium at a concentration of 0.075 mg/mL. 100 µL of the medium containing ECM was transferred into a 15 mL vented-cap conical tube containing $2.5x10^5$ passage 2 ASCs suspended in 900 µL of

complete medium. The samples were centrifuged at 300 x g for 5 minutes and cultured for 48 hours. Masson's trichrome staining was performed to confirm that the ECM particles were successfully integrated into the cell aggregates. To further verify ECM incorporation, a pilot study was performed in which the DAT and DCT particles were pre-labeled with an amine-reactive Alexa fluor® 350 succinimidyl ester (Molecular Probes, Burlington, Ontario) prior to aggregate formation using published methods [127]. At 48 hours, the aggregates were cryo-sectioned and visualized by fluorescence microscopy, with SYTOX® orange nuclear staining.

3.3.6 *In vitro* Culture Study Design

Detailed *in vitro* cell culture studies were conducted to explore the effects of the tissue-specific ECM particles on mediating the lineage-specific differentiation of the ASCs in the 3-D ASC+ECM aggregate cultures. Table 3.2 summarizes the experimental groups and culture conditions investigated for the adipogenic and chondrogenic lineages. All experiments were repeated with passage 2 ASCs sourced from 3 different donors (N=3), using the pooled DAT and DCT stocks that were previously characterized.

Table 3.2: Summary of Differentiation Studies (N=3 cell donors for each lineage).

Culture Groups	**Adipogenic Differentiation Time point = 14 days**	**Chondrogenic Differentiation Time point = 28 days**
DAT+ASCs	Complete Medium	Complete Medium
	Adipogenic Medium	Chondrogenic Medium
DCT+ASCs	Complete Medium	Complete Medium
	Adipogenic Medium	Chondrogenic Medium
ASCs Only (Control)	Complete Medium	Complete Medium
	Adipogenic Medium	Chondrogenic Medium

For the cell culture studies, ECM+ASC and ASC-alone aggregate samples were cultured for 14 or 28 days in either adipogenic or chondrogenic differentiation medium using the formulations summarized in Table 3.3. To assess whether the ECM particles or 3-D culture configuration had any inductive effects on ASC differentiation, non-induced control samples maintained in

complete medium were included for all assays, with the exception of the quantitative reverse-transcriptase-polymerase chain reaction (RT-qPCR) studies.

Table 3.3 Differentiation Medium Formulations *= only for first 72 hours

Complete Media	**Adipogenic Medium** [9]	**Chondrogenic Medium** [12]
DMEM/Ham's F12 10% FBS 1% pen-strep	DMEM:Ham's F12 1% pen-strep 33 μM biotin 17 μM pantothenate 10 μg/mL transferrin 100 nM cortisol 66 nM insulin 1 nM triiodothryonine 0.25 mM isobutylmethylxanthine * 1 μg/mL troglitazone *	DMEM:Ham's F12 10% FBS 1% pen-strep 50 μM ascorbic acid 6.25 μg/mL insulin 100 nM dexamethasone 10 ng/mL TGF-β1 (R&D Systems, CAT#: 100-B-001)

3.3.7 Adipogenic Differentiation Study

Adipogenic differentiation was assessed at 14 days by quantitative measurement of glycerol-3-phosphate dehydrogenase (GPDH) enzyme activity, IHC analysis to determine the presence of a hormonally regulated intracellular lipid protein (perilipin), and RT-qPCR analysis of adipogenic gene expression. As previously discussed, all experiments were repeated with cells isolated from 3 different cell donors (N=3).

3.3.7.1 GPDH Enzyme Activity

GPDH is an enzyme that is upregulated during triglyceride synthesis and its activity can be used as a quantitative measure of adipogenic differentiation. Following published protocols [152], intracellular GPDH activity was measured using a spectrophotometric assay with a commercially available kit (Kamiya Biomedical Company, Tukwila, WA, United States) with normalization to the total cytosolic protein levels measured using the Bio-Rad protein assay with an albumin standard (Bio-Rad Laboratories Inc., Hercules, CA). GPDH activity was measured in triplicate samples for each cell donor (n=3, N=3) at an absorbance of 450 nm using a CLARIOstar®

spectrophotometer (BMG Labtech, Ortenberg, Germany). The activity required to oxidize 1 µM of NADH in 1 minute was defined as one unit of GPDH activity.

3.3.7.2 Immunohistochemical Analysis of Perilipin Expression

ECM+ASC and ASC-alone aggregates (n=3, N=3), were fixed in 4% PFA overnight, and processed at Robart's Molecular Pathology laboratory. The fixed tissues were embedded in paraffin, sectioned (7 µm thickness) onto Superfrost® Plus microscope slides (Fisher Scientific, Ottawa, ON, Canada), and allowed to set overnight at room temperature before use. The sections were deparaffinized in 100% xylene, followed by rehydration in an ethanol series, and finally dH_2O. The slides were subjected to antigen retrieval using DAKO citrate buffer, rinsed in TBS containing 0.025% Triton X-100, and blocked with 10% goat serum for 1 hour. The samples were then incubated in rabbit polyclonal anti-perilipin (ab3526, Abcam) diluted to 1:500 in TBS with 1% BSA solution overnight. Following this, the sections were rinsed with TBS and incubated in Dylight® 650 fluorescent goat anti-rabbit IgG secondary antibody (ab96902, Abcam) diluted to 1 µg/mL in TBS with 1% BSA for one hour at room temperature. The sections were rinsed, and mounted with DAPI mounting medium for imaging with an Evos FL cell imaging system (Thermo Fisher Scientific, Ottawa, ON, Canada).

3.3.7.3 RT-qPCR Analysis of Adipogenic Gene Expression

RT-qPCR analysis was performed using TaqMan® Gene Expression Assays to assess the expression of the adipogenic markers PPARγ (Hs00234592_m1), lipoprotein lipase (LPL) (Hs00173452_m1) and adiponectin (Hs00905917_m1) in the induced samples cultured in adipogenic differentiation medium for 14 days, with IP08 (Hs00183533_m1) and GAPDH (Hs02758991_g1) included as the housekeeping genes (based on previous validation in the Flynn lab). To isolate sufficient RNA, 4 aggregates for each experimental group were pooled together.

For RNA extraction, the pooled aggregate samples were immersed in 1 mL Trizol® Reagent (Invitrogen, Burlington, Canada), sonicated, and incubated at room temperature for 5 minutes. 200 µL of chloroform (Sigma C7559) was added to the samples, which were vortexed and incubated at room temperature for 5 minutes, and then centrifuged at 12,000 x g for 15 minutes at 4°C. The upper aqueous phase was transferred to a new 1.5 mL tube, and an equal volume of chloroform:isoamyl alcohol (49:1) (Sigma C0549) was added to each tube. The samples were

vortexed and then centrifuged at 12,000 x g for 15 minutes at 4°C. Once more, the upper aqueous layer was transferred to a new 1.5 mL tube and an equal volume of 100% isopropanol was added. The samples were then inverted to mix, incubated at room temperature for 10 minutes, and centrifuged at 12,000 x g for 10 minutes at 4°C. The supernatant was removed and the RNA pellet was resuspended in 22 µL of molecular grade water. The concentration and purity of the RNA was measured using a NanoDrop 1000 spectrophotometer (Thermo Fisher Scientific, Ottawa, ON, Canada).

All samples were subjected to DNase digestion using a TURBO DNA-free kit™ (abmion AM1907, Life Technologies, Carlsbad, California) following the manufacturer's instructions. First strand cDNA synthesis was then performed using the iScript™ kit (Bio-Rad 170-8840, Mississauga, ON, Canada) following manufacturer protocols with 250 ng of input RNA. Reverse transcription was carried out in a total reaction volume of 20 µL, consisting of iScript supermix or no-RT control, and 16 µL of RNA diluted in nuclease-free water. The reaction was carried out in Bio-Rad C1000 Touch Thermal Cycler (Bio-Rad Laboratories Inc., Hercules, California) with the following conditions: 5 minutes at 25˚C, 30 minutes at 42˚C, 5 minutes at 85˚C, and then cooling to 4˚C.

For the PCR amplification, 5 µL of TaqMan® Universal Master Mix II, 3.5 µL of nuclease-free, molecular grade water, and 0.5 µL of primer were combined in each well. 1 µL of cDNA was added to each well and the reaction was carried out using a CFX384 Touch™ Real-Time PCR Detection System (Bio-Rad Laboratories Inc., Hercules, California). The conditions were as follows: 2 minutes at 50˚C, 20 s at 95˚C, and then 40 cycles of 3 s at 95˚C (denature) and 30 s at 60˚C (anneal/extend). No reverse transcriptase and no template controls were included on every plate, and all samples were analyzed in triplicate. The results were analyzed using the ΔΔCt method [204], with the ASC-alone induced group as the calibrator.

3.3.8 Chondrogenic Differentiation Study

Chondrogenic differentiation was assessed at 28 days by IHC of chondrogenic extracellular matrix proteins (collagen I and collagen II), histological analysis of GAG accumulation (safranin o), and RT-qPCR analysis of chondrogenic gene expression. As previously discussed, experiments were repeated with cells isolated from 3 different cell donors (N=3).

3.3.8.1 Immunohistochemical Analysis of Collagen II/I Expression

IHC analysis was performed to qualitatively assess the levels of collagen II and collagen I expression in the ASC+ECM and ASC-alone aggregates (n=3, N=3), following the methods described in section 3.3.4.

3.3.8.2 Histological Analysis of GAG Accumulation

Safranin O staining was performed to qualitatively assess GAG accumulation in the ASC+ECM and ASC-alone aggregates (n=2, N=3), following the methods described in section 3.3.4.

3.3.8.3 RT-qPCR Analysis of Chondrogenic Gene Expression

RT-qPCR analysis was performed to assess the expression of the chondrogenic markers SOX9 (Hs0100343_g1), cartilage oligomeric matrix protein (COMP) (Hs00164359_m1), and aggrecan (Hs00153936_m1) in the induced samples cultured in chondrogenic differentiation medium for 28 days, with UBC (Hs01871556_s1) and RPL13A (Hs04194366_g1) included as the housekeeping genes (based on previous validation in the Flynn lab). To isolate sufficient RNA, 4 aggregates for each experimental group were pooled together. The samples were analyzed following the methods for RNA isolation, cDNA synthesis and PCR amplification described in section 3.3.7.4.

3.3.8.4 Statistical Analysis

Statistical analyses were performed using GraphPad Prism 6 Software by one-way or two-way ANOVA with Tukey's post-hoc comparison of means. All data values are expressed as a mean ± standard deviation and significant differences considered when $p < 0.05$.

Chapter 4

4 Results and Discussion

4.1 Objective 1: Tissue Procurement and Decellularization

4.1.1 Adipose Tissue Decellularization

Adipose tissue was decellularized using established protocols in the Flynn lab [9]. During processing, the adipose tissue gradually transitioned into a white, highly-hydrated matrix (Figure 4.1), consistent with previous findings demonstrating effective cell and lipid extraction [9].

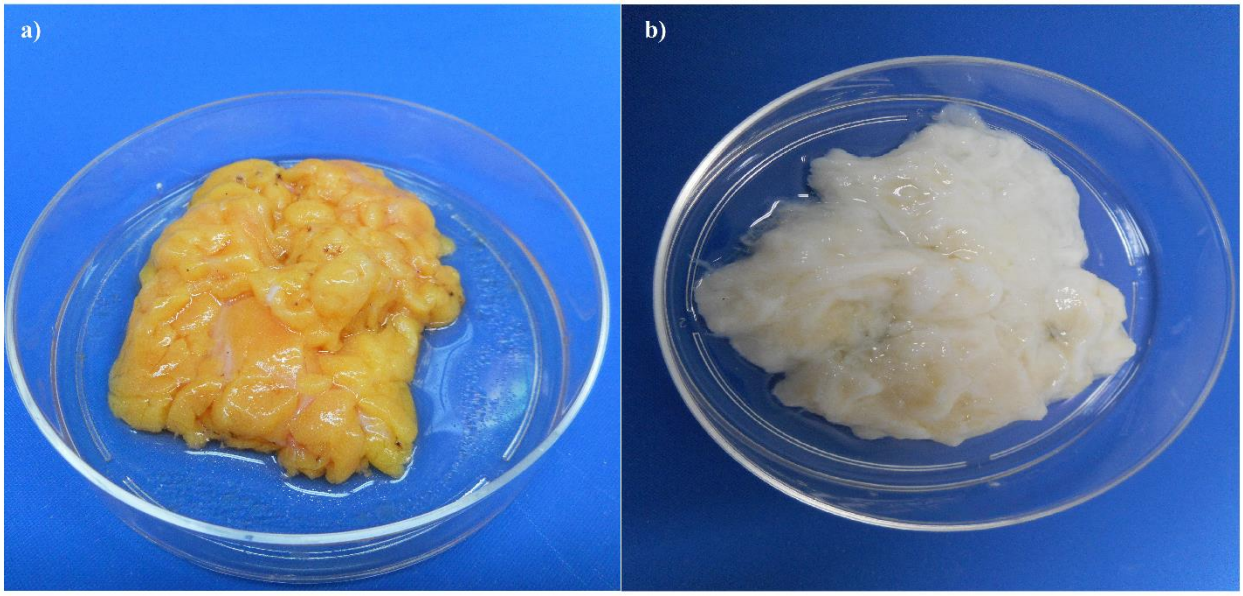

Figure 4.1 Macroscopic image of human adipose tissue (a) before and (b) after decellularization.

4.1.2 Cartilage Tissue Decellularization

Masson's trichrome and safranin O/fast green staining was performed to compare the tissue structure and composition (Figure 4.2) following decellularization with two initial cartilage decellularization protocols adapted from Xu *et al.* [136]. DAPI staining was used to identify the presence of residual nuclei in the processed tissues. These protocols, which involved 72 hours enzymatic extraction with trypsin, DNase and RNase, demonstrated notable changes in the ECM composition, including qualitatively reduced GAG content, shown in red in the safranin O/fast green stained sections, with no GAG staining visualized in the samples treated with Protocol 1 B.

Further, the decellularization processes also appeared to negatively impact the tissue integrity as the samples were easily torn during sectioning, particularly for those treated with Protocol 1B. DAPI staining revealed the presence of a large number of residual nuclei in the tissues processed with Protocol 1A, while no positive nuclear staining was visualized in the samples treated with Protocol 1B. As the goal was to identify a decellularization protocol that effectively extracted cellular components while causing minimal changes to the ECM structure and composition, these findings prompted further investigation into alternative decellularization protocols.

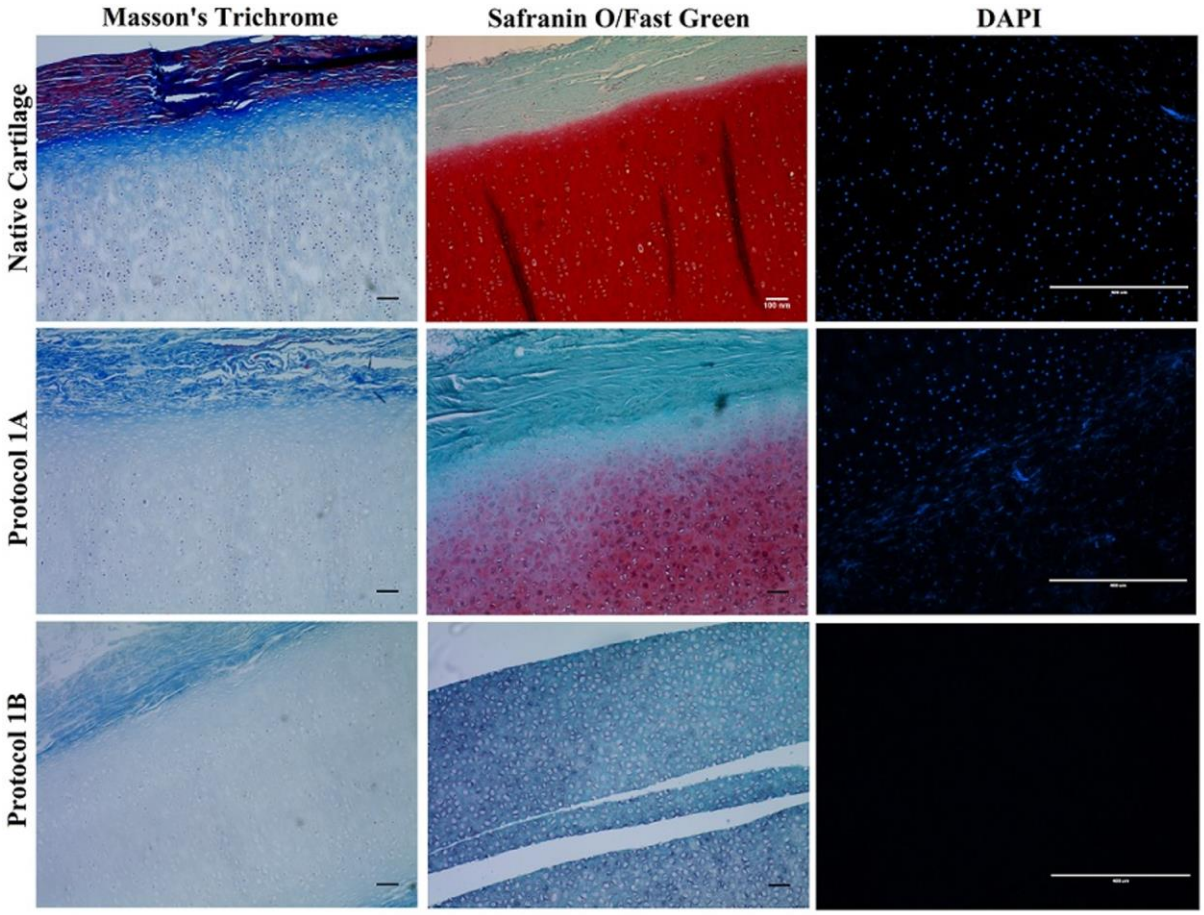

Figure 4.2 Representative histological results of the initial cartilage decellularization protocols in comparison to native cartilage controls. The first column represents Masson's trichrome stains where the cell nuclei appear black and collagen is blue. The second column represents safranin O/fast green staining. GAGs appear red and collagen appears blue/green. In the third column, DAPI staining shows cell nuclei in blue. Scale bars represent 100 μm**.**

Three alternate decellularization protocols based on the work of Woods and Grazter [201] were tested using TBP or detergent (Figure 4.3), along with a shorter 5-hour DNase and RNase treatment. From the Masson's trichrome, safranin O, and DAPI staining, Protocol 2A, comprised of 1% Triton X-100 treatment followed by 1% TBP extraction (Triton X-100/TBP), showed the most promising results. The samples processed using this protocol had qualitatively enhanced GAG staining in comparison to Protocols 1A, 1B, 2B (Triton X-100/Triton X-100) and 2C (Triton X-100/SDC) and reduced nuclei staining as compared to Protocols 1A and 2B. Relative to the initial trials, the processed tissues were more robust and easier to handle. Following the results of the second decellularization trial, a slightly modified approach (Protocol 2D) was tested using 2% Triton X-100 and 1% TBP to establish if the number of nuclei could be reduced further by increasing the detergent concentration in the early stages of processing. Masson's trichrome and DAPI staining revealed no detectable cell nuclei in the samples processed with this revised protocol, and demonstrated qualitatively better preservation of the collagen and GAG content in the ECM relative to the other protocols, with staining patterns similar to native cartilage. Therefore, based on histological analysis, the decellularization approach in Protocol 2D was chosen for all future experiments.

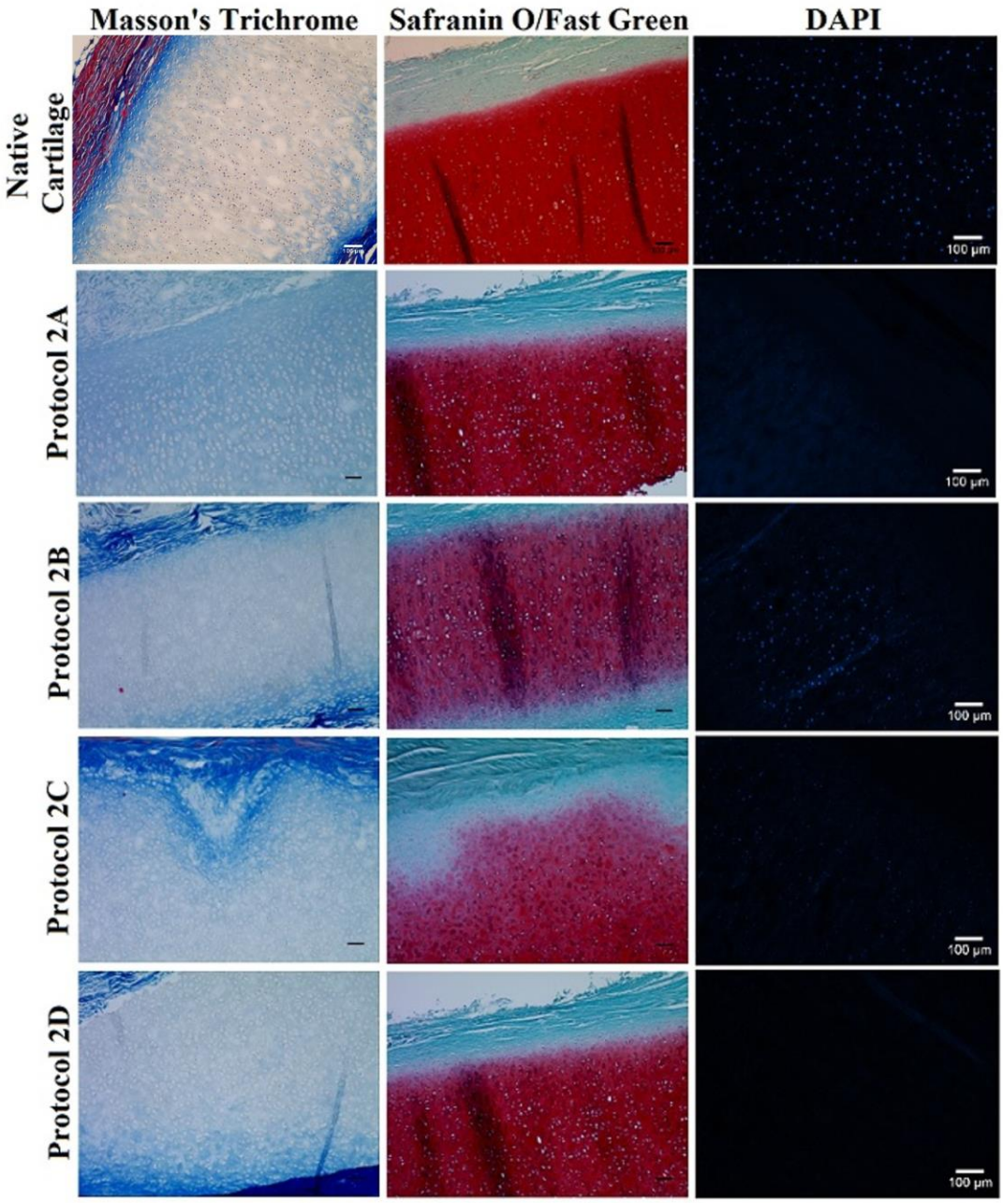

Figure 4.3. Representative histological results of the initial cartilage decellularization protocols in comparison to native cartilage controls. The first column represents Masson's trichrome stains where the cell nuclei appear black and collagen is blue. The second column represents safranin O/fast green staining (red = GAGs, blue/green = collagen). In the third column, residual nuclei are shown in blue. Scale bars represent 100 μm.

4.2 Objective 2: Milling and Characterization of ECM Particles

4.2.1 Particle Size Analysis

Lyophilization and cryogenic milling of DAT and DCT yielded a heterogeneous distribution of particle sizes. The largest yield in terms of the mass of dry particles collected was between the 45 µm and 125 µm sieves (Figure 4.4).

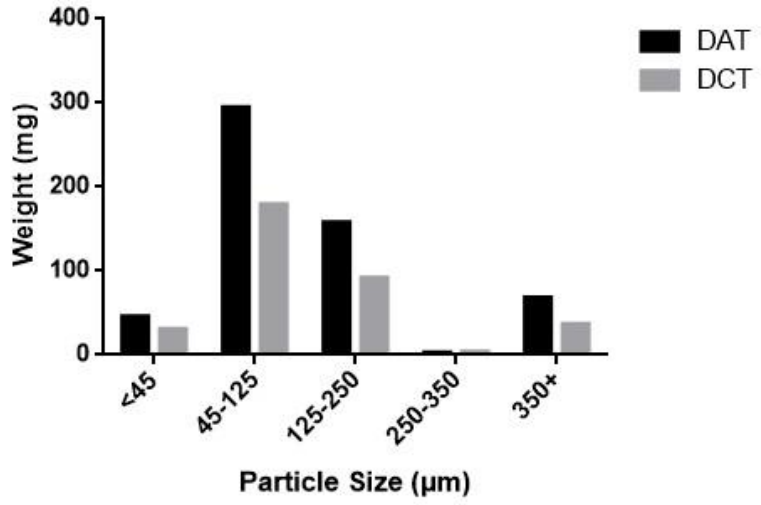

Figure 4.4: Mass of particles generated through cryo-milling DAT or DCT and sorted by size through sieving. Data presented reflects the results for three pooled donors per ECM source.

The Mastersizer analysis confirmed that the majority of the particles were in the size range of less than 125 µm (Figure 4.5). As the particles analyzed with the Mastersizer were in a hydrated state and prone to agglomeration, the second peak within each trial was suspected to be associated with particle aggregates. The results of the Kolmogorov–Smirnov test with $p < 0.05$ confirmed that the particle size distributions for the DAT and DCT particles were statistically equivalent.

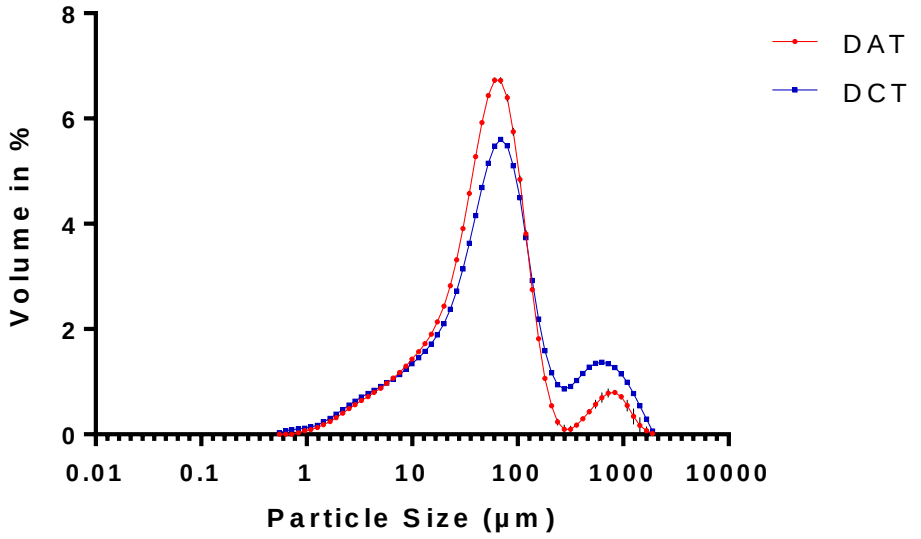

Figure 4.5 Cryo-milled DAT and DCT particle size distribution analyzed using a laser diffraction particle size analyzer. The data shown represents the average of three technical replicates (n=3) of the pooled ECM particles sourced from three donors.

4.2.2 Scanning Electron Microscopy

Based on the SEM images, both the DAT and DCT particles had an amorphous structure with some visible fibers at the surface (Figure 4.6). However, the images suggest that the DAT and DCT may have different microstructures that are distinct to each type of tissue. This could potentially alter cell-ECM interactions with regards to cell attachment, spreading, and differentiation [205]. Further, structural and compositional variations in the particles may have some impact on the properties of the cell aggregates with regards to stiffness and cell densities. However, further research would need to be done to evaluate these potential effects.

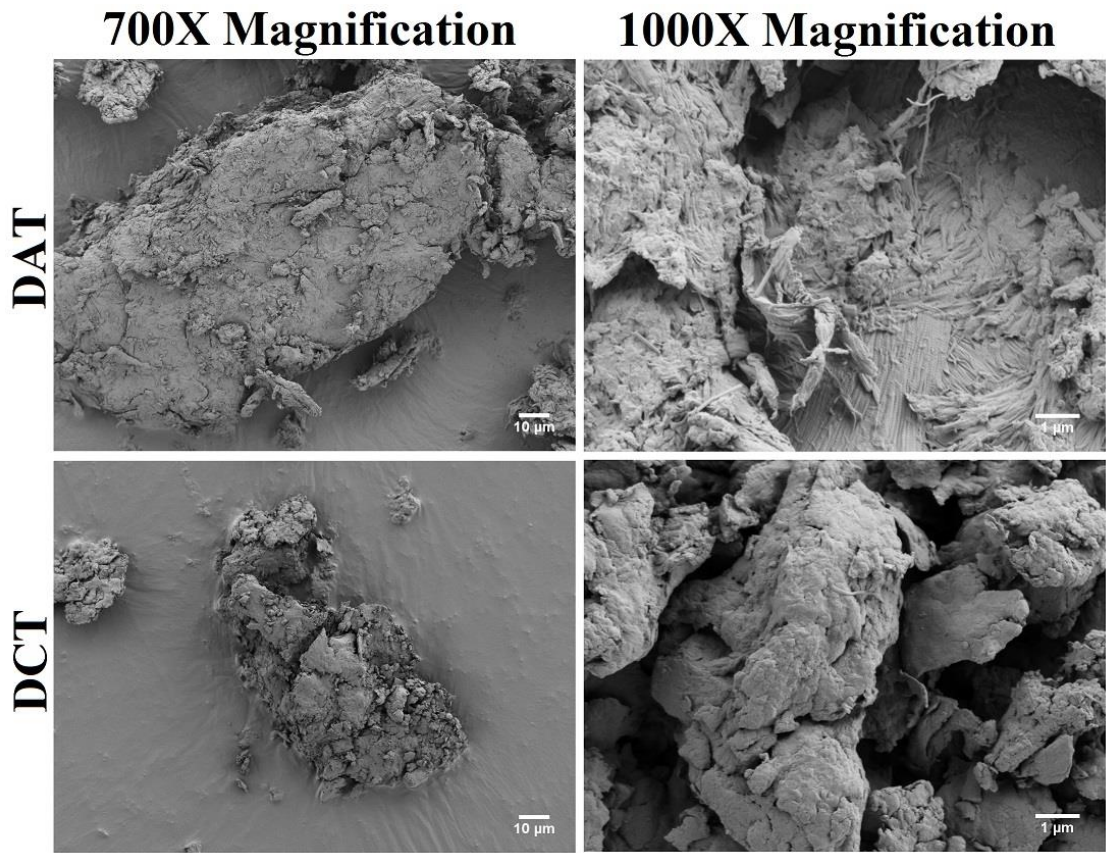

Figure 4.6 Representative SEM images of DAT and DCT particles at 700x and 1000x magnification.

4.3 Objective 3: *In Vitro* Cell Culture Studies

4.3.1 Flow Cytometry

Flow cytometry results from three donors (Figure 4.7) demonstrated that the ASCs expressed markers consistent with the expected ASC immunophenotype. Positive markers CD90, CD44, CD29, CD73, and CD105 were expressed at high levels (>90%), and the negative markers CD31, CD45, and CD146 were expressed at levels less than 2%. This is consistent with the requirements for ASCs as outlined by the International Federation for Adipose Therapeutics (IFATS) and Science and the International Society for Cellular Therapy (ISCT) guidelines [54].

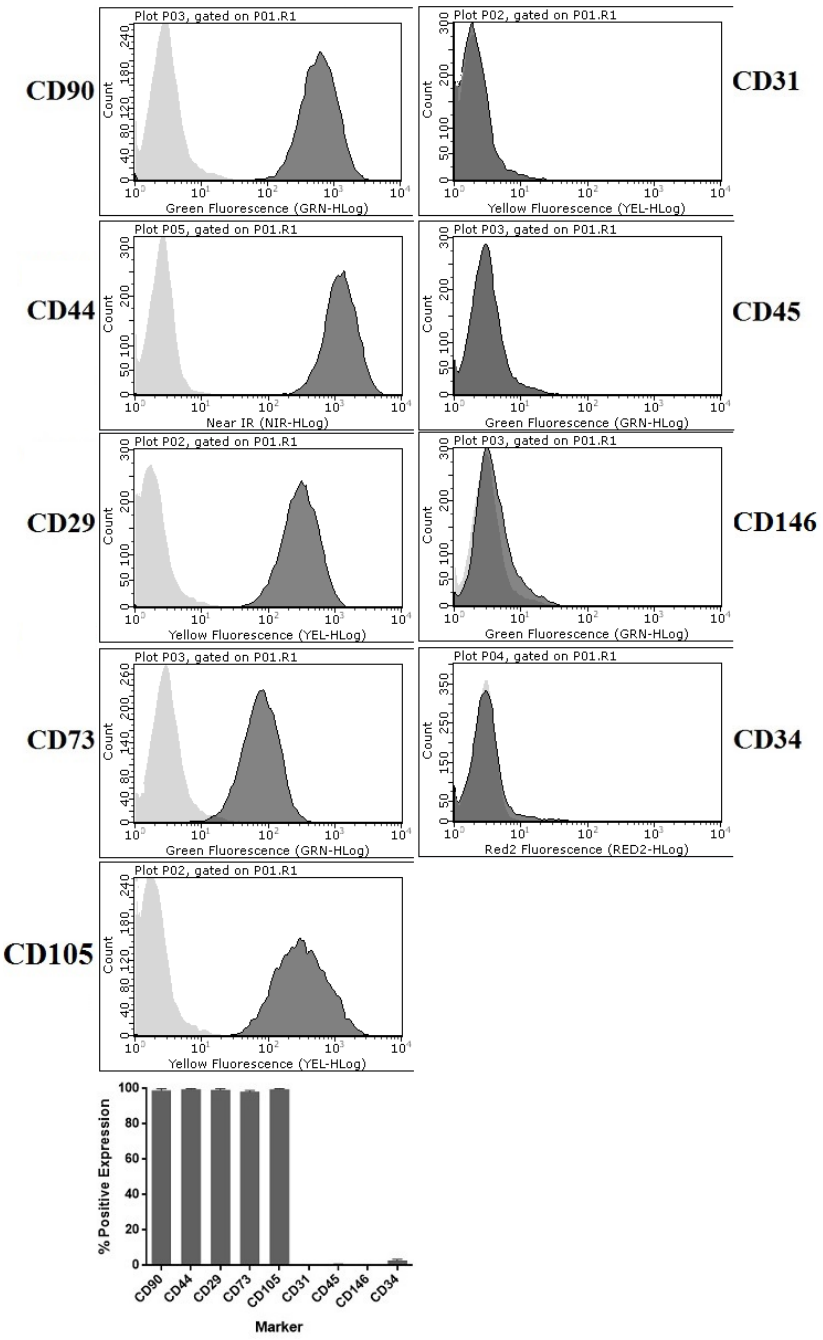

Figure 4.7: Representative histograms and average flow cytometry results of ASC marker expression at passage 1 (n=3, N=3).

4.3.2 Validation of the Chondrogenic Differentiation Medium Formulation

Since chondrogenesis requires close cell-cell contact in order to mimic the condensation process observed in native tissue formation during development [77], all *in vitro* culture studies were

carried out using the self-aggregation methods described in Section 3.3.3. The effects of two chondrogenic media formulations reported in the literature for inducing chondrogenesis of ASCs on cartilage ECM production were assessed [12][71]. A qualitatively higher ratio of collagen II:collagen I expression was observed in the ASC pellets cultured in the differentiation medium comprised of 89% DMEM/Ham's F12, 10% FBS, 1% pen-strep, 37.5 µg/mL of ascorbate-2-phosphate (A2P), 6.25 µg/mL insulin, 100 ng dexamethasone, and 10 ng/mL TGF-β1. A higher ratio of collagen II:collagen I is characteristic of cells undergoing chondrogenesis [206], [207]. The safranin O staining also demonstrated qualitatively more uniform and intense staining with this formulation, suggesting enhanced GAG accumulation (Figure 4.8) indicative of cells undergoing chondrogenesis. Based on these results indicating effective induction of ASC chondrogenesis, this chondrogenic medium formulation was used for all subsequent studies.

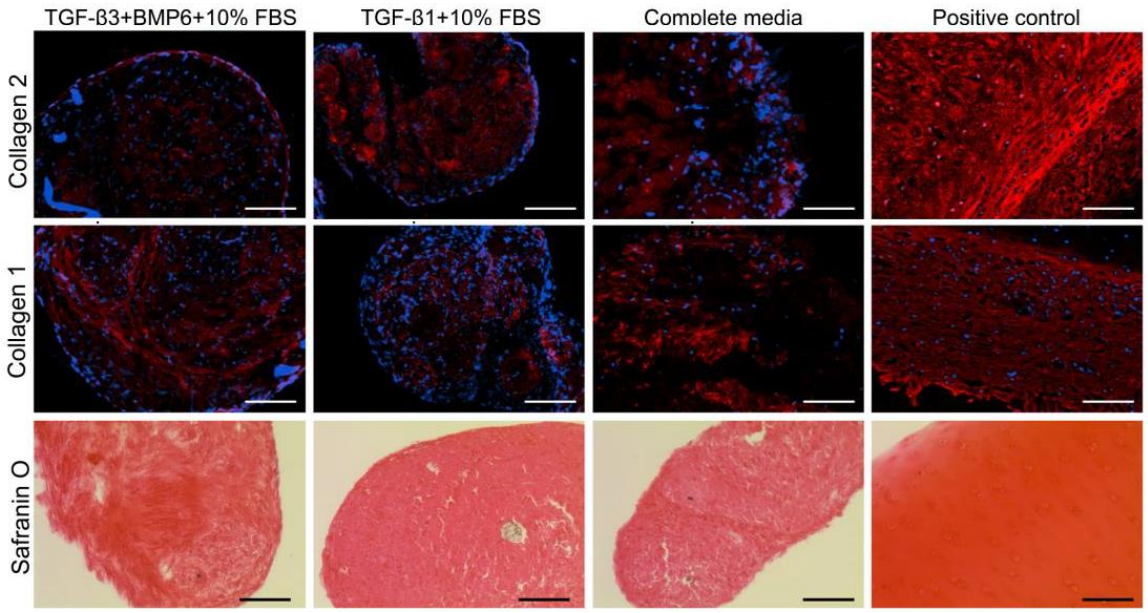

Figure 4.8 Validation of chondrogenic media formulations. ASC pellets stained for collagen II and I (red), with DAPI counterstaining (blue), after 28 days in culture (scale bars=100 µm) (n=2). Safranin O analysis showing GAG content (red) (scale bars=200 µm). Porcine auricular cartilage was used as a positive control.

4.3.3 Verification of ECM Incorporation Within the Cell Aggregates

Masson's trichrome staining was performed to confirm that the DAT or DCT particles were successfully integrated into the cell aggregates (Figure 4.9a, b) following the self-aggregation methods described in Section 3.3.3. It was confirmed that the ECM was incorporated into the aggregates, with a heterogeneous distribution. To further verify ECM incorporation, a pilot study was conducted in which the ECM particles were pre-labeled with an amine-reactive Alexa fluor® 350 succinimidyl ester. Visualization with fluorescence microscopy confirmed that the DAT and DCT particles were heterogeneously incorporated into the aggregates (Figure 4.9c, d).

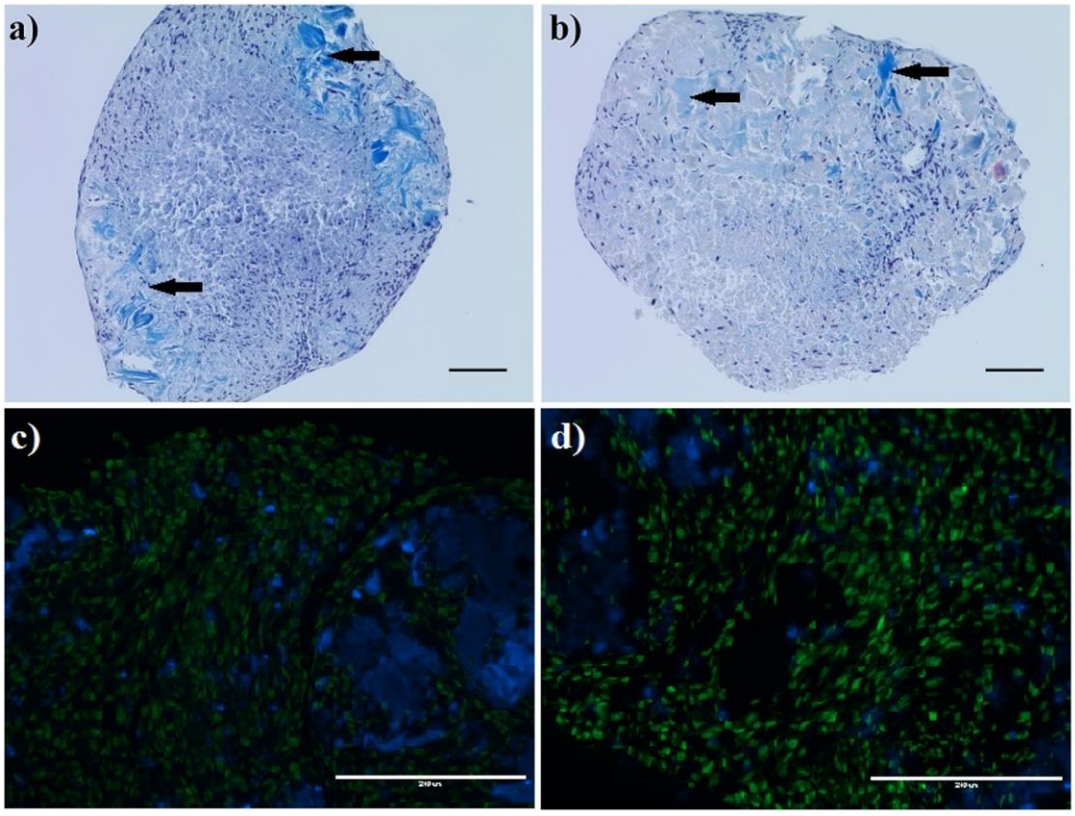

Figure 4.9 Representative staining of cell-ECM aggregates formed with DAT and DCT particles. Masson's trichrome staining of a) DAT + ASC and b) DCT +ASC aggregates showing embedded ECM particles in dark blue, with examples highlighted with arrows. Scale bars represent 100 µm. Fluorescence microscopy of Alexa fluor-labeled ECM particles (blue) in c) DAT+ASC and d) DCT+ASC aggregates with SYTOX® orange (green) nuclear counterstaining. Scale bars represent 200 µm.

4.3.4 *In Vitro* Adipogenic Study

As previously discussed, adipogenesis was assessed using analysis of GPDH enzyme activity, perilipin by IHC, and adipogenic gene expression by RT-qPCR.

4.3.4.1 GPDH Results

GPDH enzyme activity was measured as a quantitative assessment of adipogenic differentiation. For ASC donor 1 (age: 41, BMI: 28.8), the GPDH activity levels were quite low and no significant differences were observed between the groups (Figure 4.10a). It is interesting to note that this donor had the highest BMI, and previous studies have observed that decreased adipogenesis has been noted in donors with an increased BMI [41], [152]. Trends indicated that GPDH activity was higher in the induced groups when compared to the non-induced groups, as expected. The DAT+ASC induced group demonstrated the highest GPDH activity when compared to other conditions, suggesting that the DAT may be assisting with the differentiation toward the adipogenic lineage.

GPDH activity levels for donor 2 (Age:19, BMI: 26.7) were higher, with significantly higher activity levels observed in the induced conditions as compared to the non-induced conditions for the DAT+ASC group (Figure 4.10b). The data suggests that incorporating either type of ECM had a beneficial effect on adipogenic enzyme activity in the 3-D aggregate cultures. Further, the DAT+ASC induced group showed significantly higher levels of GPDH activity as compared to all other groups, indicating that adipogenesis was enhanced in the aggregates incorporating the adipose-derived ECM. Interestingly, significantly higher levels of GPDH enzyme activity were observed in the DAT+ASC non-induced samples as compared to both ASC-alone conditions, suggesting that the DAT had an adipo-inductive effect. This is consistent with what has been reported in the literature, with previous studies demonstrating DAT has the potential to induce adipogenesis when combined with various culturing methods [9], [53], [125], [148].

Similar to donor 2, GPDH activity was upregulated in donor 3 (Age:40, BMI:23.5) for induced conditions when compared to the non-induced aggregates within the same group for DAT+ASC and DCT+ASC conditions. Further, DAT+ASC induced aggregates demonstrated the highest levels of GPDH activity (Figure 4.10c), which was significantly different than all other groups. All aggregates incorporating ECM showed increased GPDH activity as compared to the ASC-

alone aggregates, suggesting that the addition of ECM in general, aids in adipogenic differentiation. In comparing the GPDH levels for the DAT+ASC non-induced group to the DCT+ASC not induced group and ASC-alone conditions, the findings again suggest that the adipose ECM had an inductive effect on ASC adipogenic differentiation.

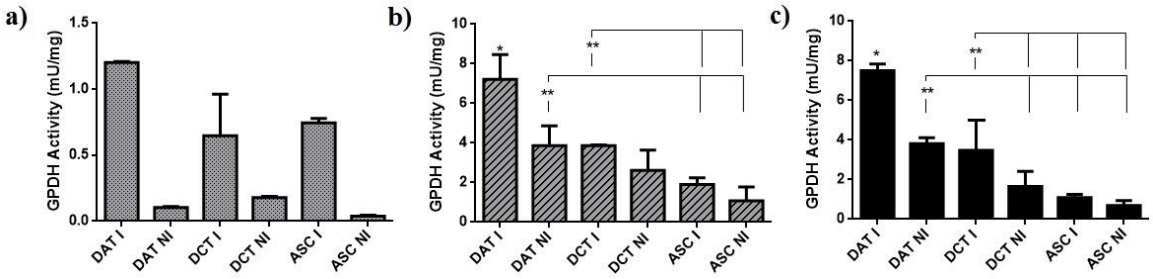

Figure 4.10 GPDH enzyme activity for (a) donor 1, (b) donor 2, and (c) donor 3 at 14 days after adipogenic induction. DAT = DAT+ASC aggregates, DCT = DCT+ASC aggregates, ASC = ASC-alone aggregates. I = induced (adipogenic medium), NI = non-induced (proliferation medium). Data represents the mean ± standard deviation (n=3). * indicates statistically different from all groups ($p < 0.05$). ** indicates statistically different from groups indicated.

4.3.4.2 Immunohistochemistry

Within mature adipocytes, the lipid droplet-cytoplasm interface is stabilized by the protein perilipin, which makes perilipin a direct indicator of intracellular lipid accumulation during adipogenesis [208]. Perilipin in pre-adipocytes will surround cell nuclei, while mature adipocytes will show positive staining surrounding the nuclei and on the surface of lipid droplets within the cell cytoplasm [208][150].

Positive perilipin staining was visualized in the DAT+ASC induced condition for donor 1 (Age:17, BMI: 27.5), as well as for the DCT+ASC induced condition. The perilipin staining demonstrated qualitatively more positive cells in the DAT+ASC induced condition (Figure 4.11a). Moreover, the positive perilipin staining in this group also qualitatively showed that the cells appear to have a more mature phenotype, with larger intracellular lipid droplets in the cells. The staining pattern of this donor was most pronounced around the periphery of the aggregates,

suggesting that the outer cells were undergoing differentiation. It is speculated that nutrient diffusion may have played a role in this response. More specifically, the outermost cells will have enhanced access to nutrients and inductive factors in the media as compared to the cells within the core of the aggregates. This could lead to more bioactive cells at the periphery and explain the staining patterns seen.

Perilipin was visualized with positive staining in cell donor 2 (Age:19, BMI:26.7) for the DAT+ASC and DCT+ASC induced conditions. Small rings can be seen around the cell nuclei in both induced groups incorporating ECM, suggesting that having some type of matrix incorporated into the aggregates is more beneficial than culturing the cells alone in a 3-D configuration. The staining was qualitatively more pronounced in the DAT+ASC induced condition, suggesting that the DAT may be more supportive of adipogenic differentiation than the DCT (Figure 4.11b).

Interestingly, positive perilipin staining was visualized for all induced conditions for cell donor 3 (Age:49, BMI:23.5), who also had the lowest BMI tested amongst donors. All three induced conditions had very obvious staining of perilipin positive cells around the exterior of the aggregates (Figure 4.11c). As discussed previously, it is speculated that this is due to the greater availability of nutrients and adipogenic supplements at the exterior surface of the aggregates. Interestingly, the DAT+ASC induced conditions not only demonstrated positive staining around the exterior of the aggregates, but also within the interior (Figure 4.12). This supports the previous findings that the DAT particles enhanced ASC adipogenic differentiation.

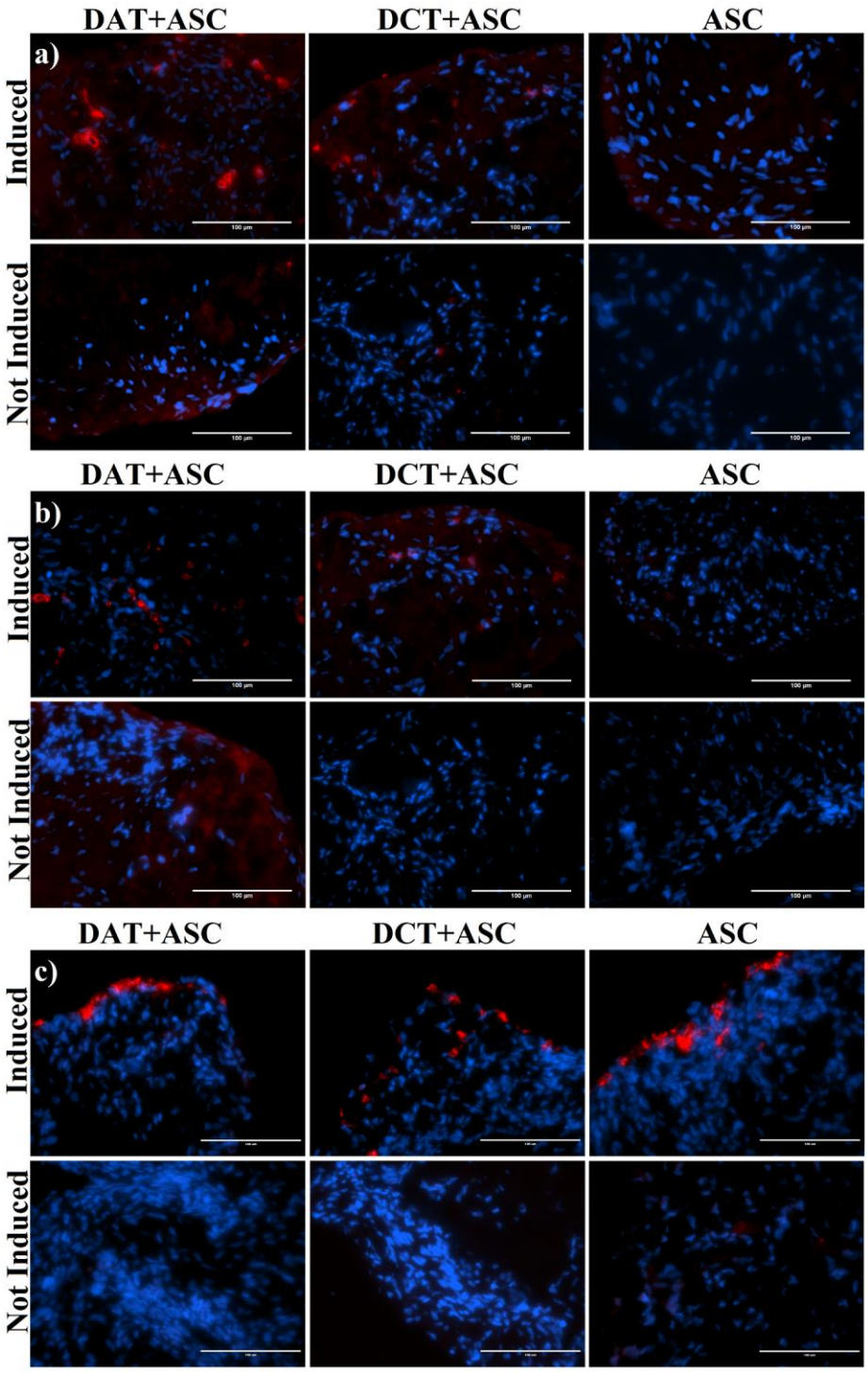

Figure 4.11 Representative IHC images of perilipin expression (red) with DAPI counterstaining (blue) for (a) donor 1, (b) donor 2, and (c) donor 3. Images shown were taken at the periphery of the aggregates. Scale bars=100 µm.

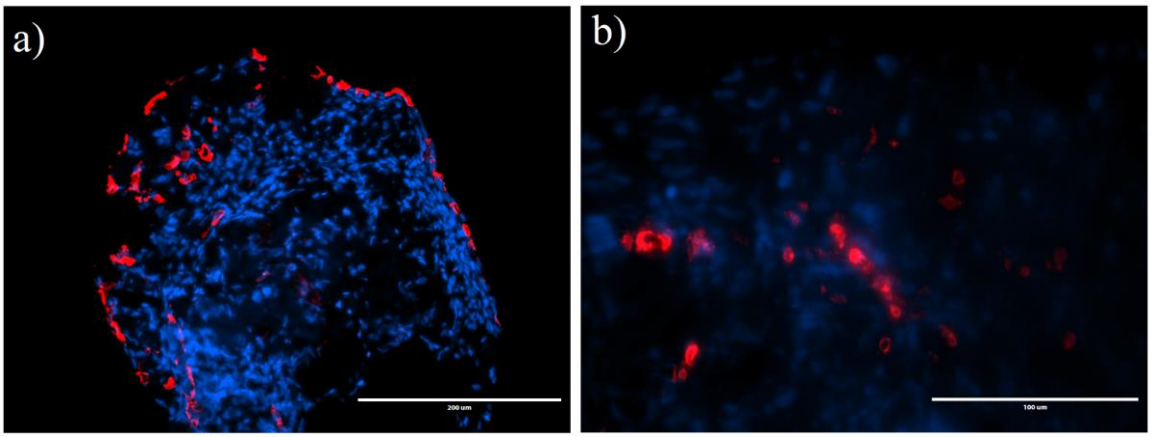

Figure 4.12 Representative IHC images of perilipin expression (red) with DAPI counterstaining (blue) for donor 3, DAT+ASC induced conditions at (a) 20x magnification and (b) 40x magnification. Perilipin positive cells were observed in the interior of the cell-ECM aggregates in this condition. Scale bars are equal to a) 200 µm and b) 100 µm.

4.3.4.3 RT-qPCR Results

Samples from a test run did not yield enough input RNA to allow for measurable readings in the non-induced conditions. Further, perilipin staining was also negative for the non-induced conditions, suggesting that intracellular lipid accumulation was minimal when the cells were maintained in proliferation medium. For these reasons, it was decided to focus the gene expression analysis on comparing the effects of incorporating the ECM on ASC adipogenesis under adipogenic differentiation conditions only.

In analyzing the donor 1 samples, a trend of enhanced expression of the early adipogenic marker PPARϒ was noted in the DAT+ASC induced conditions (Figure 4.13a). Further, the mid-marker lipoprotein lipase (LPL) and late-marker adiponectin (AdipoQ) were significantly upregulated in the DAT+ASC conditions when compared to the DCT+ASC and ASC-alone at 14 days. These results corroborate the GPDH findings that the DAT has instructive effects on promoting ASC adipogenesis. This is consistent with previous results demonstrating that DAT provides an adipo-conductive platform when incorporated into hydrogels and microcarriers [127], [125].

For donor 2 (Age:19, BMI:26.7), PPARϒ expression followed the trend seen with all markers in that expression was highest in the DAT+ASC induced conditions (Figure 4.13b), and was

significantly higher than the ASC-alone group. Similar to the GPDH and IHC results, the expression patterns for all three genes indicated that adipogenic marker expression was enhanced in the aggregates incorporating ECM. Further, significantly higher levels of LPL and AdipoQ expression were observed in the DAT+ASC group relative to all other conditions, suggesting that the adipose ECM enhanced ASC adipogenesis.

While the average fold changes were lower, similar trends were seen for cell donor 3 (Age:49, BMI:23.5) with regards to gene expression (Figure 4.13c). The aggregates with ECM showed increased LPL and adiponectin expression when compared to the ASC-alone group, suggesting that the addition of ECM aids in differentiation. Moreover, significantly higher levels of expression of these two markers were observed in the DAT+ASC group, indicating that DAT may be superior to DCT for inducing adipogenic differentiation, and validating what was seen in both the GPDH enzyme activity assay and perilipin staining.

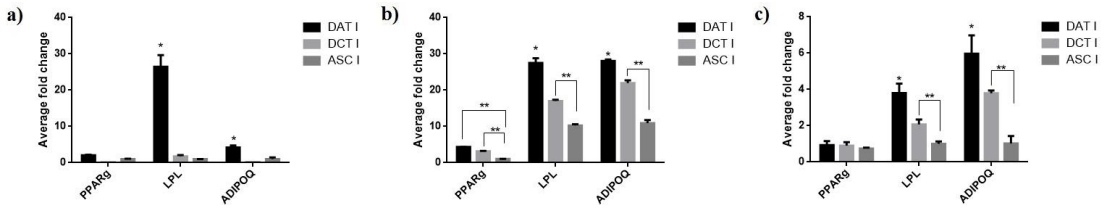

Figure 4.13 Adipogenic gene expression at 14 days for cell (a) donor 1, (b) donor 2, and (c) donor 3. Calibrated to ASC induced conditions. DAT = DAT+ASC aggregates, DCT = DCT+ASC aggregates, ASC = ASC-alone aggregates. I = induced (adipogenic medium). Data represents the mean ± standard deviation (n=3* indicates statistically different from all groups ($p < 0.05$). ** indicates statistically different from groups indicated.

4.3.5 *In Vitro* Chondrogenic Study

As previously discussed in Chapter 3, chondrogenesis was assessed using collagen II and collagen I IHC, safranin O staining of GAG accumulation, and RT-qPCR analysis of chondrogenic gene expression.

4.3.5.1 Immunohistochemistry and Histology

It has been suggested in the literature that the proteins collagen I and II are upregulated during chondrogenesis as extracellular matrix is being produced by the ASCs [206]. An increased ratio of collagen II:collagen I is expected during chondrogenesis [179].

Results from ASC donor 1 (age: 19, BMI: 26.7) demonstrated (Figure 4.14a) strong positive staining for collagen II in both DCT+ASC conditions, as well as low levels in the DAT+ASC and ASC-alone induced groups, suggesting that the cells were undergoing chondrogenesis. However, a limitation of the experimental design is that it is technically challenging to distinguish new ECM produced by the cells from the ECM within the embedded particles. Based on knowledge of the composition of adipose and cartilage ECM, it would be expected that the DAT particles would be comprised substantially of collagen I and the DCT particles of collagen II [112]. As such, it is difficult to assess how much of the collagen II in the DCT+ASC groups was synthesized by differentiating cells. It is worth noting that collagen II staining in the DCT aggregates was quite uniform, unlike the heterogeneous distribution of the particles in the aggregates seen in Figure 4.9. Based on the more homogenous staining, it is speculated that at least part of the collagen II detected was newly synthesized by the cells. IHC showed low levels of collagen I (Figure 4.15a) expression in all chondrogenic induced conditions, with no detectable expression in all non-induced controls.

IHC for donor 2 (age:17, BMI: 27.5) demonstrates collagen II accumulation appears to be enhanced in all conditions when compared to donor 1. Literature suggests that differences in expression of collagen II and collagen I between trials may be attributed to donor variability [209]. Collagen II staining was observed in all conditions, with more intense staining found in the DCT+ASC groups, with a highly uniform staining pattern observed across the entire aggregate cross-section in the induced conditions (Figure 4.14b). Interestingly, both of the DAT+ASC groups also showed very uniform collagen II expression, suggesting that the cells were undergoing chondrogenic differentiation in the presence of the DAT. In contrast, the ASC-alone samples had qualitatively reduced collagen II expression in the induced conditions, as well as no detectable levels of collagen II in the non-induced conditions, suggesting that incorporating the ECM had a positive effect on ASC chondrogenesis. The collagen I staining results indicate

that the ASC-alone group cultured in chondrogenic medium had qualitatively enhanced collagen I expression (Figure 4.15b), consistent with a less differentiated phenotype.

Collagen II staining for donor 3 (age: 50, BMI:29) was more pronounced for all induced conditions when compared to non-induced counterparts (Figure 4.14c), with the most intense staining seen in the DCT+ASC aggregates. The DAT+ASC induced group had qualitatively higher levels of expression as compared to the ASC-alone conditions, further supporting the previous findings that incorporating the ECM particles had a positive effect on the chondrogenic differentiation of the ASCs. Interestingly, when magnification was increased to 20X, induced conditions that included either DAT or DCT showed positive collagen II staining similar to native cartilage, with evidence of a possible pericellular matrix region around the cells (Figure 4.16). For this cell donor, collagen I was detected in all groups, with qualitatively enhanced expression in the DCT induced and not induced conditions (Figure 4.15c).

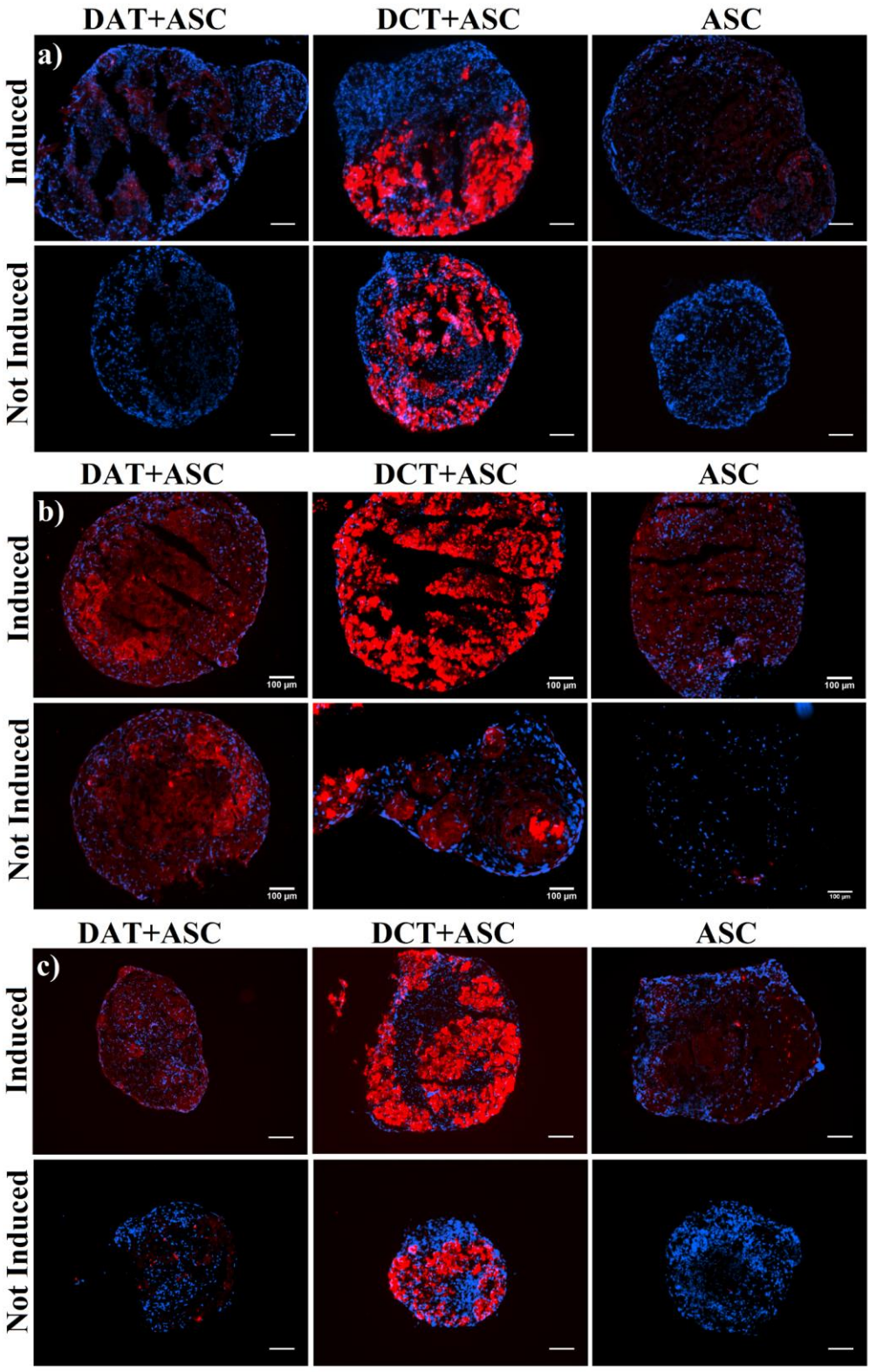

Figure 4.14 Representative images of collagen II staining (red) with DAPI counterstaining (blue) from (a) donor 1, (b) donor 2, and (c) donor 3. Scale bars = 100 µm.

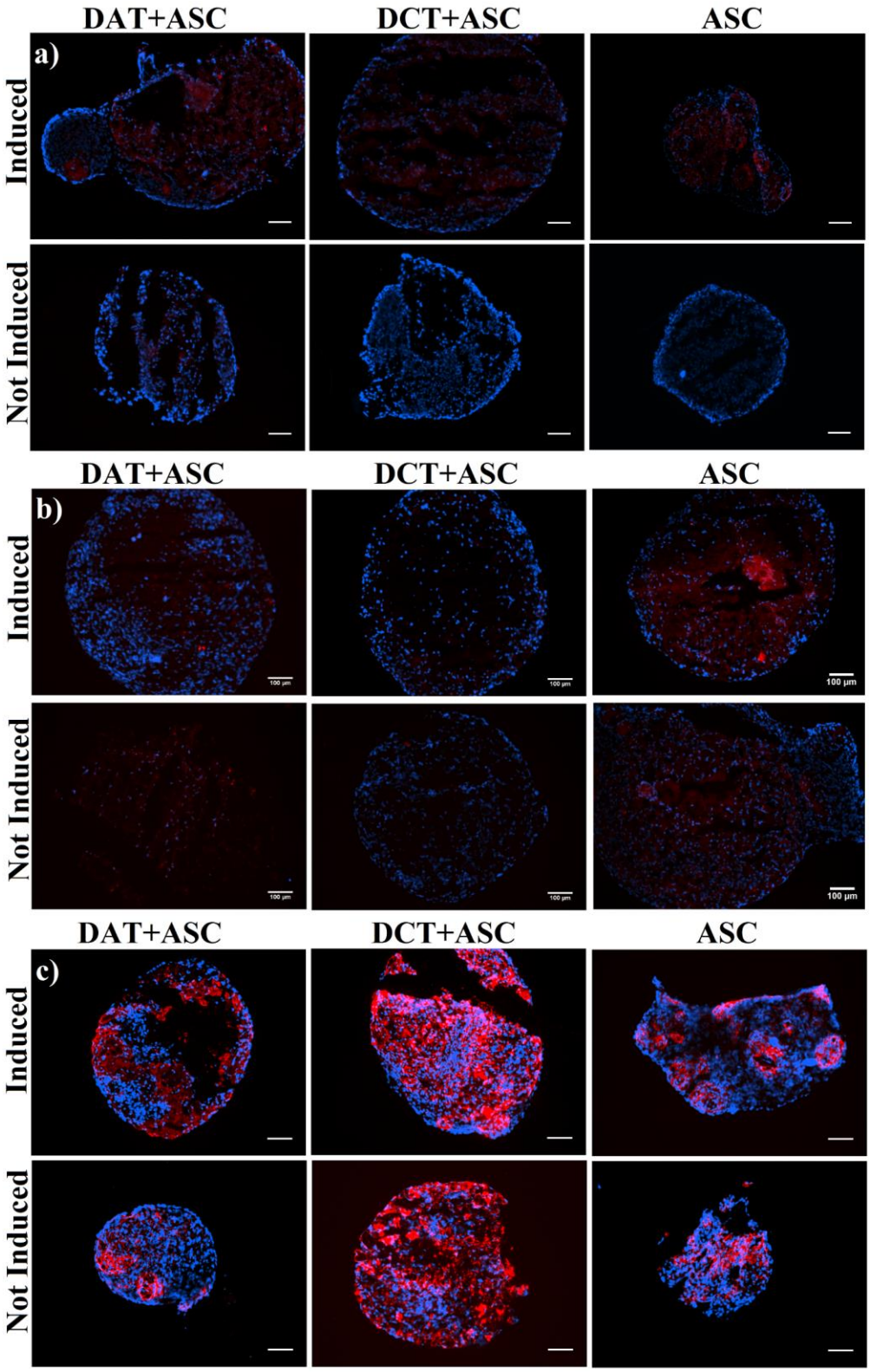

Figure 4.15 Representative images of collagen I (red) staining with DAPI counterstaining (blue) from (a) donor 1, (b) donor 2 and, (c) donor 3. Scale bars = 100 µm.

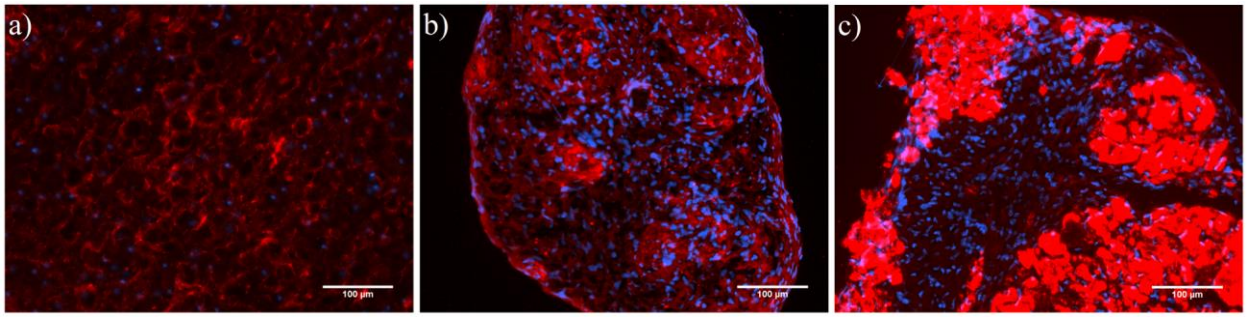

Figure 4.16 Representative 20X images of collagen II staining with DAPI counterstaining from donor 3. Induced conditions with (a) native porcine auricular cartilage (b) DAT+ASC and (c) DCT+ASC groups. Scale bars = 100 µm.

Safranin O staining was used to visualize GAG accumulation within the aggregates (Figure 4.17a). Qualitatively darker staining was observed in the DCT+ASC induced condition than the other groups cultured in chondrogenic medium, which is suggestive of increased GAG content. It is worth noting that the aggregates cultured in the induced conditions from all donors were macroscopically larger than the non-induced controls, suggesting there may be enhanced ECM deposition in the cultures maintained in chondrogenic medium. This is supported by literature suggesting that factors such as TGF-β1 and A2P upregulate synthesis of cartilage-specific matrix containing GAGs and a higher ratio of collagen II:collagen I [78][179].

For donors 2 (Figure 4.17b) and 3 (Figure 4.17c), safranin O staining suggested that induced conditions displayed consistently more homogenous, darker stains when compared to not induced conditions. This confirmed what was seen with collagen II and collagen I IHC staining. DCT+ASC conditions produced more intense and homogenous staining for GAG accumulation when compared to the DAT+ASC conditions. The combination of data from collagen II/collagen I IHC and safranin O staining was suggestive of enhanced chondrogenic ECM accumulation in the DCT+ASC group relative to either DAT+ASCs or ASC-alone.

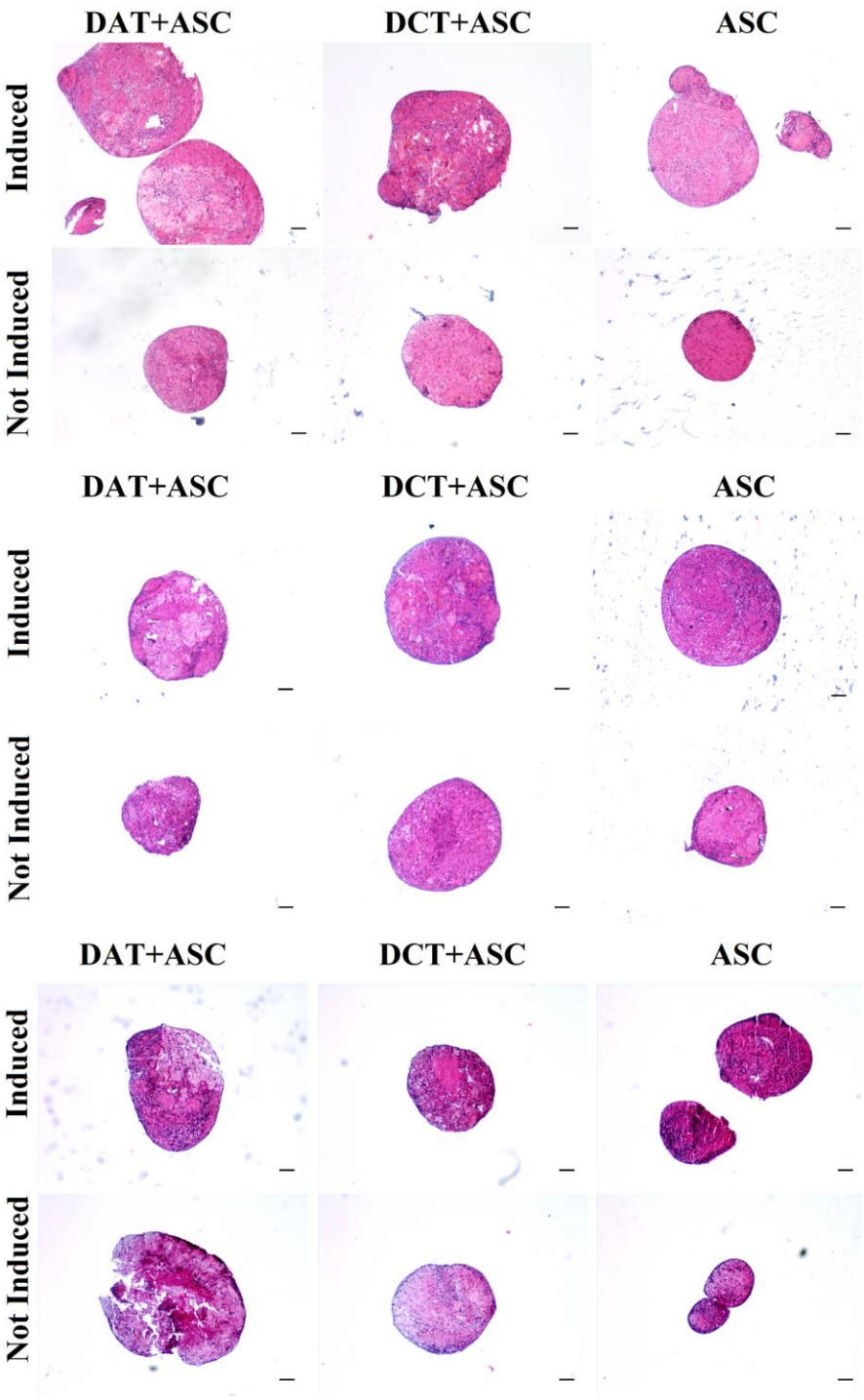

Figure 4.17 Representative images of safranin O staining for (a) donor 1, (b) donor 2, and (c) donor 3. Safranin O staining of GAG content (red) present in cell aggregates. Scale bars = 100 µm.

4.3.5.2 RT-qPCR Results

To complement the qualitative staining results, RT-qPCR analysis was performed to assess the expression of the chondrogenic markers SOX9, COMP, and aggrecan in the induced samples cultured in chondrogenic medium, with UBC and RPL13A included as the housekeeping genes.

The gene expression results showed very consistent patterns across all three donors (Figure 4.18). Results from donor 1 (Figure 4.18a) show a trend for enhanced SOX9 gene expression and significantly higher levels of AGG gene expression in the DCT+ASC experimental group as compared to the other two groups. Interestingly, the DAT+ASC group demonstrated significant upregulation of the COMP gene as compared to the other conditions. One possibility is that COMP gene expression may have peaked earlier in the DCT+ASC group when compared to the DAT+ASC conditions, causing the results seen. A similar study saw chondrogenic genes upregulated after one week in studies combining decellularized cartilage with bone-marrow-derived stem cells (bMSCs) [210]. While RT-qPCR quantitatively measures gene expression, it only provides information about the levels of gene expression at the point in time when the samples were processed. Given that gene expression patterns can vary considerably as differentiation progresses, average fold changes would very likely be different if the samples were assessed at an earlier or later time point. Since COMP has been reported as an early/mid marker and AGG as a late-stage marker of human mesenchymal stem cell (MSC) chondrogenesis [211], it is possible that the DCT+ASC group had a more differentiated phenotype, although further studies with additional time points and markers would be required to verify this interpretation.

While the average fold change values were generally higher, in comparing the groups, the gene expression patterns for donor 2 were very similar to donor 1. DAT induced conditions for donor 2 (Figure 4.18b) show a trend of enhanced SOX9 expression in both groups that incorporate ECM. Two-way ANOVA results indicate significantly elevated COMP expression in the DAT+ASC group relative to all other conditions, as well as in the DCT+ASC group as compared to the ASC-alone samples. Additionally, similar to donor 1, AGG was significantly upregulated in the DCT+ASC aggregates when compared to both the DAT+ASC and ASC-alone groups.

Results from the RT-qPCR analysis for donor 3 (Figure 4.18c) were very similar to those of donor 1. Again, trends indicated enhanced SOX9 expression in the DCT+ASC group. Similar to the other donors, results indicated that the DAT+ASC group showed elevated COMP expression when compared to the DCT+ASC and ASC-alone groups, and that the DCT+ASC group had enhanced COMP expression when compared to the ASC-alone group. This suggests that the addition of ECM is superior to ASC-alone for promoting chondrogenic differentiation. Moreover, AGG gene expression was again significantly enhanced in the DCT+ASC group, potentially suggestive of a more differentiated phenotype.

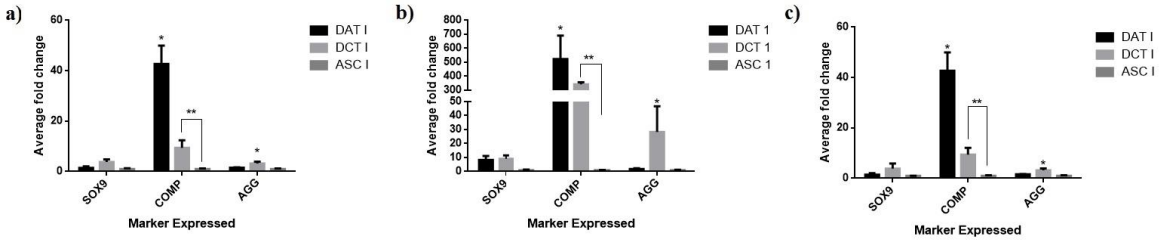

Figure 4.18 Chondrogenic gene expression at 28 days for (a) cell donor 1, (b) donor 2 and, (c) donor 3. Calibrated to ASC induced conditions. DAT = DAT+ASC aggregates, DCT = DCT+ASC aggregates, ASC = ASC-alone aggregates. I = induced (adipogenic medium). Data represents the mean ± standard deviation (n=3). * indicates statistically different from all groups ($p < 0.05$). ** indicates statistically different from groups indicated.

Results and trends from this study suggest that incorporating ECM promotes chondrogenic gene expression relative to ASC-alone, which is consistent with the IHC staining results. A limitation of this study is that only one time point was analyzed. As discussed, it would be interesting to look at a time series in future studies to analyze changes in gene expression among the different conditions. The COMP protein plays an important role in growth, division, cell attachment, and apoptosis in cartilage tissue [72]. This non-collagenous protein has been shown to interact with SOX9 to promote chondrogenic activity of MSCs from cellular condensation to terminal differentiation [72], [211]. COMP is upregulated in chondroprogenitors through to terminal differentiation [72], while AGG is typically regarded as a mature chondrocyte matrix gene [212]. One study showed that COMP levels in human MSCs induced to differentiate in 3-D alginate gels peaked around 12 days, while AGG levels peaked beyond 24 days, raising the need for a

time series including time points at 7 and 14 days [211]. Additionally, other late expression markers such as lubricin (PRG4) and matrilin-1, as well as the hypertrophic marker collagen X, could be assessed at 28 days to corroborate the speculations made above.

Chapter 5

5 Conclusions

As the emerging field of tissue engineering and regenerative medicine continues to expand upon the knowledge of the extracellular matrix (ECM), it becomes apparent that there is greater need for tissue-specific cell-based therapies. Tissues such as cartilage have a limited regenerative capacity and require assistance in order to return functionality back to the tissue. Each tissue within the body has a specific structure and function, providing a rationale for the use of tissue-specific scaffolds for regenerative purposes. While research has investigated the effects of tissue-specific biomaterials and scaffolds on differentiation, few studies to date have focused on the effects of multiple ECM sources on directing the lineage-specific differentiation of stem cells [8], [148]. This begs the question, do tissues require a specific ECM or will the addition of any type of ECM aid in the differentiation of stem/stromal cells? Incorporating decellularized ECM sourced from adipose tissue or cartilage into cell aggregate cultures provides insight into the potential importance of using tissue-specific ECM to guide differentiation and/or to act as a natural scaffold for the regeneration of adipose or cartilage tissue. Decellularized matrices represent an attractive biomaterial for 3-D scaffolds because they retain a complex mixture of functional and structural proteins from natural tissue sources [82].

Detergent-free methods of decellularization had been previously established in order to fabricate decellularized adipose tissue (DAT). In order to examine the effects of DAT and decellularized cartilage tissue (DCT), an examination of various cartilage decellularization protocols based on the literature was required. Successful decellularization of the ECM required removal of cellular materials while maintaining the integrity of the native tissue. Several different protocols were tested. A protocol was developed that successfully removed cellular material while macroscopically preserving the collagen and GAG within the ECM, which involved: repeated freeze/thaw cycles, osmotic cell lysis through washes in hypotonic Tris buffers, 5-hour enzymatic digestion with trypsin/EDTA, and rinses in a high salt buffer containing 2% Triton X-100, followed by 1% tributyl-phosphate (TBP). Successful decellularization of cartilage was achieved through removal of cellular contents as visualized by Masson’s trichrome and DAPI staining. GAG retention was also qualitatively maintained through the use of this protocol.

DAT and DCT were lyophilized and milled into ECM particles. The particles were then sorted by size, collecting those captured between 45 μm and 125 μm screens. The resulting particles were characterized using dynamic light scattering and scanning electron microscopy. It was concluded that a heterogeneous mixture of particle sizes was achieved through the process, with some structural differences noted between the two types of ECM.

Finally, *in vitro* culture studies were conducted to assess the potential effects of the tissue-specific ECM on the lineage-specific differentiation of human adipose-derived stem/stromal cells (ASCs). First, chondrogenic media formulations were tested and culture methods were established for creating the cell-ECM aggregates. Subsequently, *in vitro* cell culture studies were conducted to investigate adipogenesis and chondrogenesis of aggregates comprised of (i) DAT+ASCs, (ii) DCT+ASCs, and (iii) ASC-alone, cultured in both differentiation and proliferation media.

The results demonstrated that the addition of ECM generally improved differentiation for both adipogenesis and chondrogenesis, as demonstrated by analysis of protein expression and confirmed with RT-qPCR. Both adipogenic and chondrogenic markers were upregulated in conditions containing ECM when compared to the ASC-alone groups.

Adipogenesis was assessed by glycerol-3-phosphate dehydrogenase (GPDH) activity, perilipin immunohistochemistry (IHC) and RT-qPCR. The GPDH results consistently demonstrated that GPDH expression was higher in all induced aggregates when compared to the corresponding non-induced controls. The DAT+ASC groups consistently showed the highest levels of GPDH activity, suggesting that incorporating the DAT enhanced adipogenesis relative to either the DCT+ASCs or ASC-alone. Perilipin results confirmed this finding, as the DAT induced conditions consistently stained positive for perilipin, with the cells qualitatively having a more mature phenotype associated with larger intracellular lipid droplets. For the third cell donor, positive perilipin staining was visualized around the edges of the aggregates for all induced conditions. However, the DAT induced aggregates were the only group that also demonstrated perilipin staining within the interior of the aggregates in this set of samples. RT-qPCR results consistently demonstrated that the DAT+ASC induced conditions had larger fold changes for the adipogenic markers LPL and adiponectin. Taken together, the findings support that the DAT has

adipo-inductive and adipo-conductive properties and is superior to either the DCT or ASCs alone for inducing adipogenesis within 3-D aggregate cultures.

Chondrogenesis was assessed by comparing collagen II and collagen I expression, as higher expression of collagen II is related to increased chondrogenic activity. A limitation of this study was that it was difficult to discern newly synthesized matrix from the ECM in the particles that were incorporated into the aggregates. IHC results demonstrated once again that the inclusion of ECM had a positive effect on differentiation relative to culturing the ASCs alone. The DCT+ASC samples consistently demonstrated more intense fluorescent staining for collagen II than the other conditions, but as mentioned previously, it was difficult to differentiate between the ECM particles and newly-synthesized matrix within the aggregates. Safranin O staining demonstrated darker staining in all induced conditions, and when combined with the IHC results, supported the conclusion that incorporating either type of ECM in the aggregates enhanced cartilage matrix synthesis. The uniformity of the response may suggest that incorporating DCT may be superior to DAT in terms of collagen II/collagen I production, but further studies would be required to verify this interpretation. Results of RT-qPCR studies showed trends that the DCT+ASC group had enhanced SOX9 expression at 28 days when compared to the other groups. Further, RT-qPCR results for all three donors show that COMP gene expression was upregulated for both the DAT+ASC and DCT+ASC groups when compared to ASC-alone at 28-days, with significantly higher expression in the DAT+ASC group. Additional time points may demonstrate different results at 7 and 14 days, as several studies have seen SOX9 and COMP levels peak between 6 and 14 days [1], [211]. Additionally, all donors demonstrated that AGG gene expression was upregulated in DCT+ASCs when compared to either DAT+ASCs or ASC-alone, and supports the theory that the DCT+ASC aggregates may be more terminally differentiated than other groups. Additional gene expression studies would help to confirm this hypothesis.

Towards the development of tissue-specific cell-based strategies for tissue engineering, the data obtained highlights the potential effects that the ECM has on the differentiation of ASCs and demonstrates a promising use of decellularized ECM materials for the development of tissue-specific instructive platforms for directing mesenchymal stem/stromal cell (MSC) differentiation.

5.1 Future Recommendations

Short-term goals to build from the work presented in this thesis include further application of fluorescent labeling of the DAT and DCT particles prior to incorporation in the cell-ECM aggregates to assist in distinguishing the newly-synthesized ECM from the ECM particles during IHC analyses. This would give a better indication of collagen II and collagen I production, particularly in the DCT+ASC conditions. It would also be interesting to look at chondrogenic differentiation at earlier time points of 7 and 14 days to see how gene expression changes in the earlier stages of chondrogenesis. One study showed increased gene expression levels in cell-ECM aggregates incorporating DCT at 24 hours and 7 days [1]. It would also be beneficial to look at wider array of chondrogenic genes such as SOX5, SOX6, COLII, lubricin, matrilin-1 and COLX. A more quantitative assay such as the Blyscan™ sulphated GAG assay kit or DMMB assay could also be done to give more quantitative results to complement the safranin O staining. It would also be worthwhile to repeat the adipogenic studies to further validate trends with additional cell donors. This would clarify the results of this study and may provide more insight into whether there are differences between the aggregates incorporating DAT and DCT.

Porcine auricular cartilage was used as an ECM source for this study as a proof of concept. It would be interesting to examine a different cartilage source, such as fibrocartilage or hyaline cartilage, to see if the tissue source has an impact on the chondrogenic differentiation of the ASCs. Additionally, it would be worth exploring human cartilage as a source of DCT, although this would be more challenging to obtain. Expanding on the overall strategy for this project, it would be worth examining decellularization of other tissues such as bone, skin, and muscle. Using similar methods, ASCs and ECM could be combined and differentiated towards the osteogenic, endothelial, and myogenic lineages in order to gain a broader understanding of the potential effects of tissue-specific ECM.

Alternatively, it would be interesting to investigate the manipulation of the DCT as a scaffolding material. If the DCT were enzymatically digested, this could allow for the fabrication of ECM-dervied foams, microcarriers, and sheets. These alternative scaffold formats would allow for better control of the architecture of the scaffold and potentially better control of the distribution of ECM compared to the cells. This was a limitation in this project that could be addressed through the manipulation of the ECM materials. More specifically, it was difficult to control the

distribution of the ECM and the cells, leading to heterogeneous cell-ECM aggregates. Using ECM-derived microcarriers, for example, might solve this problem, and would still allow for the 3-D culture conditions required for chondrogenesis. The porosity could also be controlled, which may aid in cell infiltration into the scaffold, which is a common problem with current cartilage tissue engineering methods [123].

In terms of long-term goals for the work presented in this thesis, incorporating the ECM particles into other materials, such as hydrogels would be an interesting way to examine the effects the ECM has on differentiation where nutrient availability could be limited. Some recent studies have suggested that ECM-derived materials can provide an instructive microenvironment for directing stem/stromal cell fate [8], [192]. ECM particles could also be incorporated into injectables, to develop clinically-translational cell-based therapies using the ECM as an instructive component to direct stem cell differentiation. Testing these results with various decellularized tissues to examine the tissue-specific effects could be first accomplished *in vitro.*

In terms of *in vivo* work, murine models can be used to examine the effects of tissue-specific cell-ECM therapies. Incorporating various scaffold types into different tissues can aid in the understanding of how the ECM can affect cellular fate *in vivo.* Additionally, it should be proposed that cell-based therapies continue to incorporate naturally-derived ECM into experiments, as this has shown promise for aiding the proliferation and differentiation of stem/stromal cells both *in vitro* and *in vivo*.

References

[1] J. S. Choi, H.-J. Yang, B. S. Kim, J. D. Kim, J. Y. Kim, B. Yoo, K. Park, H. Y. Lee, and Y. W. Cho, "Human extracellular matrix (ECM) powders for injectable cell delivery and adipose tissue engineering.," *J. Control. Release*, vol. 139, no. 1, pp. 2–7, Oct. 2009.

[2] K. E. M. Benders, P. R. van Weeren, S. F. Badylak, D. B. F. Saris, W. J. A. Dhert, and J. Malda, "Extracellular matrix scaffolds for cartilage and bone regeneration.," *Trends Biotechnol.*, vol. 31, no. 3, pp. 169–76, Mar. 2013.

[3] Y. C. Choi, J. S. Choi, C. H. Woo, and Y. W. Cho, "Stem cell delivery systems inspired by tissue-specific niches.," *J. Control. Release*, vol. 193, pp. 42–50, Nov. 2014.

[4] K. A. Moore, "Stem Cells and Their Niches," *Science (80-.).*, vol. 311, no. 5769, pp. 1880–1885, Mar. 2006.

[5] J. P. Lanza, Robert; Langer, Robert; Vacanti, *Principles of Tissue Engineering*. Academic Press, 2011.

[6] S. F. Badylak, "The extracellular matrix as a scaffold for tissue reconstruction," *Semin. Cell Dev. Biol.*, vol. 13, no. 5, pp. 377–383, Oct. 2002.

[7] J. Zellner, M. Mueller, A. Berner, T. Dienstknecht, R. Kujat, M. Nerlich, B. Hennemann, M. Koller, L. Prantl, M. Angele, and P. Angele, "Role of mesenchymal stem cells in tissue engineering of meniscus.," *J. Biomed. Mater. Res. A*, vol. 94, no. 4, pp. 1150–61, Sep. 2010.

[8] A. Skardal, L. Smith, S. Bharadwaj, A. Atala, S. Soker, and Y. Zhang, "Tissue specific synthetic ECM hydrogels for 3-D in vitro maintenance of hepatocyte function.," *Biomaterials*, vol. 33, no. 18, pp. 4565–75, Jun. 2012.

[9] L. E. Flynn, "The use of decellularized adipose tissue to provide an inductive microenvironment for the adipogenic differentiation of human adipose-derived stem cells," *Biomaterials*, vol. 31, no. 17, pp. 4715–4724, Jun. 2010.

[10] J. M. Gimble, A. J. Katz, and B. A. Bunnell, "Adipose-Derived Stem Cells for Regenerative Medicine," *Circ. Res.*, vol. 100, no. 9, pp. 1249–1260, Apr. 2007.

[11] H.-T. Liao, "Osteogenic potential: Comparison between bone marrow and adipose-derived mesenchymal stem cells," *World J. Stem Cells*, vol. 6, no. 3, p. 288, Jul. 2014.

[12] Y. Zhao, "The Characterization of Bovine Adipose-Derived Stem Cells in Conventional and Co-culture Environments for Tissue Engineering," *Queen's University*, 2011. [Online]. Available: file:///M:/Danielle Heinbuch/Downloads/Zhao_Yimu_201102_Msc.PDF.

[13] K. Liu, G. D. Zhou, W. Liu, W. J. Zhang, L. Cui, X. Liu, T. Y. Liu, and Y. Cao, "The dependence of in vivo stable ectopic chondrogenesis by human mesenchymal stem cells on chondrogenic differentiation in vitro.," *Biomaterials*, vol. 29, no. 14, pp. 2183–92, May 2008.

[14] O. Naveiras and G. Q. Daley, "Stem cells and their niche: a matter of fate.," *Cell. Mol. Life Sci.*, vol. 63, no. 7–8, pp. 760–6, Apr. 2006.

[15] S. F. Badylak, "Xenogeneic extracellular matrix as a scaffold for tissue reconstruction.," *Transpl. Immunol.*, vol. 12, no. 3–4, pp. 367–77, Apr. 2004.

[16] J. Hodde, "Naturally Occurring Scaffolds for Soft Tissue Repair and Regeneration," Jul. 2004.

[17] S. Cebotari, H. Mertsching, K. Kallenbach, S. Kostin, O. Repin, A. Batrinac, C. Kleczka, A. Ciubotaru, and A. Haverich, "Construction of Autologous Human Heart Valves Based on an Acellular Allograft Matrix," *Circulation*, vol. 106, no. 90121, pp. I–63–68, Sep. 2002.

[18] S. F. Badylak, D. Taylor, and K. Uygun, "Whole-Organ Tissue Engineering: Decellularization and Recellularization of Three-Dimensional Matrix Scaffolds," Jul. 2011.

[19] H. C. Ott, T. S. Matthiesen, S.-K. Goh, L. D. Black, S. M. Kren, T. I. Netoff, and D. A.

Taylor, “Perfusion-decellularized matrix: using nature’s platform to engineer a bioartificial heart,” *Nat. Med.*, vol. 14, no. 2, pp. 213–221, Feb. 2008.

[20] S. Schwarz, L. Koerber, A. F. Elsaesser, E. Goldberg-Bockhorn, A. M. Seitz, L. Dürselen, A. Ignatius, P. Walther, R. Breiter, and N. Rotter, “Decellularized Cartilage Matrix as a Novel Biomatrix for Cartilage Tissue-Engineering Applications,” *Tissue Eng. Part A*, vol. 18, p. 120720085805006, 2012.

[21] T. Woods and P. F. Gratzer, “Effectiveness of three extraction techniques in the development of a decellularized bone-anterior cruciate ligament-bone graft.,” *Biomaterials*, vol. 26, no. 35, pp. 7339–49, Dec. 2005.

[22] A. J. Sutherland, E. C. Beck, S. C. Dennis, G. L. Converse, R. A. Hopkins, C. J. Berkland, and M. S. Detamore, “Decellularized cartilage may be a chondroinductive material for osteochondral tissue engineering.,” *PLoS One*, vol. 10, no. 5, p. e0121966, Jan. 2015.

[23] B. T. Estes, B. O. Diekman, J. M. Gimble, and F. Guilak, “Isolation of adipose-derived stem cells and their induction to a chondrogenic phenotype.,” *Nat. Protoc.*, vol. 5, no. 7, pp. 1294–311, Jul. 2010.

[24] H. Z. W. E. and G. S.-T. <p>K. El Sayed, “Stimulated Chondrogenesis via Chondrocytes Co-culturing,” *J. Biochips Tissue Chips*.

[25] R. McBeath, D. M. Pirone, C. M. Nelson, K. Bhadriraju, and C. S. Chen, “Cell Shape, Cytoskeletal Tension, and RhoA Regulate Stem Cell Lineage Commitment,” *Dev. Cell*, vol. 6, no. 4, pp. 483–495, Apr. 2004.

[26] A. J. Friedenstein, K. V Petrakova, A. I. Kurolesova, and G. P. Frolova, “Heterotopic of bone marrow. Analysis of precursor cells for osteogenic and hematopoietic tissues.,” *Transplantation*, vol. 6, no. 2, pp. 230–47, Mar. 1968.

[27] A. P. Beltrami, L. Barlucchi, D. Torella, M. Baker, F. Limana, and S. Chimenti, “Adult cardiac stem cells are multipotent and support myocardial regeneration.,” *Cell*, vol. 114, no. 6, pp. 763–76, Sep. 2003.

[28] J. G. Toma, M. Akhavan, K. J. L. Fernandes, F. Barnabé-Heider, A. Sadikot, D. R. Kaplan, and F. D. Miller, "Isolation of multipotent adult stem cells from the dermis of mammalian skin," *Nat. Cell Biol.*, vol. 3, no. 9, pp. 778–784, Sep. 2001.

[29] P. A. Zuk, M. Zhu, H. Mizuno, J. Huang, J. W. Futrell, A. J. Katz, P. Benhaim, H. P. Lorenz, and M. H. Hedrick, "Multilineage cells from human adipose tissue: implications for cell-based therapies.," *Tissue Eng.*, vol. 7, no. 2, pp. 211–28, Apr. 2001.

[30] M. F. Pittenger, A. M. Mackay, S. C. Beck, and R. K. Jaiswal, "Multilineage potential of adult human mesenchymal stem cells.," *Science*, vol. 284, no. 5411, pp. 143–7, Apr. 1999.

[31] S. A. Wexler, C. Donaldson, P. Denning-Kendall, C. Rice, B. Bradley, and J. M. Hows, "Adult bone marrow is a rich source of human mesenchymal 'stem' cells but umbilical cord and mobilized adult blood are not," *Br. J. Haematol.*, vol. 121, no. 2, pp. 368–374, Apr. 2003.

[32] L. Flynn, G. D. Prestwich, J. L. Semple, and K. A. Woodhouse, "Adipose tissue engineering in vivo with adipose-derived stem cells on naturally derived scaffolds.," *J. Biomed. Mater. Res. A*, vol. 89, no. 4, pp. 929–41, Jun. 2009.

[33] J. M. Gimble, B. A. Bunnell, E. S. Chiu, and F. Guilak, "Concise Review: Adipose-Derived Stromal Vascular Fraction Cells and Stem Cells: Let's Not Get Lost in Translation," *Stem Cells*, vol. 29, no. 5, pp. 749–754, May 2011.

[34] B. Peterson, J. Zhang, R. Iglesias, M. Kabo, M. Hedrick, P. Benhaim, and J. R. Lieberman, "Healing of Critically Sized Femoral Defects, Using Genetically Modified Mesenchymal Stem Cells from Human Adipose Tissue," *http://dx.doi.org/10.1089/ten.2005.11.120*, 2005.

[35] M. Corselli, C. W. Chen, M. Crisan, L. Lazzari, and B. Peault, "Perivascular Ancestors of Adult Multipotent Stem Cells," *Arterioscler. Thromb. Vasc. Biol.*, vol. 30, no. 6, pp. 1104–1109, Jun. 2010.

[36] Y. Zhao, S. D. Waldman, and L. E. Flynn, "The effect of serial passaging on the proliferation and differentiation of bovine adipose-derived stem cells.," *Cells. Tissues.*

Organs, vol. 195, no. 5, pp. 414–27, Jan. 2012.

[37] P. C. Baer, "Adipose-derived mesenchymal stromal/stem cells: An update on their phenotype in vivo and in vitro.," *World J. Stem Cells*, vol. 6, no. 3, pp. 256–65, Jul. 2014.

[38] J. M. Gimble, A. J. Katz, and B. A. Bunnell, "Adipose-Derived Stem Cells for Regenerative Medicine," *Circ. Res.*, vol. 100, no. 9, pp. 1249–1260, Apr. 2007.

[39] M. Zhu, E. Kohan, J. Bradley, M. Hedrick, P. Benhaim, and P. Zuk, "The effect of age on osteogenic, adipogenic and proliferative potential of female adipose-derived stem cells.," *J. Tissue Eng. Regen. Med.*, vol. 3, no. 4, pp. 290–301, Jun. 2009.

[40] M. S. Choudhery, M. Badowski, A. Muise, J. Pierce, and D. T. Harris, "Donor age negatively impacts adipose tissue-derived mesenchymal stem cell expansion and differentiation.," *J. Transl. Med.*, vol. 12, p. 8, 2014.

[41] V. van Harmelen, T. Skurk, K. Röhrig, Y.-M. Lee, M. Halbleib, I. Aprath-Husmann, and H. Hauner, "Effect of BMI and age on adipose tissue cellularity and differentiation capacity in women," *Int. J. Obes.*, vol. 27, no. 8, pp. 889–895, Aug. 2003.

[42] B. M. Schipper, K. G. Marra, W. Zhang, A. D. Donnenberg, and J. P. Rubin, "Regional anatomic and age effects on cell function of human adipose-derived stem cells.," *Ann. Plast. Surg.*, vol. 60, no. 5, pp. 538–44, May 2008.

[43] V. Russo, C. Yu, P. Belliveau, A. Hamilton, and L. E. Flynn, "Comparison of human adipose-derived stem cells isolated from subcutaneous, omental, and intrathoracic adipose tissue depots for regenerative applications.," *Stem Cells Transl. Med.*, vol. 3, no. 2, pp. 206–17, Feb. 2014.

[44] A. E. Aksu, J. P. Rubin, J. R. Dudas, and K. G. Marra, "Role of gender and anatomical region on induction of osteogenic differentiation of human adipose-derived stem cells.," *Ann. Plast. Surg.*, vol. 60, no. 3, pp. 306–22, Mar. 2008.

[45] J. Gimble and F. Guilak, "Adipose-derived adult stem cells: isolation, characterization, and differentiation potential.," *Cytotherapy*, vol. 5, no. 5, pp. 362–9, Jan. 2003.

[46] J. M. Gimble, W. Grayson, F. Guilak, M. J. Lopez, and G. Vunjak-Novakovic, “Adipose tissue as a stem cell source for musculoskeletal regeneration.,” *Front. Biosci. (Schol. Ed).*, vol. 3, pp. 69–81, Jan. 2011.

[47] B. M. Strem, K. C. Hicok, M. Zhu, I. Wulur, Z. Alfonso, R. E. Schreiber, J. K. Fraser, and M. H. Hedrick, “Multipotential differentiation of adipose tissue-derived stem cells,” *Keio J. Med.*, vol. 54, no. 3, pp. 132–141, 2005.

[48] H. Takemitsu, D. Zhao, I. Yamamoto, Y. Harada, and M. Michishita, “Comparison of bone marrow and adipose tissue-derived canine mesenchymal stem cells,” *BMC Vet. Res.*, vol. 8, no. 1, p. 150, 2012.

[49] W.-S. Kim, B.-S. Park, J.-H. Sung, J.-M. Yang, S.-B. Park, S.-J. Kwak, J.-S. Park, and P. A. Zuk, “Wound healing effect of adipose-derived stem cells: a critical role of secretory factors on human dermal fibroblasts.,” *J. Dermatol. Sci.*, vol. 48, no. 1, pp. 15–24, Oct. 2007.

[50] S. P. Blaber, R. A. Webster, C. J. Hill, E. J. Breen, and D. Kuah, “Analysis of in vitro secretion profiles from adipose-derived cell populations,” *J. Transl. Med.*, vol. 10, no. 1, p. 172, 2012.

[51] R. Yañez, A. Oviedo, M. Aldea, J. A. Bueren, and M. L. Lamana, “Prostaglandin E2 plays a key role in the immunosuppressive properties of adipose and bone marrow tissue-derived mesenchymal stromal cells,” *Exp. Cell Res.*, vol. 316, no. 19, pp. 3109–3123, 2010.

[52] J. Rehman, D. Traktuev, J. Li, S. Merfeld-Clauss, C. J. Temm-Grove, J. E. Bovenkerk, C. L. Pell, B. H. Johnstone, R. V Considine, and K. L. March, “Secretion of angiogenic and antiapoptotic factors by human adipose stromal cells.,” *Circulation*, vol. 109, no. 10, pp. 1292–8, Mar. 2004.

[53] T. T. Y. Han, S. Toutounji, B. G. Amsden, and L. E. Flynn, “Adipose-derived stromal cells mediate in vivo adipogenesis, angiogenesis and inflammation in decellularized adipose tissue bioscaffolds,” *Biomaterials*, vol. 72, pp. 125–137, Dec. 2015.

[54] P. Bourin, B. A. Bunnell, L. Casteilla, M. Dominici, A. J. Katz, K. L. March, H. Redl, J. P. Rubin, K. Yoshimura, and J. M. Gimble, "Stromal cells from the adipose tissue-derived stromal vascular fraction and culture expanded adipose tissue-derived stromal/stem cells: a joint statement of the International Federation for Adipose Therapeutics and Science (IFATS) and the International So," *Cytotherapy*, vol. 15, no. 6, pp. 641–8, Jun. 2013.

[55] E. D. Rosen, C. J. Walkey, P. Puigserver, and B. M. Spiegelman, "Transcriptional regulation of adipogenesis," *Genes Dev.*, vol. 14, no. 11, pp. 1293–1307, 2000.

[56] B. O. Diekman, C. R. Rowland, D. P. Lennon, A. I. Caplan, and F. Guilak, "Chondrogenesis of adult stem cells from adipose tissue and bone marrow: induction by growth factors and cartilage-derived matrix.," *Tissue Eng. Part A*, vol. 16, no. 2, pp. 523–33, Feb. 2010.

[57] T. M. Loftus and M. D. Lane, "Modulating the transcriptional control of adipogenesis," *Curr. Opin. Genet. Dev.*, vol. 7, no. 5, pp. 603–608, 1997.

[58] F. M. Gregoire, C. M. Smas, and H. S. Sul, "Understanding adipocyte differentiation," *Physiological Reviews*, vol. 78, no. 3. pp. 783–809, 1998.

[59] J. Frith and P. Genever, "Transcriptional control of mesenchymal stem cell differentiation.," *Transfus. Med. hemotherapy Off. Organ der Dtsch. Gesellschaft fur̈ Transfusionsmedizin und Immunhaḿatologie*, vol. 35, no. 3, pp. 216–27, Jun. 2008.

[60] J.-E. Lee and K. Ge, "Transcriptional and epigenetic regulation of PPARγ expression during adipogenesis.," *Cell Biosci.*, vol. 4, p. 29, 2014.

[61] C. M. Smas and H. S. Sul, "Control of adipocyte differentiation," *Biochemical Journal*, vol. 309, no. 3. pp. 697–710, 1995.

[62] L. Fajas, J.-C. Fruchart, and J. Auwerx, "Transcriptional control of adipogenesis," *Curr. Opin. Cell Biol.*, vol. 10, no. 2, pp. 165–173, Apr. 1998.

[63] S. R. Farmer, "Transcriptional control of adipocyte formation.," *Cell Metab.*, vol. 4, no. 4, pp. 263–73, Oct. 2006.

[64] M. J. Reginato, S. L. Krakow, S. T. Bailey, and M. A. Lazar, “Prostaglandins Promote and Block Adipogenesis through Opposing Effects on Peroxisome Proliferator-activated Receptor,” *J. Biol. Chem.*, vol. 273, no. 4, pp. 1855–1858, Jan. 1998.

[65] Q. Q. Tang and M. D. Lane, “Role of C/EBP homologous protein (CHOP-10) in the programmed activation of CCAAT/enhancer-binding protein-beta during adipogenesis.,” *Proc. Natl. Acad. Sci. U. S. A.*, vol. 97, no. 23, pp. 12446–50, Nov. 2000.

[66] O. A. MacDougald, S. Mandrup, B. B. Kahn, and J. S. Flier, “Adipogenesis: forces that tip the scales,” *Trends Endocrinol. Metab.*, vol. 13, no. 1, pp. 5–11, Jan. 2002.

[67] B. A. Bunnell, M. Flaat, C. Gagliardi, B. Patel, and C. Ripoll, “Adipose-derived stem cells: Isolation, expansion and differentiation,” *Methods*, vol. 45, no. 2, pp. 115–120, 2008.

[68] M. A. Scott, V. T. Nguyen, B. Levi, and A. W. James, “Current Methods of Adipogenic Differentiation of Mesenchymal Stem Cells,” *http://dx.doi.org/10.1089/scd.2011.0040*, 2011.

[69] N. C. Foster, J. R. Henstock, Y. Reinwald, and A. J. El Haj, “Dynamic 3D culture: Models of chondrogenesis and endochondral ossification,” *Birth Defects Res. Part C Embryo Today Rev.*, vol. 105, no. 1, pp. 19–33, Mar. 2015.

[70] B. T. Estes and F. Guilak, “Three-dimensional culture systems to induce chondrogenesis of adipose-derived stem cells.,” *Methods Mol. Biol.*, vol. 702, pp. 201–17, 2011.

[71] N.-C. Cheng, B. T. Estes, H. A. Awad, and F. Guilak, “Chondrogenic differentiation of adipose-derived adult stem cells by a porous scaffold derived from native articular cartilage extracellular matrix.,” *Tissue Eng. Part A*, vol. 15, no. 2, pp. 231–41, Feb. 2009.

[72] M. B. Goldring, K. Tsuchimochi, and K. Ijiri, “The control of chondrogenesis,” *J. Cell. Biochem.*, vol. 97, no. 1, pp. 33–44, Jan. 2006.

[73] H. Akiyama, “Control of chondrogenesis by the transcription factor Sox9,” *Mod. Rheumatol.*, vol. 18, no. 3, pp. 213–219, Jun. 2008.

[74] T. Ikeda, H. Kawaguchi, S. Kamekura, N. Ogata, Y. Mori, K. Nakamura, S. Ikegawa, and U. Chung, “Distinct roles of Sox5, Sox6, and Sox9 in different stages of chondrogenic differentiation,” *J. Bone Miner. Metab.*, vol. 23, no. 5, pp. 337–340, Aug. 2005.

[75] V. Lefebvre, R. R. Behringer, B. de Crombrugghe, and R. Cancedda, “L-Sox5, Sox6 and Sox9 control essential steps of the chondrocyte differentiation pathway,” *Osteoarthr. Cartil.*, vol. 9, pp. S69–S75, Aug. 2001.

[76] V. Lefebvre and P. Smits, “Transcriptional control of chondrocyte fate and differentiation,” *Birth Defects Res. Part C Embryo Today Rev.*, vol. 75, no. 3, pp. 200–212, Sep. 2005.

[77] S. Ghosh, M. Laha, S. Mondal, S. Sengupta, and D. L. Kaplan, “In vitro model of mesenchymal condensation during chondrogenic development.,” *Biomaterials*, vol. 30, no. 33, pp. 6530–40, Nov. 2009.

[78] A. W. James, Y. Xu, J. K. Lee, R. Wang, and M. T. Longaker, “Differential effects of TGF-beta1 and TGF-beta3 on chondrogenesis in posterofrontal cranial suture-derived mesenchymal cells in vitro.,” *Plast. Reconstr. Surg.*, vol. 123, no. 1, pp. 31–43, Jan. 2009.

[79] C. D. Grimsrud, P. R. Romano, M. D’Souza, J. E. Puzas, P. R. Reynolds, R. N. Rosier, and R. J. O’Keefe, “BMP-6 is an autocrine stimulator of chondrocyte differentiation.,” *J. Bone Miner. Res.*, vol. 14, no. 4, pp. 475–82, Apr. 1999.

[80] K.-H. Choi, B. H. Choi, S. R. Park, B. J. Kim, and B.-H. Min, “The chondrogenic differentiation of mesenchymal stem cells on an extracellular matrix scaffold derived from porcine chondrocytes.,” *Biomaterials*, vol. 31, no. 20, pp. 5355–65, Jul. 2010.

[81] E.-J. Kim, S.-W. Cho, J.-O. Shin, M.-J. Lee, and K.-S. Kim, “Ihh and Runx2/Runx3 Signaling Interact to Coordinate Early Chondrogenesis: A Mouse Model,” *PLoS One*, vol. 8, no. 2, p. e55296, Feb. 2013.

[82] T. W. Gilbert, T. L. Sellaro, and S. F. Badylak, “Decellularization of tissues and organs.,” *Biomaterials*, vol. 27, no. 19, pp. 3675–83, Jul. 2006.

[83] Y. Zhao, S. D. Waldman, and L. E. Flynn, “Adipose tissue engineering with naturally derived scaffolds and adipose-derived stem cells.,” *Biomaterials*, vol. 26, no. 12, pp. 109–30, Dec. 2013.

[84] H. Lu, T. Hoshiba, N. Kawazoe, I. Koda, M. Song, and G. Chen, “Cultured cell-derived extracellular matrix scaffolds for tissue engineering.,” *Biomaterials*, vol. 32, no. 36, pp. 9658–66, Dec. 2011.

[85] F. Pati, J. Jang, D.-H. Ha, S. Won Kim, J.-W. Rhie, J.-H. Shim, D.-H. Kim, and D.-W. Cho, “Printing three-dimensional tissue analogues with decellularized extracellular matrix bioink.,” *Nat. Commun.*, vol. 5, 2014.

[86] A. Divoux and K. Clément, “Architecture and the extracellular matrix: the still unappreciated components of the adipose tissue,” *Obes. Rev.*, vol. 12, no. 5, pp. e494–e503, May 2011.

[87] A. J. Engler, S. Sen, H. L. Sweeney, and D. E. Discher, “Matrix elasticity directs stem cell lineage specification.,” *Cell*, vol. 126, no. 4, pp. 677–89, Aug. 2006.

[88] M. F. Goody and C. A. Henry, “Dynamic interactions between cells and their extracellular matrix mediate embryonic development,” *Mol. Reprod. Dev.*, vol. 77, no. 6, pp. 475–488, Jun. 2010.

[89] F. Gattazzo, A. Urciuolo, and P. Bonaldo, “Extracellular matrix: a dynamic microenvironment for stem cell niche.,” *Biochim. Biophys. Acta*, vol. 1840, no. 8, pp. 2506–19, Aug. 2014.

[90] B. Eckes, D. Kessler, M. Aumailley, and T. Krieg, “Springer Seminars in Immunopathology Interactions of fibroblasts with the extracellular matrix: implications for the understanding of fibrosis The extracellular matrix in fibrosis,” *Springer Semin Immunopathol*, vol. 21, 2000.

[91] J. D. Mott and Z. Werb, “Regulation of matrix biology by matrix metalloproteinases,” *Curr. Opin. Cell Biol.*, vol. 16, no. 5, pp. 558–564, 2004.

[92] C. B. Foldager, W. S. Toh, A. H. Gomoll, B. R. Olsen, and M. Spector, “Distribution of Basement Membrane Molecules, Laminin and Collagen Type IV, in Normal and Degenerated Cartilage Tissues.,” *Cartilage*, vol. 5, no. 2, pp. 123–32, Apr. 2014.

[93] M. AUMAILLEY and N. SMYTH, “The role of laminins in basement membrane function,” *J. Anat.*, vol. 193, no. 1, pp. 1–21, Jul. 1998.

[94] L. Bruckner-Tuderman and C. Has, “Disorders of the cutaneous basement membrane zone—The paradigm of epidermolysis bullosa,” *Matrix Biol.*, vol. 33, pp. 29–34, 2014.

[95] T. W. Gilbert, T. L. Sellaro, and S. F. Badylak, “Decellularization of tissues and organs.,” *Biomaterials*, vol. 27, no. 19, pp. 3675–83, Jul. 2006.

[96] C. Streuli, “Extracellular matrix remodelling and cellular differentiation,” *Curr. Opin. Cell Biol.*, vol. 11, no. 5, pp. 634–640, Oct. 1999.

[97] B. Alberts, A. Johnson, J. Lewis, M. Raff, K. Roberts, and P. Walter, “The Extracellular Matrix of Animals.” Garland Science, 2002.

[98] V. Catalán, J. Gómez-Ambrosi, A. Rodríguez, and G. Frühbeck, “Role of extracellular matrix remodelling in adipose tissue pathophysiology: relevance in the development of obesity.,” *Histol. Histopathol.*, vol. 27, no. 12, pp. 1515–28, Dec. 2012.

[99] E. C. M. Mariman and P. Wang, “Adipocyte extracellular matrix composition, dynamics and role in obesity,” *Cell. Mol. Life Sci.*, vol. 67, no. 8, pp. 1277–1292, Apr. 2010.

[100] S. S. Choe, J. Y. Huh, I. J. Hwang, J. I. Kim, and J. B. Kim, “Adipose Tissue Remodeling: Its Role in Energy Metabolism and Metabolic Disorders.,” *Front. Endocrinol. (Lausanne).*, vol. 7, p. 30, 2016.

[101] I. Nakajima, H. Aso, T. Yamaguchi, and K. Ozutsumi, “Adipose tissue extracellular matrix: newly organized by adipocytes during differentiation,” *Differentiation*, vol. 63, no. 4, pp. 193–200, Aug. 1998.

[102] C. Gentili and R. Cancedda, “Cartilage and bone extracellular matrix.,” *Curr. Pharm.*

Des., vol. 15, no. 12, pp. 1334–48, 2009.

[103] J.-L. Chen, L. Duan, W. Zhu, J. Xiong, and D. Wang, "Extracellular matrix production in vitro in cartilage tissue engineering.," *J. Transl. Med.*, vol. 12, p. 88, 2014.

[104] H. Lodish, A. Berk, S. L. Zipursky, P. Matsudaira, D. Baltimore, and J. Darnell, "Collagen: The Fibrous Proteins of the Matrix," 2000.

[105] K. Gelse, E. Pöschl, and T. Aigner, "Collagens—structure, function, and biosynthesis," *Adv. Drug Deliv. Rev.*, vol. 55, no. 12, pp. 1531–1546, 2003.

[106] C. Frantz, K. M. Stewart, V. M. Weaver, A. D. Akintola, and Z. L. Crislip, "The extracellular matrix at a glance.," *J. Cell Sci.*, vol. 123, no. Pt 24, pp. 4195–200, Dec. 2010.

[107] L. Debelle and A. M. Tamburro, "Elastin: molecular description and function," *Int. J. Biochem. Cell Biol.*, vol. 31, no. 2, pp. 261–272, 1999.

[108] J. Aziz, H. Shezali, Z. Radzi, N. A. Yahya, N. H. Abu Kassim, J. Czernuszka, and M. T. Rahman, "Molecular Mechanisms of Stress-Responsive Changes in Collagen and Elastin Networks in Skin," *Skin Pharmacol. Physiol.*, vol. 29, no. 4, pp. 190–203, 2016.

[109] C. Pérez-Rico, G. Pascual, S. Sotomayor, and Á. Asúnsolo, "Elastin Development-Associated Extracellular Matrix Constituents of Subepithelial Connective Tissue in Human Pterygium," *Investig. Opthalmology Vis. Sci.*, vol. 55, no. 10, p. 6309, Oct. 2014.

[110] A. Houghton, P. Quintero, L. A. Marconcini, S. D. Shapiro, and D. Perkins, "Elastin fragments drive disease progression in a murine model of emphysema," 2006.

[111] D. Paulsen, *Lange Histology and Cell Biology*, 5th ed. The McGraw-Hill Companies, Inc., 2010.

[112] B. Alberts, A. Johnson, J. Lewis, M. Raff, K. Roberts, and P. Walter, "The Extracellular Matrix of Animals," 2002.

[113] F. N. Ghadially, J. M. Lalonde, and J. H. Wedge, "Ultrastructure of normal and torn

menisci of the human knee joint.," *J. Anat.*, vol. 136, no. Pt 4, pp. 773–91, Jun. 1983.

[114] P. J. Roughley and E. R. Lee, "Cartilage proteoglycans: Structure and potential functions," *Microsc. Res. Tech.*, vol. 28, no. 5, pp. 385–397, Aug. 1994.

[115] J. Halper and M. Kjaer, "Basic Components of Connective Tissues and Extracellular Matrix: Elastin, Fibrillin, Fibulins, Fibrinogen, Fibronectin, Laminin, Tenascins and Thrombospondins," Springer Netherlands, 2014, pp. 31–47.

[116] P. J. Roughley and E. R. Lee, "Cartilage proteoglycans: Structure and potential functions," *Microsc. Res. Tech.*, vol. 28, no. 5, pp. 385–397, Aug. 1994.

[117] H. Lodish, A. Berk, S. L. Zipursky, P. Matsudaira, D. Baltimore, and J. Darnell, "Noncollagen Components of the Extracellular Matrix," 2000.

[118] E. Hay, *Cell Biology of Extracellular Matrix: Second Edition - Google Books*, 2nd ed. Boston: Springer Science.

[119] L. Schaefer and R. M. Schaefer, "Proteoglycans: from structural compounds to signaling molecules.," *Cell Tissue Res.*, vol. 339, no. 1, pp. 237–46, Jan. 2010.

[120] U. Freymann, M. Endres, K. Neumann, H.-J. Scholman, L. Morawietz, and C. Kaps, "Expanded human meniscus-derived cells in 3-D polymer-hyaluronan scaffolds for meniscus repair.," *Acta Biomater.*, vol. 8, no. 2, pp. 677–85, Feb. 2012.

[121] J. L. Ong, M. R. Appleford, and G. Mani, *Introduction to Biomaterials: Basic Theory with Engineering Applications*, vol. 7. Cambridge University Press, 2013.

[122] R. Langer and D. A. Tirrell, "Designing materials for biology and medicine," *Nature*, vol. 428, no. 6982, pp. 487–492, Apr. 2004.

[123] C. W. Cheng, L. D. Solorio, and E. Alsberg, "Decellularized tissue and cell-derived extracellular matrices as scaffolds for orthopaedic tissue engineering.," *Biotechnol. Adv.*, vol. 32, no. 2, pp. 462–84, Jan. .

[124] N. W. Garrigues, D. Little, J. Sanchez-Adams, D. S. Ruch, and F. Guilak, "Electrospun

cartilage-derived matrix scaffolds for cartilage tissue engineering.," *J. Biomed. Mater. Res. A*, vol. 102, no. 11, pp. 3998–4008, Nov. 2014.

[125] C. Yu, J. Bianco, C. Brown, L. Fuetterer, J. F. Watkins, A. Samani, and L. E. Flynn, "Porous decellularized adipose tissue foams for soft tissue regeneration," *Biomaterials*, vol. 34, no. 13, pp. 3290–3302, Apr. 2013.

[126] D. A. Young, D. O. Ibrahim, D. Hu, and K. L. Christman, "Injectable hydrogel scaffold from decellularized human lipoaspirate.," *Acta Biomater.*, vol. 7, no. 3, pp. 1040–9, Mar. 2011.

[127] H. K. Cheung, T. T. Y. Han, D. M. Marecak, J. F. Watkins, B. G. Amsden, and L. E. Flynn, "Composite hydrogel scaffolds incorporating decellularized adipose tissue for soft tissue engineering with adipose-derived stem cells," *Biomaterials*, vol. 35, no. 6, pp. 1914–1923, 2014.

[128] C. Yu, J. Bianco, C. Brown, L. Fuetterer, J. F. Watkins, A. Samani, and L. E. Flynn, "Porous decellularized adipose tissue foams for soft tissue regeneration," *Biomaterials*, vol. 34, no. 13, pp. 3290–3302, 2013.

[129] R. C. Thomson, M. J. Yaszemski, J. M. Powers, and A. G. Mikos, "Fabrication of biodegradable polymer scaffolds to engineer trabecular bone," *http://dx.doi.org/10.1163/156856295X00805*, 2012.

[130] Y. Y. Gong, J. X. Xue, W. J. Zhang, G. D. Zhou, W. Liu, and Y. Cao, "A sandwich model for engineering cartilage with acellular cartilage sheets and chondrocytes.," *Biomaterials*, vol. 32, no. 9, pp. 2265–73, Mar. 2011.

[131] L. E. Flynn, "The use of decellularized adipose tissue to provide an inductive microenvironment for the adipogenic differentiation of human adipose-derived stem cells.," *Biomaterials*, vol. 31, no. 17, pp. 4715–24, Jun. 2010.

[132] L. Flynn, J. L. Semple, and K. A. Woodhouse, "Decellularized placental matrices for adipose tissue engineering.," *J. Biomed. Mater. Res. A*, vol. 79, no. 2, pp. 359–69, Nov. 2006.

[133] B. D. Elder, S. V Eleswarapu, and K. A. Athanasiou, “Extraction techniques for the decellularization of tissue engineered articular cartilage constructs.,” *Biomaterials*, vol. 30, no. 22, pp. 3749–56, Aug. 2009.

[134] B. Dhandayuthapani, Y. Yoshida, T. Maekawa, D. S. Kumar, B. Dhandayuthapani, Y. Yoshida, T. Maekawa, and D. S. Kumar, “Polymeric Scaffolds in Tissue Engineering Application: A Review,” *Int. J. Polym. Sci.*, vol. 2011, pp. 1–19, 2011.

[135] P. M. Crapo, T. W. Gilbert, and S. F. Badylak, “An overview of tissue and whole organ decellularization processes.,” *Biomaterials*, vol. 32, no. 12, pp. 3233–43, Apr. 2011.

[136] H. Xu, B. Xu, Q. Yang, X. Li, X. Ma, Q. Xia, Y. Zhang, C. Zhang, Y. Wu, and Y. Zhang, “Comparison of decellularization protocols for preparing a decellularized porcine annulus fibrosus scaffold.,” *PLoS One*, vol. 9, no. 1, p. e86723, Jan. 2014.

[137] A. M. Seddon, P. Curnow, and P. J. Booth, “Membrane proteins, lipids and detergents: not just a soap opera,” *Biochim. Biophys. Acta - Biomembr.*, vol. 1666, no. 1, pp. 105–117, 2004.

[138] T. Arnold, D. Linke, T. Arnold, and D. Linke, “The Use of Detergents to Purify Membrane Proteins,” in *Current Protocols in Protein Science*, Hoboken, NJ, USA: John Wiley & Sons, Inc., 2008, pp. 4.8.1–4.8.30.

[139] J. S. Cartmell and M. G. Dunn, “Effect of chemical treatments on tendon cellularity and mechanical properties.,” *J. Biomed. Mater. Res.*, vol. 49, no. 1, pp. 134–40, Jan. 2000.

[140] C. R. Deeken, A. K. White, S. L. Bachman, B. J. Ramshaw, D. S. Cleveland, T. S. Loy, and S. A. Grant, “Method of preparing a decellularized porcine tendon using tributyl phosphate.,” *J. Biomed. Mater. Res. B. Appl. Biomater.*, vol. 96, no. 2, pp. 199–206, Feb. 2011.

[141] M. B. Cole, “Alteration of cartilage matrix morphology with histological processing.,” *J. Microsc.*, vol. 133, no. Pt 2, pp. 129–40, Feb. 1984.

[142] S. B. Lumpkins, N. Pierre, and P. S. McFetridge, “A mechanical evaluation of three

decellularization methods in the design of a xenogeneic scaffold for tissue engineering the temporomandibular joint disc," *Acta Biomater.*, vol. 4, no. 4, pp. 808–816, 2008.

[143] K. E. M. Benders, P. R. van Weeren, S. F. Badylak, D. B. F. Saris, W. J. A. Dhert, and J. Malda, "Extracellular matrix scaffolds for cartilage and bone regeneration.," *Trends Biotechnol.*, vol. 31, no. 3, pp. 169–76, Mar. 2013.

[144] S. Schwarz, L. Koerber, A. F. Elsaesser, E. Goldberg-Bockhorn, A. M. Seitz, L. Dürselen, A. Ignatius, P. Walther, R. Breiter, and N. Rotter, "Decellularized Cartilage Matrix as a Novel Biomatrix for Cartilage Tissue-Engineering Applications," *Tissue Eng. Part A*, vol. 18, no. 21–22, pp. 2195–2209, Nov. 2012.

[145] E. J. Lehr, G. R. Rayat, B. Chiu, T. Churchill, and L. E. McGann, "Decellularization reduces immunogenicity of sheep pulmonary artery vascular patches," *J. Thorac. Cardiovasc. Surg.*, vol. 141, no. 4, pp. 1056–1062, Apr. 2011.

[146] D. W. Jackson, E. S. Grood, P. Wilcox, D. L. Butler, T. M. Simon, and J. P. Holden, "The effects of processing techniques on the mechanical properties of bone-anterior cruciate ligament-bone allografts. An experimental study in goats.," *Am. J. Sports Med.*, vol. 16, no. 2, pp. 101–5.

[147] E. Kheir, T. Stapleton, D. Shaw, Z. Jin, J. Fisher, and E. Ingham, "Development and characterization of an acellular porcine cartilage bone matrix for use in tissue engineering.," *J. Biomed. Mater. Res. A*, vol. 99, no. 2, pp. 283–94, Nov. 2011.

[148] A. E. B. Turner and L. E. Flynn, "Design and characterization of tissue-specific extracellular matrix-derived microcarriers.," *Tissue Eng. Part C. Methods*, vol. 18, no. 3, pp. 186–97, Mar. 2012.

[149] P. Trayhurn and J. H. Beattie, "Physiological role of adipose tissue: white adipose tissue as an endocrine and secretory organ," *Proc. Nutr. Soc.*, vol. 60, no. 03, pp. 329–339, Aug. 2001.

[150] J. T. Tansey, C. Sztalryd, E. M. Hlavin, A. R. Kimmel, and C. Londos, "The central role of perilipin a in lipid metabolism and adipocyte lipolysis.," *IUBMB Life*, vol. 56, no. 7, pp.

379–85, Jul. 2004.

[151] K. N. Frayn, P. Arner, H. Yki-Järvinen, W. S. Snyder, A. Strawford, and F. Antelo, “Fatty acid metabolism in adipose tissue, muscle and liver in health and disease.,” *Essays Biochem.*, vol. 42, no. 5, pp. 89–103, 2006.

[152] V. Russo, C. Yu, P. Belliveau, A. Hamilton, and L. E. Flynn, “Comparison of human adipose-derived stem cells isolated from subcutaneous, omental, and intrathoracic adipose tissue depots for regenerative applications.,” *Stem Cells Transl. Med.*, vol. 3, no. 2, pp. 206–17, Feb. 2014.

[153] E. E. Kershaw and J. S. Flier, “Adipose Tissue as an Endocrine Organ,” *http://dx.doi.org/10.1210/jc.2004-0395*, 2009.

[154] D. unglaub Silverthorn, *Human physiology : an integrated approach*, 6th ed. San Francisco: Pearson, 2007.

[155] G. Fantuzzi, C. C. Wang, M. L. Goalstone, B. Draznin, C. A. Curat, and A. Miranville, “Adipose tissue, adipokines, and inflammation.,” *J. Allergy Clin. Immunol.*, vol. 115, no. 5, pp. 911–9; quiz 920, May 2005.

[156] A. Smorlesi, A. Frontini, A. Giordano, and S. Cinti, “The adipose organ: white-brown adipocyte plasticity and metabolic inflammation,” *Obes. Rev.*, vol. 13, no. S2, pp. 83–96, Dec. 2012.

[157] J. Nedergaard, T. Bengtsson, and B. Cannon, “Unexpected evidence for active brown adipose tissue in adult humans.,” *Am. J. Physiol. Endocrinol. Metab.*, vol. 293, no. 2, pp. E444–52, Aug. 2007.

[158] M. Ward and K. M. Ajuwon, “Regulation of pre-adipocyte proliferation and apoptosis by the small leucine-rich proteoglycans, biglycan and decorin.,” *Cell Prolif.*, vol. 44, no. 4, pp. 343–51, Aug. 2011.

[159] K. Bolton, D. Segal, and K. Walder, “The small leucine-rich proteoglycan, biglycan, is highly expressed in adipose tissue of Psammomys obesus and is associated with obesity

and type 2 diabetes.," *Biologics*, vol. 6, pp. 67–72, 2012.

[160] J. Sottile, "Regulation of angiogenesis by extracellular matrix," *Biochim. Biophys. Acta - Rev. Cancer*, vol. 1654, no. 1, pp. 13–22, 2004.

[161] J. Hubbell, "Matrix-bound growth factors in tissue repair.," *Swiss Med. Wkly.*, vol. 136, no. 25–26, pp. 387–91, Jun. 2006.

[162] S. Hippenstiel, M. Krüll, A. Ikemann, W. Risau, and M. Clauss, "VEGF induces hyperpermeability by a direct action on endothelial cells.," *Am. J. Physiol.*, vol. 274, no. 5 Pt 1, pp. L678–84, May 1998.

[163] A. Sukarto, C. Yu, L. E. Flynn, and B. G. Amsden, "Co-delivery of adipose-derived stem cells and growth factor-loaded microspheres in RGD-grafted N-methacrylate glycol chitosan gels for focal chondral repair.," *Biomacromolecules*, vol. 13, no. 8, pp. 2490–502, Aug. 2012.

[164] S. Schwarz, L. Koerber, A. F. Elsaesser, E. Goldberg-Bockhorn, A. M. Seitz, L. Dürselen, A. Ignatius, P. Walther, R. Breiter, and N. Rotter, "Decellularized Cartilage Matrix as a Novel Biomatrix for Cartilage Tissue-Engineering Applications," *Tissue Eng. Part A*, vol. 18, no. 21–22, pp. 2195–2209, Nov. 2012.

[165] B. N. Brown, J. M. Freund, L. Han, J. P. Rubin, J. E. Reing, E. M. Jeffries, M. T. Wolf, S. Tottey, C. A. Barnes, B. D. Ratner, and S. F. Badylak, "Comparison of three methods for the derivation of a biologic scaffold composed of adipose tissue extracellular matrix.," *Tissue Eng. Part C. Methods*, vol. 17, no. 4, pp. 411–21, Apr. 2011.

[166] B. Zvarova, F. E. Uhl, J. J. Uriarte, Z. D. Borg, A. L. Coffey, N. R. Bonenfant, D. J. Weiss, and D. E. Wagner, "Residual Detergent Detection Method for Nondestructive Cytocompatibility Evaluation of Decellularized Whole Lung Scaffolds.," *Tissue Eng. Part C. Methods*, vol. 22, no. 5, pp. 418–28, May 2016.

[167] S. Cebotari, I. Tudorache, T. Jaekel, A. Hilfiker, S. Dorfman, W. Ternes, A. Haverich, and A. Lichtenberg, "Detergent decellularization of heart valves for tissue engineering: toxicological effects of residual detergents on human endothelial cells.," *Artif. Organs*,

vol. 34, no. 3, pp. 206–10, Mar. 2010.

[168] B. Cody, K. Miljan, F. Lydia, L. Gilles, and F. Lauren, “The proteomic characterization of decellularized adipose tissue bioscaffolds for applications in soft tissue regeneration,” *Front. Bioeng. Biotechnol.*, vol. 4, 2016.

[169] H. Muir, “The chondrocyte, architect of cartilage. Biomechanics, structure, function and molecular biology of cartilage matrix macromolecules,” *BioEssays*, vol. 17, no. 12, pp. 1039–1048, Dec. 1995.

[170] A. J. Sophia Fox, A. Bedi, and S. A. Rodeo, “The basic science of articular cartilage: structure, composition, and function.,” *Sports Health*, vol. 1, no. 6, pp. 461–8, Nov. 2009.

[171] J. A. Buckwalter and L. C. Rosenberg, “Electron microscopic studies of cartilage proteoglycans.,” *Electron Microsc. Rev.*, vol. 1, no. 1, pp. 87–112, 1988.

[172] B. Young, J. Lowe, A. Stevens, and J. Heath, *Wheater’s Functional Histology: A Text and Colour Atlas, 5th Edition: 9780443068508: Medicine & Health Science Books @ Amazon.com*, 5th ed. Elsevier Limited, 2006.

[173] C. McDevitt and J. Marcelino, “Composition of Articular Cartilage,” *Sports Med. Arthrosc.*, vol. 2, no. 1, pp. 1–12, 1994.

[174] K. Mithoefer, T. McAdams, R. J. Williams, P. C. Kreuz, and B. R. Mandelbaum, “Clinical efficacy of the microfracture technique for articular cartilage repair in the knee: an evidence-based systematic analysis.,” *Am. J. Sports Med.*, vol. 37, no. 10, pp. 2053–63, Oct. 2009.

[175] W. R. J. McDevitt C.A., “The ultrastructure and biochemistry of meniscal cartilage,” *Clinical Orthopaedics and Related Research*, 1990. .

[176] C. Chung and J. A. Burdick, “Engineering cartilage tissue.,” *Adv. Drug Deliv. Rev.*, vol. 60, no. 2, pp. 243–62, Jan. 2008.

[177] J. Hasan, J. Fisher, and E. Ingham, “Current strategies in meniscal regeneration.,” *J.*

Biomed. Mater. Res. B. Appl. Biomater., vol. 102, no. 3, pp. 619–34, Apr. 2014.

[178] C. G. Wilson, J. F. Nishimuta, and M. E. Levenston, "Chondrocytes and meniscal fibrochondrocytes differentially process aggrecan during de novo extracellular matrix assembly.," *Tissue Eng. Part A*, vol. 15, no. 7, pp. 1513–22, Jul. 2009.

[179] M. K. Murphy, D. J. Huey, J. C. Hu, and K. A. Athanasiou, "TGF-β1, GDF-5, and BMP-2 stimulation induces chondrogenesis in expanded human articular chondrocytes and marrow-derived stromal cells.," *Stem Cells*, vol. 33, no. 3, pp. 762–73, Mar. 2015.

[180] J. E. Ratner, B. D., Hoffman, A. S., Schoen, F. J., & Lemons, *Biomaterials science: an introduction to materials in medicine*. 2004.

[181] S. Mirsadraee, H. E. Wilcox, S. A. Korossis, J. N. Kearney, K. G. Watterson, J. Fisher, and E. Ingham, "Development and characterization of an acellular human pericardial matrix for tissue engineering.," *Tissue Eng.*, vol. 12, no. 4, pp. 763–73, Apr. 2006.

[182] F. Mwale, "Composition of Intervertebral Disc," *Eur. Cells Mater.*, vol. 8, pp. 58–64, 2004.

[183] A. J. Sutherland, E. C. Beck, S. C. Dennis, G. L. Converse, and R. A. Hopkins, "Decellularized Cartilage May Be a Chondroinductive Material for Osteochondral Tissue Engineering," *PLoS One*, vol. 10, no. 5, p. e0121966, May 2015.

[184] J. M. Gimble, A. J. Katz, and B. A. Bunnell, "Adipose-Derived Stem Cells for Regenerative Medicine," *Circ. Res.*, vol. 100, no. 9, pp. 1249–1260, Apr. 2007.

[185] A. R. Poole, T. Kojima, T. Yasuda, F. Mwale, M. Kobayashi, and S. Laverty, "Composition and structure of articular cartilage: a template for tissue repair.," *Clin. Orthop. Relat. Res.*, no. 391 Suppl, pp. S26–33, Oct. 2001.

[186] L. Han, A. J. Grodzinsky, and C. Ortiz, "Nanomechanics of the Cartilage Extracellular Matrix.," *Annu. Rev. Mater. Res.*, vol. 41, pp. 133–168, Jul. 2011.

[187] C. Liu, "Transcriptional mechanism of COMP gene expression and chondrogenesis.," *J.*

Musculoskelet. Neuronal Interact., vol. 5, no. 4, pp. 340–1.

[188] E. L. Radin, F. de Lamotte, and P. Maquet, "Role of the menisci in the distribution of stress in the knee.," *Clin. Orthop. Relat. Res.*, no. 185, pp. 290–4, May 1984.

[189] M. B. Pabbruwe, W. Kafienah, J. F. Tarlton, S. Mistry, D. J. Fox, and A. P. Hollander, "Repair of meniscal cartilage white zone tears using a stem cell/collagen-scaffold implant.," *Biomaterials*, vol. 31, no. 9, pp. 2583–91, Mar. 2010.

[190] N.-C. Cheng, B. T. Estes, H. A. Awad, and F. Guilak, "Chondrogenic differentiation of adipose-derived adult stem cells by a porous scaffold derived from native articular cartilage extracellular matrix.," *Tissue Eng. Part A*, vol. 15, no. 2, pp. 231–41, Feb. 2009.

[191] J. Herwig, E. Egner, and E. Buddecke, "Chemical changes of human knee joint menisci in various stages of degeneration.," *Ann. Rheum. Dis.*, vol. 43, no. 4, pp. 635–40, Aug. 1984.

[192] S. Jia, L. Liu, W. Pan, G. Meng, C. Duan, L. Zhang, Z. Xiong, and J. Liu, "Oriented cartilage extracellular matrix-derived scaffold for cartilage tissue engineering.," *J. Biosci. Bioeng.*, vol. 113, no. 5, pp. 647–53, May 2012.

[193] U. Freymann, M. Endres, U. Goldmann, M. Sittinger, and C. Kaps, "Toward scaffold-based meniscus repair: effect of human serum, hyaluronic acid and TGF-ß3 on cell recruitment and re-differentiation.," *Osteoarthritis Cartilage*, vol. 21, no. 5, pp. 773–81, May 2013.

[194] M. T. Conconi, P. De Coppi, R. Di Liddo, S. Vigolo, G. F. Zanon, P. P. Parnigotto, and G. G. Nussdorfer, "Tracheal matrices, obtained by a detergent-enzymatic method, support in vitro the adhesion of chondrocytes and tracheal epithelial cells.," *Transpl. Int.*, vol. 18, no. 6, pp. 727–34, Jun. 2005.

[195] Lumpkins SB, Pierre N, and McFetridge PS., "A mechanical evaluation of three decellularization methods in the design of a xenogeneic scaffold for tissue engineering the temporomandibular join... - PubMed - NCBI," *Acta Biomater*, vol. 4, no. 4, pp. 808–816, 2008.

[196] T. W. Stapleton, J. Ingram, J. Katta, R. Knight, S. Korossis, J. Fisher, and E. Ingham, "Development and characterization of an acellular porcine medial meniscus for use in tissue engineering.," *Tissue Eng. Part A*, vol. 14, no. 4, pp. 505–18, Apr. 2008.

[197] Q. Yang, J. Peng, Q. Guo, J. Huang, L. Zhang, J. Yao, F. Yang, S. Wang, W. Xu, A. Wang, and S. Lu, "A cartilage ECM-derived 3-D porous acellular matrix scaffold for in vivo cartilage tissue engineering with PKH26-labeled chondrogenic bone marrow-derived mesenchymal stem cells.," *Biomaterials*, vol. 29, no. 15, pp. 2378–87, May 2008.

[198] H. Lu, T. Hoshiba, N. Kawazoe, and G. Chen, "Comparison of decellularization techniques for preparation of extracellular matrix scaffolds derived from three-dimensional cell culture.," *J. Biomed. Mater. Res. A*, vol. 100, no. 9, pp. 2507–16, Sep. 2012.

[199] H.-W. Cheng, Y.-K. Tsui, K. M. C. Cheung, D. Chan, and B. P. Chan, "Decellularization of chondrocyte-encapsulated collagen microspheres: a three-dimensional model to study the effects of acellular matrix on stem cell fate.," *Tissue Eng. Part C. Methods*, vol. 15, no. 4, pp. 697–706, Dec. 2009.

[200] Y. Y. Gong, J. X. Xue, W. J. Zhang, G. D. Zhou, W. Liu, and Y. Cao, "A sandwich model for engineering cartilage with acellular cartilage sheets and chondrocytes," *Biomaterials*, vol. 32, no. 9, pp. 2265–2273, 2011.

[201] T. Woods and P. F. Gratzer, "Effectiveness of three extraction techniques in the development of a decellularized bone-anterior cruciate ligament-bone graft.," *Biomaterials*, vol. 26, no. 35, pp. 7339–49, Dec. 2005.

[202] L. E. Flynn, G. D. Prestwich, J. L. Semple, and K. A. Woodhouse, "Proliferation and differentiation of adipose-derived stem cells on naturally derived scaffolds.," *Biomaterials*, vol. 29, no. 12, pp. 1862–71, Apr. 2008.

[203] M. Neupane, C.-C. Chang, M. Kiupel, and V. Yuzbasiyan-Gurkan, "Isolation and Characterization of Canine Adipose–Derived Mesenchymal Stem Cells," *Tissue Eng. Part A*, vol. 0, no. 0, p. 080422095744451, Apr. 2008.

[204] K. J. Livak and T. D. Schmittgen, “Analysis of relative gene expression data using real-time quantitative PCR and the 2(-Delta Delta C(T)) Method.,” *Methods*, vol. 25, no. 4, pp. 402–8, Dec. 2001.

[205] A. M. Pizzo, K. Kokini, L. C. Vaughn, B. Z. Waisner, and S. L. Voytik-Harbin, “Extracellular matrix (ECM) microstructural composition regulates local cell-ECM biomechanics and fundamental fibroblast behavior: a multidimensional perspective.,” *J. Appl. Physiol.*, vol. 98, no. 5, pp. 1909–21, May 2005.

[206] I. Garza-Veloz, V. J. Romero-Diaz, M. L. Martinez-Fierro, I. A. Marino-Martinez, M. Gonzalez-Rodriguez, H. G. Martinez-Rodriguez, M. A. Espinoza-Juarez, D. A. Bernal-Garza, R. Ortiz-Lopez, and A. Rojas-Martinez, “Analyses of chondrogenic induction of adipose mesenchymal stem cells by combined co-stimulation mediated by adenoviral gene transfer.,” *Arthritis Res. Ther.*, vol. 15, no. 4, p. R80, Jan. 2013.

[207] W. S. Toh, X.-M. Guo, A. B. Choo, K. Lu, E. H. Lee, and T. Cao, “Differentiation and enrichment of expandable chondrogenic cells from human embryonic stem cells in vitro.,” *J. Cell. Mol. Med.*, vol. 13, no. 9B, pp. 3570–90, Sep. 2009.

[208] B. K. Straub, B. Gyoengyoesi, M. Koenig, M. Hashani, L. M. Pawella, E. Herpel, W. Mueller, S. Macher-Goeppinger, H. Heid, and P. Schirmacher, “Adipophilin/perilipin-2 as a lipid droplet-specific marker for metabolically active cells and diseases associated with metabolic dysregulation.,” *Histopathology*, vol. 62, no. 4, pp. 617–31, Mar. 2013.

[209] L. Pilgaard, P. Lund, M. Duroux, T. Fink, M. Ulrich-Vinther, K. Søballe, and V. Zachar, “Effect of oxygen concentration, culture format and donor variability on in vitro chondrogenesis of human adipose tissue-derived stem cells.,” *Regen. Med.*, vol. 4, no. 4, pp. 539–48, Jul. 2009.

[210] A. J. Sutherland, E. C. Beck, S. C. Dennis, G. L. Converse, R. A. Hopkins, C. J. Berkland, and M. S. Detamore, “Decellularized cartilage may be a chondroinductive material for osteochondral tissue engineering.,” *PLoS One*, vol. 10, no. 5, p. e0121966, Jan. 2015.

[211] J. Xu, W. Wang, M. Ludeman, K. Cheng, T. Hayami, J. C. Lotz, and S. Kapila,

"Chondrogenic Differentiation of Human Mesenchymal Stem Cells in Three-Dimensional Alginate Gels," *Tissue Eng. Part A*, vol. 14, no. 5, pp. 667–680, May 2008.

[212] M. J. Zuscik, M. J. Hilton, X. Zhang, D. Chen, and R. J. O'Keefe, "Regulation of chondrogenesis and chondrocyte differentiation by stress," *J. Clin. Invest.*, vol. 118, no. 2, pp. 931–941, 2008.

Appendix A

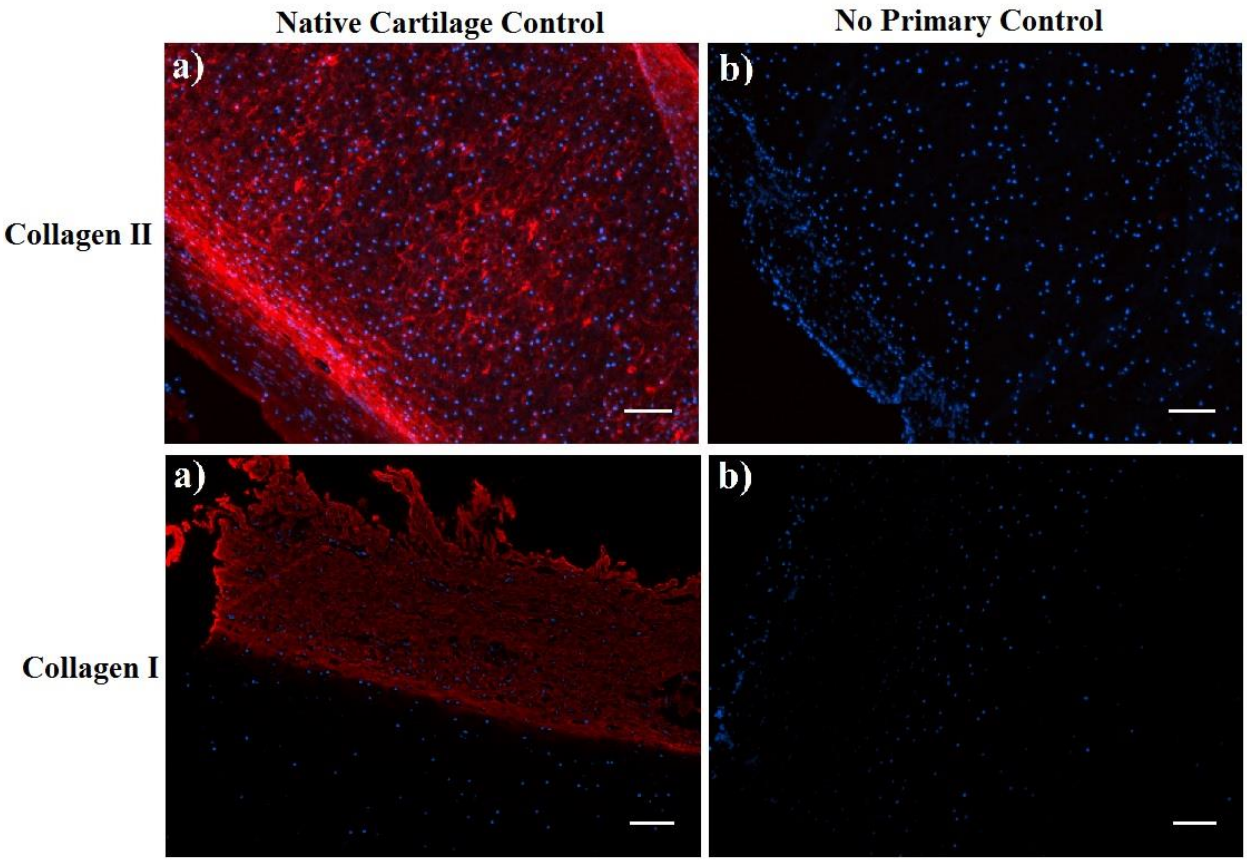

Figure A.1: Immunohistochemical of collagen II and collagen I (red) staining with DAPI counterstaining (blue) on (a) porcine cartilage (COL II) and skin (COL I) and, (b) with no primary controls. Scale bars = 100 µm (n=2).

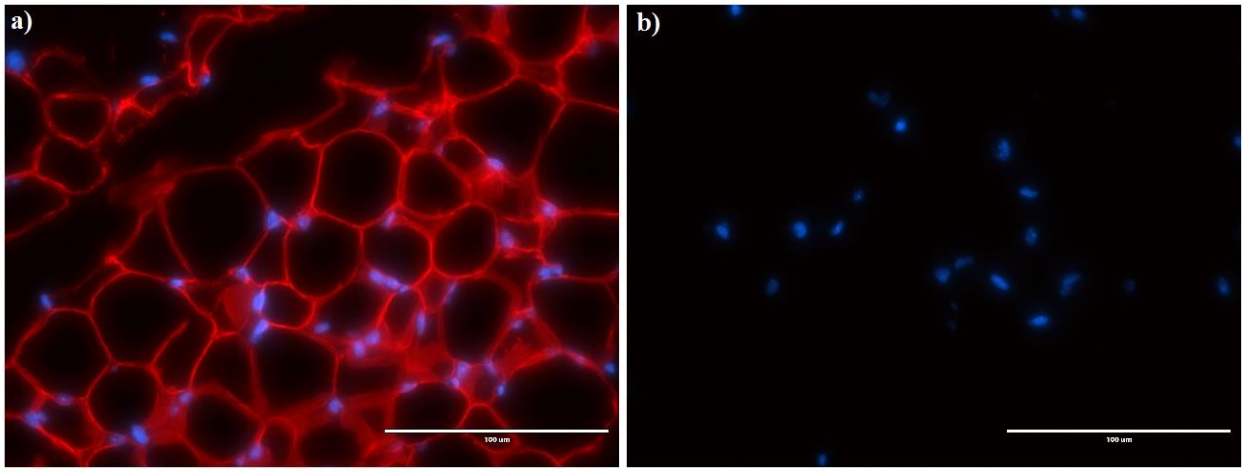

Figure A 2: Immunohistochemical of perilipin (red) staining with DAPI counterstaining (blue) on (a) murine adipose tissue and, (b) with no primary controls. Scale bars = 100 µm (n=2).

Curriculum Vitae

Name:	Danielle Heinbuch
Post-secondary Education and Degrees:	University of Waterloo Waterloo, Ontario, Canada 2009-2014 B.Sc. (Kinesiology), Biology Minor, Co-op The University of Western Ontario London, Ontario, Canada 2014 -Present M.E.Sc. Candidate
Honours and Awards:	Graduate Research Assistant 2014-2016 Dean's Honor Roll University of Waterloo 2013-2014 Academic All-Canadian University of Waterloo 2013-2014
Related Work Experience	Teaching Assistant The University of Western Ontario 2014-2016 Teaching Assistant University of Waterloo 2012-2014